計畫編號：NHRI-EX91-9102BC

國家衛生研究院九十一年度整合性醫藥衛生科技研究計畫

以精簡雜交和基因微矩陣技術探討肺腺癌治病機轉
Study of carcinogenic mechanisms of lung adenocarcinoma

計畫名稱

年度成果報告

執 行 機 構：中山醫學大學

計 畫 主 持 人：蔡菁華

執 行 期 間：91 年 1 月 1 日 至 91 年 12 月 31 日

計畫名稱：以精簡雜交和基因微矩陣技術探討肺腺癌治病機轉

計畫編號：NHRI-EX91-9102BC

執行機構：中山醫學大學

計畫主持人：蔡菁華

研究人員：

關鍵字：肺腺癌、精簡雜交基因庫、差異性雜交反應篩選法 (differential screening) 、致癌基因、抑癌基因、同步定量 PCR 系統

壹、九十一年度計畫研究成果摘要

近數十年來，歐美國家罹患肺癌的病人有顯著的增加，而在台灣，衛生署統計民國 90 年的 10 大死亡原因中惡性腫瘤仍居首位，其中肺癌的死亡率在男性癌症死亡原因中位居第二位，僅少於肝癌 1.4 個百分比，但在女性的死亡率卻高居首位，綜合男性與女性的癌症死亡原因中仍以肺癌爲第一。根據世界衛生組織對於原發性肺癌的分類主要可分成 4 大類：鱗狀細胞癌（squamous cell carcinoma）、肺腺癌（adenocarcinoma）、小細胞癌（small cell carcinoma）與大細胞癌（large cell carcinoma）。其中鱗狀細胞癌與小細胞癌和抽煙有密切的關係，對於絕大多數不抽煙的台灣女性肺癌病人中以肺腺癌的罹患率最高。值得注意的是近年來男性肺腺癌病人的發生率也逐漸的居於領先的局勢。因此探討肺腺癌病人的肺正常組織與癌組織間基因表現的差異性，將有助於我們發現新的致癌基因或抑癌基因。研究這些可能的致癌基因或抑癌基因將可以提高我們對肺腺癌形成的了解，並期望對於肺腺癌的治療、診段、或預防上提供一些重要的訊息。

爲了尋找可能的致癌基因或抑癌基因，本實驗室利用精簡雜交反應建立

了兩個精簡基因庫；其一是利用大量的正常組織中的 cDNA 減去肺腺癌組織中之表現量相同的基因 (T-N 精簡基因庫) ，另一基因庫是利用大量的肺腺癌組織中的 cDNA 減去正常組織中之表現量相同的基因 (N-T 精簡基因庫)。由於此雜交反應經過數次的 PCR 反應，每一個 cDNA 已經被大量的放大，因此基因庫裡的基因重複性很高。爲了降低成本並有效率的將這些在正常組織與腫瘤組織鐘表現量有差異的基因鑑定出來，我們實驗室發展了差異性雜交反應篩選法(differential screening)。

差異性雜交反應篩選法是將精簡雜交基因庫裡的 cDNA 利用 PCR 反應將其放大，點於兩張 Nylon 轉漬膜上，再利用精簡雜交基因庫裡的 cDNA 製成正常組織較專一的探針和肺腺癌組織較專一的探針分別進行雜交反應。此雜交反應可將經精簡雜交反應後漏網之魚-未被剔除的表現量相同的基因，再度找出並剔除。其餘具有差異表現量的基因被集合起來製成第一組的 positive probes。此 positive probes 將用來剔除下一組差異性雜交反應中已重複出現的基因。在第二組差異性雜交反應中篩選出來的新的具有差異性表現基因再被集合起來與第一組的 positive probes 製成第二組的 positive probes。此 positive probes 即用來篩選第三組差異性雜交反應中新的具有差異性表現的基因。以此列推，直到用精簡雜交基因庫裡的 cDNA probes 找出的具有差異性表現基因與 positve probes 都有雜交反應時，我們再進行一組新的反應以確定結果後停止篩選。每一個精簡基因庫一共進行了五至六組的 differential screening。

經過此 differential screening，從 N-T 精簡基因庫裡篩選了 174 個含差異性表現量 cDNA 的細胞株，並從 T-N 精簡基因庫裡得到了 105 個含差異性表現量 cDNA。欲了解這些基因的內容，我們將這些基因定序，並將於

differential screening 裡遺漏的重複性基因再次剔除。最後我們由 174 個 N-T 精簡基因庫裡得到 76 個不重複的表現量有差異的基因，並從 105 個 T-N 精簡基因庫裡得到 37 個不重複的表現量有差異的基因。

欲了解這些經由 differential screening 出來的表現量有差異的基因是否在不同病人的組織中具有差異的表現量，同步定量 PCR 系統(realtime PCR)被用來定量這些基因在不同病人的表現量。當同一個被用來製造精簡雜交基因庫的病人組織用來進行 realtime PCR，初步分析六個表現量有差異的基因 (N6, N8, N21, N28, N42, 和N47)發現這些基因在此病人的正常組織中表現量分別高於肺癌組織約 282, 13, 446, 3468, 2702 和 156 倍。

本實驗室希望由此貳精簡基因庫裡找出尚未被研究的基因進行更深入的研究，因此當定序的結果顯示出尚未被研究的基因時，這些基因即被用來合成一對引子(primers)，並用來進行 realtime PCR 反應。由於我們需要利用 realtime PCR 進一步的證明這些表現量有差異的基因在肺腺癌的形成是否具有實質的意義，而進行 realtime PCR 反應所需的試劑非常的昂貴，因此我們花了一些時間發展這個試劑以節省成本。

我們實驗室目前除了繼續利用realtime PCR進行鑑定這些精簡基因庫裡的基因是否真的具有差異性的表現，我們選了兩個新的基因, N6 和 N21 進行較深入的研究。由於我們感興趣的是一些未被研究的新基因，因此我們建立了肺正常組織、肺腺癌組織及肺癌細胞株等三個 cDNA 基因庫，以利於尋找全長基因。目前我們正在尋找 N6 和 N21 的全長基因。

由於肺癌的腫瘤組織並非全爲癌細胞，因此 total RNA 裡包含了癌細胞

和非癌細胞。解決這個問題可以利用 microdisector 將腫瘤組織中之癌細胞分別取出，但此法非常不經濟，不適合於基因篩選用。 因此使用 total RNA 進行 PCR 反應不能精確的反應出腫瘤組織與鄰近正常組織中基因表現的差異性。爲了證實 realtime PCR 的結果並鑑定感興趣的基因表現於何種型態的細胞，我們正在進行組織定位雜交反應。

除了利用 realtime RT-PCR 偵測基因的差異表現量，並以此爲篩選的依據進行更深入的研究，我們正在發展另一個新的技術 - siRNA (small interefering RNA)，期望利用此技術阻止表現量有差異的基因的細胞表現，藉以觀察這些基因與正常細胞或癌細胞的生長或死亡有沒有關細。這個技術特別適合我們使用，因爲此技術對於得到全長 cDNA 幾百分之百的精確定序較無關，而精簡基因庫裡的基因都只是片段定序的。因此，當這個技術成熟時，這些被篩選過的基因將被分別或幾個一組的送入細胞內進行抑制作用。

貳、九十一年度計畫著作一覽表

註：群體計畫(PPG)者，不論是否提出各子計畫資料，都必須提出總計畫整合之資料
若爲群體計畫，請勾選本表屬於: □子計畫； 或 □總計畫(請自行整合)

1.列出貴計畫於本年度中之所有計畫產出於下表，包含已發表或已被接受發表之文獻、已取得或被接受之專利、擬投稿之手稿（manuscript）以及專著等。

2.「計畫產出名稱」欄位：請依「臺灣醫誌」參考文獻方式撰寫;

3.「產出型式」欄位：填寫該產出爲國內期刊、、國外期刊、專利、手稿或專著等。

4.「SCI」欄位：Science Citation Index，若發表之期刊爲 SCI 所包含者，請在欄位上填寫該期刊當年度之 impact factor。

5.「致謝與否」欄位：請註明該成果產出之致謝單位。若該成果產出有註明衛生署資助字樣者，請以 DOH 註明；若該成果產出有註明國家衛生研究院委託資助字樣者，請以 NHRI 註明；若該成果產出有註明衛生署及國家衛生研究院資助字樣者，請合併以 DOH&NHRI 註明；若該成果產出有註明非上述機構資助字樣者，請以機構全銜註明。
舉例如下:

序號	計畫產出名稱	產出型式	SCI*	致謝與否
例	Hsiu SL, Huang TY, Hou YC., Chin DH, Chao PDL. Comparison of Metabolic Pharmacokinetics of Naringin and Naringenin in Rabbits. Life Sciences 2002 Feb 15, 70:1481-1489.	國外期刊	1.808	NHRI
1.	Identification of novel bovine RPE and retinal genes by subtractive hybridization. Sharma S, Chang JT, Della NG, Campochiaro PA, Zack DJ. Mol Vis. 2002 Jul 16;8:251-8.	國外期刊	2.779	National Instiute of Health (NIH)
2.	Cloning and characterization of a human beta,beta-carotene-15,15'-dioxygenase that is highly expressed in the retinal pigment epithelium. Yan W, Jang GF, Haeseleer F, Esumi N, Chang JT, Kerrigan M, Campochiaro M, Campochiaro P, Palczewski K, Zack DJ. Genomics. 2001 Mar 1;72(2):193-202.	國外期刊	3.425	NIH
3.	Expression and permeation properties of the K(+) channel Kir7.1 in the retinal pigment epithelium. Shimura M, Yuan Y, Chang JT, Zhang S, Campochiaro PA, Zack DJ, Hughes BA. J Physiol. 2001 Mar 1;531(Pt	國外期刊	4.455	NIH

	2):329-46.			
4.	Identification of genes involved in lung tumorigenesis via suppressive subtractive hybridization Huey-Ling Hung , Huey-Tsu Huang, Ming-Ji. Fann, Yu-chung Wu, Wen-Hu Hsu and Jinghua-Tsai Chang 2002 生醫年會	研討會論文		
5.				
6.				
7.				
8.				
9.				

*本表如不敷使用，請自行影印。

參、九十一年度計畫重要研究成果產出統計表

註：群體計畫(PPG)者，不論是否提出各子計畫資料，都必須提出總計畫整合之資料
若爲群體計畫，請勾選本表屬於: □子計畫； 或 □總計畫(請自行整合)

(係指執行九十一年度計畫之所有研究產出成果)

科技論文篇數			技術移轉			技術報告
	國內	國外	類型	經費	項數	篇
期刊論文	篇	篇	技術輸入	千元	項	技術創新 項
研討會論文	1 篇	篇	技術輸出	千元	項	著作權(核准) 項
專著	篇	篇	技術擴散	千元	項	專利權(核准) 項

〔註〕:

期刊論文：指在學術性期刊上刊登之文章，其本文部份一般包含引言、方法、結果、及討論，並且一定有參考文獻部分，未在學術性期刊上刊登之文章（研究報告等）與博士或碩士論文，則不包括在內。

研討會論文：指參加學術性會議所發表之論文，且尚未在學術性期刊上發表者。

專　　著：爲對某項學術進行專門性探討之純學術性作品。

技術報告：指從事某項技術之創新、設計及製程等研究發展活動所獲致的技術性報告且未公開發表者。

技術移轉：指技術由某個單位被另一個單位所擁有的過程。我國目前之技術轉移包括下列三項：一、技術輸入。二、技術輸出。三、技術擴散。

技術輸入：藉僑外投資、與外國技術合作、投資國外高科技事業等方式取得先進之技術引進國內者。

技術輸出：指直接供應國外買主具生產能力之應用技術、設計、顧問服務及專利等。我國技術輸出方包括整廠輸出、對外投資、對外技術合作及顧問服務等四種。

技術擴散：指政府引導式的技術移轉方式，即由財團法人、國營事業或政府研究機構將其開發之技術擴散至民間企業之一種單向移轉（政府移轉民間）。

技術創新：指研究執行中產生的技術，且有詳實技術資料文件者。

肆、九十一年度計畫重要研究成果

註：群體計畫(PPG)者，不論是否提出各子計畫資料，都必須提出總計畫整合之資料
若爲群體計畫，請勾選本表屬於: □子計畫； 或 □總計畫(請自行整合)

1.計畫之新發現或新發明

本計劃所產生的兩個精簡基因庫裡有許多的基因目前尚未被研究，我們希望研究這些基因能增加人類對於肺癌形成的了解，而這些基因對於肺癌的實質貢獻則有待更深入的研究。

2.計畫對學術界或產業界具衝擊性（impact）之研究成果

由於此計畫所篩選出來的基因數目很多，已超過一個實驗室所能操作的範圍。因此當我們進一步證實這些基因的專一性之後，我們歡迎對於肺癌研究有興趣的實驗室共同研究這些基因。

3.計畫對民眾具教育宣導之研究成果

此部份將爲規劃對一般民眾教育或宣導研究成果之依據，請以淺顯易懂之文字簡述研究成果，內容以不超過 300 字爲原則。

肺癌的死亡率位居所有癌症死亡率之首並非因其罹患率最高所致，主要是缺乏早期偵測的方法，大部分的肺癌被診斷出來時已經轉移了，唯有初期肺癌的診斷才有機會防止癌細胞的轉移。另一個要因是肺癌細胞的抗藥性非常的強，經過化學治療後，復發的癌細胞幾乎對所有的藥物都產生抗藥性。

欲有效的提高肺癌的存活率，我們必須對肺癌的形成充份了解，而尋找參與肺癌形成的基因是最直接的方法。這些基因可以當作肺癌早期篩選的指標或提供新的治療途徑。而人類最大的夢想是預防癌症的發生，達到這些夢想沒有捷徑，只有將那些能促進癌化的基因一個個研究清楚。我們實驗室朝著這個目標，建立了可能參與肺癌

形成的精簡基因庫以供我們或其他有志之士共同研究。

4.技術移轉（註明成果或技術名稱、移轉對象及概略情形）

5.技術推廣（註明成果或技術名稱、移轉對象及概略情形）

6.業界合作成效（註明成果或技術名稱、移轉對象及概略情形）

7.成效評估（技術面、經濟面、社會面、整合綜效）

本研究屬於肺癌的基本研究，我們已有效的將可能參與肺腺癌形成的部分基因收集於兩個基因庫裡，並已完成初步的篩選工作。

8.下年度工作構想及重點之妥適性

(1)本計劃下年度將利用基因微矩陣，將這些表現量有差異的基因點在轉漬膜上，在將不同病人的腫瘤組織和鄰近的正常組織的 RNA 製成探針進行雜較反應。如此將可更有效率的篩選與肺癌形成有關的基因。

(2)除了利用表現量的差異來篩選基因外，我們將用 siRNA 的系統檢視這些基因是否影響正常細胞的功能或者能抑制癌細胞的生長。

9.檢討與展望

本實驗室下個年度的重點在於利用功能分析(functional analysis)來進一步篩選基因，並致力於個別基因的研究。

伍、九十一年度計畫所培訓之研究人員

註：群體計畫(PPG)者，不論是否提出各子計畫資料，都必須提出總計畫整合之資料
若爲群體計畫，請勾選本表屬於: □子計畫； 或 □總計畫(請自行整合)

種類			人數	備註
專任人員	1. 博士後研究人員	訓練中		
		已結訓		
	2. 碩士級研究人員	訓練中	4	2 人爲碩士班二年級，2 人爲碩士班一年級
		已結訓		
	3. 學士級研究人員	訓練中		
		已結訓		
	4. 其他	訓練中		
		已結訓		
兼任人員	1. 博士班研究生	訓練中		
		已結訓		
	2. 碩士班研究生	訓練中		
		已結訓		
醫師		訓練中		
		已結訓		
特殊訓練課程				

註： 1.特殊訓練課程請於備註欄說明所訓練課程名稱

2.本表如不敷使用，請自行影印

陸、參與九十一年度計畫所有人力之職級分析

註：群體計畫(PPG)者，不論是否提出各子計畫資料，都必須提出總計畫整合之資料
若爲群體計畫，請勾選本表屬於: □子計畫； 或 □總計畫(請自行整合)

職級	所含職級類別	參與人次
第一級	研究員、教授、主治醫師	1 人
第二級	副研究員、副教授、總醫師	人
第三級	助理研究員、講師、住院醫師	人
第四級	研究助理、助教、實習醫師	人
第五級	技術人員	人
第六級	支援人員	人
合計		人

〔註〕

第一級：研究員、教授、主治醫師、簡任技正，若非以上職稱則相當於博士滿三年、碩士滿六年、或學士滿九年之研究經驗者。

第二級：副研究員、副教授、助研究員、助教授、總醫師、薦任技正，若非以上職稱則相當於博士、碩士滿三年、學士滿六年以上之研究經驗者。

第三級：助理研究員、講師、住院醫師、技士，若非以上職稱則相當於碩士、或學士滿三年以上之研究經驗者。

第四級：研究助理、助教、實習醫師，若非以上職稱則相當於學士、或專科滿三年以上之研究經驗者。

第五級：指目前在研究人員之監督下從事與研究發展有關之技術性工作，且具備下列資格之一者屬之：具初（國）中、高中（職）、大專以上畢業者，或專科畢業目前從事研究發展，經驗未滿三年者。

第六級：指在研究發展執行部門參與研究發展有關之事務性及雜項工作者，如人事，會計、秘書、事務人員及維修、機電人員等。

柒、參與九十一年度計畫所有人力之學歷分析

註：群體計畫(PPG)者，不論是否提出各子計畫資料，都必須提出總計畫整合之資料
若爲群體計畫，請勾選本表屬於: □子計畫； 或 □總計畫(請自行整合)

類別	學歷別	參與人次
1	博士	1 人
2	碩士	人
3	學士	人
4	專科	人
5	博士班研究生	人
6	碩士班研究生	4 人
7	其他	人
合計		人

捌、參與九十一年度計畫之所有協同合作之研究室

群體計畫(PPG)者，不論是否提出各子計畫資料，都必須提出總計畫整合之資料
若爲群體計畫，請勾選本表屬於: □子計畫 □總計畫(請自行整合)

機構	研究室名稱	研究室負責人

玖、九十一年度之著作抽印本或手稿

依「貳、九十一年度計畫著作一覽表」所列順序附上文獻抽印本或手稿。

Molecular Vision 2002; 8:251-8 <http://www.molvis.org/molvis/v8/a32>
Received 29 November 2001 | Accepted 9 July 2002 | Published 16 July 2002

Identification of novel bovine RPE and retinal genes by subtractive hybridization

Shiwani Sharma,[1] Jinghua T. Chang,[2] Neil G. Della,[1] Peter A. Campochiaro,[2,3] Donald J. Zack[2,3,4]

(The first three authors contributed equally to this publication)

[1]Department of Ophthalmology, Flinders University, Bedford Park, South Australia, Australia; Departments of [2]Ophthalmology, [3]Neuroscience, and [4]Molecular Biology and Genetics, The John Hopkins University School of Medicine, Baltimore, MD

Purpose: Understanding of the specialized function of the retinal pigment epithelium (RPE) can be aided by the identification and characterization of genes that are preferentially expressed in the RPE. With this aim, we undertook a systematic effort to identify and begin characterization of such genes.

Methods: A subtracted bovine RPE cDNA library was generated through subtractive hybridization using a single-stranded circular bovine RPE cDNA library as target and biotinylated mRNA from bovine heart and liver as alternate drivers. Approximately one thousand of the resulting subtracted cDNA clones were partially sequenced and analyzed, and a non-redundant set of one hundred of these cDNAs were examined for tissue expression pattern using a mini-Northern blot procedure and for identity by sequence analysis.

Results: The subtraction method successfully allowed the enrichment of cDNAs that are preferentially expressed in the RPE. Out of the analyzed clones, expression of forty-five clones was verifiable by Northern blotting. Of these, a significant proportion of cDNAs were preferentially expressed in the RPE. We observed that the expression of some subtracted cDNAs was restricted to the retina and no expression was detected in the RPE. These retinal clones were obtained in addition to RPE clones presumably because the initial RPE RNA population was contaminated with a small proportion of retinal RNA. Two thirds of the identified RPE and retinal cDNAs are likely to represent novel genes because they do not have homology to known genes in the databases.

Conclusions: Genes that are specifically or predominantly expressed in the RPE/retina are likely to be important for retinal function. We have identified novel cDNAs from bovine RPE and retina by subtractive hybridization. These cDNAs can be used as starting material for the identification of corresponding human genes expressed in the RPE and retina. The human genes thus identified are likely to contain good candidate genes for retinal disease.

The retina and RPE, well-defined structures in the eye, perform highly specialized functions. These functions require the involvement of a number of highly specialized genes that are likely to be preferentially expressed in the retina and RPE. The identification of such genes is pivotal in understanding the molecular basis of structure and function in the retina and RPE, and is likely to provide good candidate genes for the study of retinal disease genetics. Screening methods such as subtractive-, differential-, or suppression subtractive-hybridization have been employed for the identification of retina-specific genes [1-5]. A number of retinal genes such as *NRL*, *AOC2*, HRG4, *mrdgB* and CRB1 have been identified using these methods [5-9].

Earlier studies reporting the identification of RPE-specific genes involved the generation of subtracted cDNA libraries from human RPE-cell line [10] or human RPE and choroid [3]. As only a limited amount of RPE is recovered from a human eye, this restricts the use of subtractive hybridization approach for the identification of RPE-specific human genes. To overcome this problem, we constructed a subtracted cDNA library from bovine RPE. Bovine eyes were used because of their ready availability for mRNA extraction. In this paper, we report the use of a modified subtractive hybridization method for efficient generation of a subtracted bovine RPE cDNA library. We also present the expression and sequence analyses data for a set of hundred subtracted bovine cDNA clones obtained from this library. This subtractive hybridization strategy allowed us to identify a number of novel bovine genes that are predominantly expressed in the RPE and are potentially important in the function and dysfunction of the retina.

Correspondence to: Dr. Shiwani Sharma, Department of Ophthalmology, Flinders Medical Centre, Flinders Drive, Bedford Park, SA 5042, Australia; Phone: 61 08 8204 5892; FAX: 61 08 8277 0899; email: shiwani.sharma@flinders.edu.au

METHODS

Generation of single-stranded (ss) circular bovine RPE cDNA library: A unidirectional bovine RPE cDNA library with $5x10^6$ independent phages was constructed in Uni-ZAP XR vector (Stratagene, La Jolla, CA). The library was amplified once to attain the titre of $5x10^{10}$ pfu/ml. To generate ss circular cDNA, the library was excised in vivo with ExAssist helper phage (Stratagene) following the manufacturer's instructions with some modifications. The phage particles were precipitated with 30% PEG/1.6 M NaCl at 4 °C overnight. The residual bacterial cells were removed by repeated centrifugation. The resulting phage preparation was treated with 200 μg DNase I at

37 °C for 30 min to digest any double-stranded (ds) DNA. The ss phagemid DNA was isolated by phenol/ chloroform extraction of phage particles followed by chloroform extraction and subsequent ethanol precipitation. The ss DNA pellet was resuspended in TE buffer, pH 7.6.

Isolation and biotinylation of driver mRNA: Total RNA was extracted from bovine heart and liver by the guanidinium/ acid phenol extraction method [11]. The poly-A^+ RNA was isolated by passing total RNA through a poly-dT cellulose column (Gibco BRL, Life Technologies) and purifying according to the manufacturer's protocol. The recovery of poly-A^+ RNA after two rounds of purification was about 1.9% of the starting total RNA.

For biotinylation, 50 µg of driver mRNA was mixed with 50 µl of photobiotin (long arm, SP-1020, Vector Laboratories). The solution was irradiated for 20 min in an ice bath with the tube cap open and at a distance of 10 cm from a sunlamp (150 W, Flood). The reaction was stopped with a final concentration of 100 mM Tris-HCl pH 9.0. The unbound biotin was removed by extraction with water-saturated isobutanol four to seven times or until the organic phase was colourless. The biotinylated mRNA was then extracted with chloroform to remove isobutanol, and precipitated with ethanol. The biotinylation and ethanol precipitation were repeated and biotinylated driver mRNA was finally resuspended in 50 µl H_2O.

Subtractive hybridization and transformation: The ss RPE cDNA library was subjected to four rounds of hybridization with biotinylated heart or liver mRNA as alternate drivers. Typically, 2 ng of ss circular library cDNA containing $>1x10^7$ phagemids was mixed with 5 µg of biotinylated driver mRNA and ethanol precipitated. The cDNA/RNA pellet was dissolved in 5 µl H_2O and following addition of an equal volume of 2X hybridization buffer (100 mM HEPES pH 7.6, 500 mM NaCl, 4 mM EDTA, 80% formamide), the solution was covered with mineral oil and heated at 95 °C for 5 min. Hybridization was carried out at 52 °C for 24 h. After hybridization, mineral oil was removed and 40 µl of 1X hybridization buffer was added to the reaction mix. To separate the hybridized and unhybridized biotinylated mRNAs, 10 µl of streptavidin (SA5000, Vector Laboratories) was added to the hybridization reaction and incubated at room temperature for 10 min with frequent mixing. After phenol/ chloroform extraction, the organic phase was again extracted with 50 µl of 1X hybridization buffer and the two aqueous phases were pooled. The streptavidin extraction was repeated twice again by adding 10 µl of streptavidin each time. After two rounds of chloroform extraction, 5 µg of another lot of biotinylated driver mRNA was added to the solution and ethanol precipitated. The hybridization procedure was repeated four times using heart and liver biotinylated mRNAs as alternate drivers.

After the last round of phenol/chloroform extraction, subtracted ss circular cDNA was ethanol precipitated and resuspended in 20µl H_2O. The ss circular cDNA was electroporated into electrocompetent MC1061 strain of *E. coli* and plated onto LB agar plates suplemented with ampicillin, X-gal and IPTG. About 1000 transformants/µl of ss circular cDNA were recovered. The blue/white selection of β-galactosidase expression was used to differentiate between recombinant and non-recombinant colonies.

Sequencing and sequence analysis: The sequencing reactions were performed with the fluorescence-labelled dideoxynucleotide (Prism, Applied Biosystems) using M13 (-20) and M13 reverse primers, and analysed on an ABI model 3700 Version 3.6 automated sequencer (Applied Biosystems). Sequences were analysed at the NCBI (National Center for Biotechnology Information) against the non-redundant nucleotide (nr), protein (Swissprot), human Expressed Sequence Tag (hEST) and human genome sequence (htgs) databases using the Basic Local Alignment Search Tool (BLAST).

Northern blot analysis: Northern blot analyses were performed on mini-Northern blots with RNA from bovine retina, RPE, kidney/muscle, heart/liver and brain. The total RNA from each tissue was extracted using the RNAzol B reagent (Tel-Test, Inc. TX, USA). The RNA from kidney and muscle and from heart and liver were pooled prior to Northern blotting. Each RNA sample (7 µg) was size fractionated on a 1% formaldehyde-agarose gel, and transferred and immobilised onto Hybond XL membrane (Amersham Pharmacia Biotech). Multiple mini-Northern blots were simultaneously prepared in this manner. Each blot was hybridized in 3 ml hybridization solution (6X SSC, 5X Denhardt's solution, 1% SDS, 50% deionised formamide) at 42 °C for 18-20 h. Up to ten blots were hybridized with ten different probes at a time. Radiolabelled probes were prepared in a 20 µl reaction volume using the Megaprime DNA labelling kit (Amersham Pharmacia Biotech). Blots were washed in 2X SSC, 0.1%SDS and 0.2X SSC, 0.1%SDS at 42 °C. An additional wash in 0.2X SSC, 0.1%SDS at 65 °C was performed if required. The hybridized blots were exposed overnight on a PhosphorImager screen and scanned using the ImageQuant software (Molecular Dynamics).

RESULTS & DISCUSSION

Generation of subtracted bovine RPE cDNA library: We generated a subtracted bovine RPE cDNA library to identify genes specifically or predominantly expressed in mammalian RPE. Subtraction was performed between a ss circular bovine RPE cDNA library and biotinylated mRNA from bovine heart and liver. The heart and liver were chosen as driver tissues for subtraction as they are developmentally different from the posterior of the eye where RPE resides. This subtraction was expected to allow the enrichment of genes expressed in RPE, a tissue of neural origin. The subtraction method required only 2 ng of ss circular RPE cDNA library as a starting material, allowing the use of more than 1000-fold molar excess of driver mRNA to target cDNA, which helped in obtaining efficient subtraction. The subtracted ss circular library cDNA was electroporated into MC1061 *E. coli* cells without converting into ds DNA. Rubenstein et al. [12] reported about 100 to 1000 fold higher transformation efficiency of ds DNA as compared to ss DNA, depending upon the amount of DNA used for transformation, however, we found only 2-3 fold difference in the transformation efficiency between ds and ss DNA (data not shown).

Following the initial partial sequencing of approximately 1,000 subtracted bovine cDNA clones, a set of one hundred non-redundant clones was chosen for further analysis. Upon sequence analysis (which was initially done in 1999), two clones were found in duplicate and seven clones matched to known mammalian gene sequences. Out of these seven, one bovine clone was homologous to mammalian Stra6, expressed at the blood-organ barriers including the RPE [13]. Another cDNA clone was a variant of bovine rhodopsin [14]. Three cDNAs were homologous to genes of neuronal origin, including the human photoreceptor-specific nuclear receptor PNR [15], DRES9 expressed in the neural retinal and central nervous system [16], and DnaJ expressed in human brain [17]. Two bovine clones corresponded to housekeeping genes. Homology of the subtracted bovine cDNAs to Stra6 and neuronal genes indicates that the subtractive hybridization method allowed the enrichment of genes expressed in tissues of neural origin. After excluding the duplicate clones and those homologous to known genes, subsequent investigation was carried out on ninety-one subtracted clones.

Expression analysis: The expression of ninety-one subtracted bovine cDNAs was analyzed by mini-Northern blotting on total RNA from bovine retina, RPE, kidney/muscle, heart/liver and brain. The heart/liver RNA was included on the Northern blots to determine the efficiency of the subtraction protocol. Expression in kidney/muscle RNA would represent any non-ocular expression of the subtracted cDNAs. Northern blot analysis revealed the tissue distribution of fifty percent of the cDNA clones. Expression of half of the subtracted cDNAs was undetectable under the Northern hybridization conditions used in this study suggesting possibly a very low level of expression of their respective transcripts. North-

Table 1. Summary of the expression patterns of subtracted bovine cDNAs

Expression pattern	Number of clones
RPE	11
RPE and retina	11
RPE, retina and brain	2
RPE and kidney/muscle	1
RPE, retina and kidney/muscle	1
All tissues tested but high in RPE	1
All tissues tested but high in RPE and retina	2
Retina	13
Retina and brain	3
Total	45

Expression of the subtracted bovine cDNAs was analysed in bovine retinal, RPE, kidney/muscle, heart/liver and brain tissues by Northern blot analysis. The table shows the various expression patterns observed and the number of clones exhibiting each expression pattern.

Table 2. Subtracted bovine cDNAs homologous to known mammalian genes

Clone name	Expression in this study	Homology to known gene	Species	Reference
Homology to bovine genes:				
S779	Retina	Guanine nucleotide binding protein, gamma subunit in cones	Bovine	[18]
S810, S1932	RPE	SFRP5	Bovine	[20]
S774	RPE	RGR	Bovine	[21]
S1934, S2066	Retina, RPE	RGR	Bovine	[21]
S2084	Retina, RPE	Retinal cyclic GMP phosphodiesterase gamma-subunit	Bovine	[19]
Homology to retinal disease genes:				
S709	Retina, RPE	PHR1	Human, mouse	[24]
S1926	Retina, RPE	NRL	Human	[6]
S2077	Retina, RPE	HRG4, RRG4	Human, rat	[7]
Homology to other genes				
S727	RPE	Stra6	Mouse	[12]
S743	Retina, RPE	WDR6	Human	[41]
S751	Retina, brain	TTYH1	Human	[30]
S766	Retina, brain	40S ribosomal protein S13	Human	
S905	All tissues tested	Glyoxalase 1	Human	[26]
S1631	All tissues tested	SH3PX1	Human	
S1929	Retina, RPE	ACP33	Human	[28]
S1944	Retina, RPE, kidney/muscle	Cytochrome b5 reductase 1	Human, bovine	[42,43]
S1947	RPE	Melastatin	Mouse, human	[44]

BLAST analysis was performed for each cDNA query sequence against the non-redundant nucleotide, protein, human EST and human genomic sequence databases. The Northern blot and BLAST analyses results are tabulated.

em blot analysis of poly-A$^+$ RNA may reveal the transcripts and tissue distribution of these cDNAs. Out of the 45 bovine cDNAs, whose expression was detected on Northern blots, 29 were expressed in the RPE (Table 1). Of these 29 cDNAs, 11 were specifically expressed in the bovine RPE and another 11 were expressed in both RPE and retina. Two cDNAs were expressed in the retina and brain in addition to RPE, and five cDNAs had expression in one or more non-ocular tissues besides RPE. The RPE expression of approximately two thirds of the cDNA clones demonstrates that the subtractive hybridization method employed in this study successfully enabled the enrichment of genes expressed in the bovine RPE. Only three out of 45 clones were expressed in heart/liver, the driver tissues used for subtraction, further supporting the validity of the subtraction method. Sixteen of the 45 cDNAs had no RPE expression but were instead expressed in the retina. The expression of thirteen of these 16 clones was restricted to the retina and three clones were expressed in the retina as well as brain. The identification of these cDNAs indicated that the starting "RPE" RNA population was contaminated with a small proportion of retinal RNA. As bovine retina is strongly adherent to the RPE, it is difficult to completely dissect the retina away from the underlying RPE. Hence, while removing the retina from the eye-cup, some photoreceptor outer segments and probably cells remain attached to the eye-cup and thus are inadvertently collected along with the RPE cells. Obtaining retinal genes during this study in fact worked to our advantage. In addition to identifying RPE expressed genes, we also identified some potentially interesting genes that are predominantly expressed in the bovine retina.

Sequence analysis: Additional sequence data were obtained for the 45 clones whose tissue distribution was detected by Northern analysis. The BLAST analyses for these cDNAs were repeated against the nucleotide, protein, human EST and human genome sequence databases at NCBI in 2000 and 2001. The additional sequence information of these clones revealed that two clones were present in duplicate. Nineteen of the remaining 43 clones had significant homology to known mammalian genes whereas 24 subtracted clones did not match to any known genes in the database.

Out of the nineteen clones with homology to known mammalian genes, seven corresponded to known bovine RPE/retinal genes (Table 2). The cDNAs S779 and S2084 represented bovine genes involved in the phototransduction process [18,19]. The clones S810 and S1932 corresponded to different regions of the RPE-specific gene *SFRP5* that was previ-

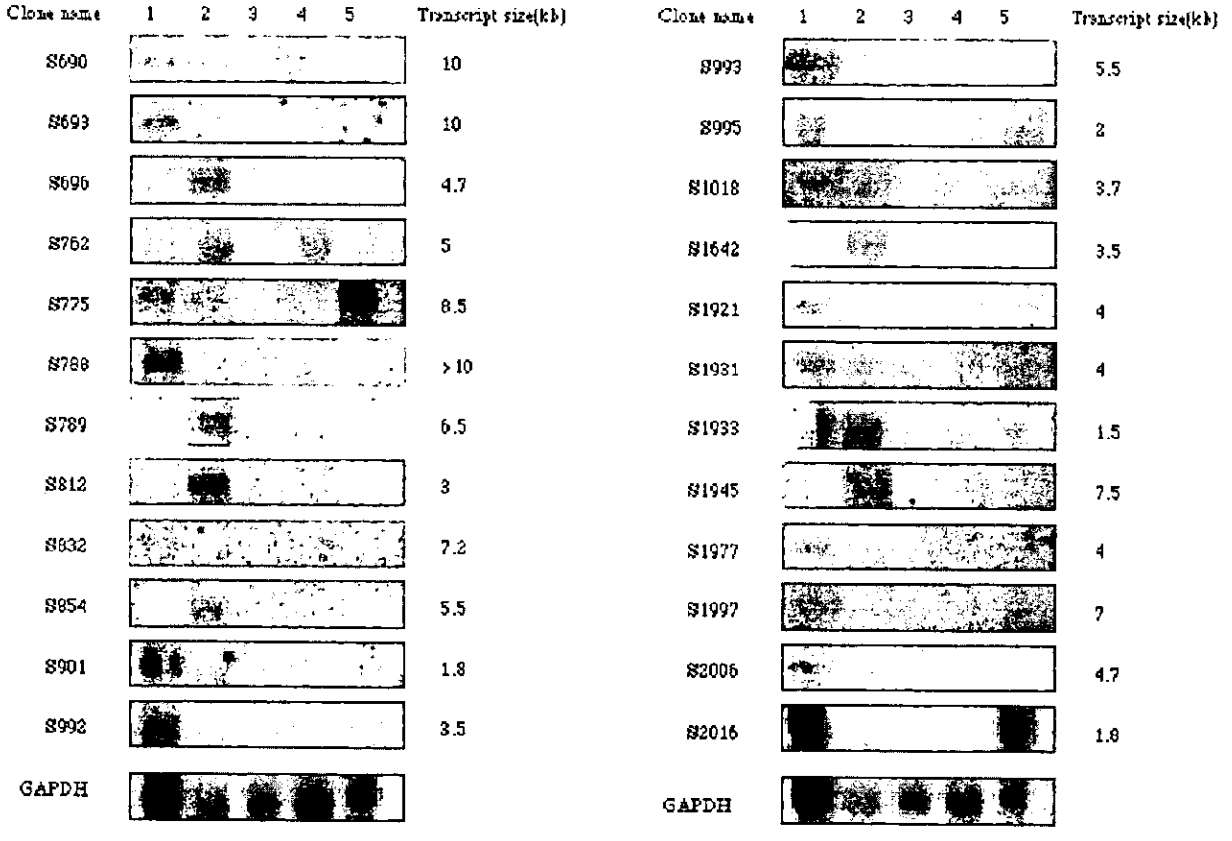

Figure 1. Northern blot analysis of total RNA from ocular and non-ocular bovine tissues. Seven µg each of retinal (lane 1), RPE (lane 2), heart/liver (lane 3), kidney/muscle (lane 4), and brain (lane 5) RNA were probed with each radiolabelled subtracted bovine cDNA. The cDNAs used as probes and the detected transcript sizes are shown. GAPDH=Glyceraldehyde-phosphate dehydrogenase.

ously isolated from this subtracted library [20]. S774, S1934 and S2066 were homologues of the bovine RPE-retinal G protein coupled receptor RGR [21]. In the present study, S774 detected a 3.4 kb transcript in the RPE, whereas S1934 and S2066 hybridized to a 1.5 kb transcript in both the RPE and retina. These results are consistent with the reported RGR expression in the bovine RPE and retina [21]. RGR binds to all-*trans*-retinal and is involved in the formation of 11-*cis*-retinal in mice [22]. Mutations in the human gene encoding RGR have been associated with retinitis pigmentosa [23]. Identification of RGR from the subtracted bovine library is encouraging as it means that the subtracted clones can be a useful resource for the identification of novel genes important for retinal function and in retinal disease. Three bovine cDNAs were orthologues of the human retinal genes, *PHR1* [24], *NRL* [6] and HRG4 [7], respectively. Mutations in the photoreceptor-specific genes *NRL* and HRG4 lead to autosomal dominant retinitis pigmentosa and dominant cone-rod dystrophy, respectively [25,26]. Their homology to known human retinal disease genes reiterates that the subtracted bovine cDNAs can be a valuable starting material for the identification of novel retinal disease genes, found as orthologues of the bovine RPE/retinal cDNAs. The transcript sizes of the bovine orthologues of *PHR1*, *NRL* and HRG4 corresponded to the transcripts encoded by these genes in the human retina (data not shown).. However, as opposed to the retinal expression reported for the human genes [6,7,24], the bovine orthologues were expressed in both the bovine retina and RPE. "Expression" of these genes in the bovine RPE is most likely due to a retinal contamination in the RPE, although the possibility of species-specific difference in RPE expression cannot be excluded.

Table 3. Novel bovine cDNAs expressed in the bovine RPE/retina

Bovine clone	GenBank Accession number	Database homology	Human UniGene identifier
S690	AF451165		
S693	AF451166		
S696	AF451167	DKFZp586B0621	Hs.157211
S762	AF451168	KIAA1522	Hs.322735
S775	AF451169		
S788	AF451170	RP4-791K14*	
S789	AF451171		
S812	AF451172	AdRab-G, FJ30107	Hs.343553
S832	AF451173	KIAA1157	Hs.21894
S854	AF451174		
S901	AF451175		
S992	AF451176		
S993	AF451177		
S995	AF451178		
S1018	AF451179		
S1642	AF451180		
S1921	AF451181		
S1931	AF451183		
S1933	AF451184		
S1945	AF451185	RP1 163G9*	
S1977	AF451186		
S1997	AF451187	KIAA0562	Hs.200595
S2006	AF451188	FLJ10018	Hs.322045
S2016	AF451189		

*Human BAC (Bacterial artificial chromosome) clone

For each cDNA the GenBank accession number, any homology to uncharacterised human sequences and the corresponding Unigene identification are listed.

Nine of the nineteen clones were orthologues of known mammalian genes originally cloned from non-ocular tissues (Table 2). The knowledge about the function of these genes in non-ocular tissues combined with the present finding of their expression in the RPE/retina can be extremely useful in elucidating the biochemical pathways involved in retinal function and dysfunction. For example, the bovine cDNA S905, expressed in the retina and RPE in this study was an orthologue of the human Glyoxalase 1 (*Glo 1*) [27], a gene ubiquitously expressed in human tissues. We have detected *Glo 1* expression in the human retina and RPE (S Sharma, unpublished data). *Glo 1* is involved in detoxification of methylglyoxal, a by-product of the cellular glycolytic pathway [28]. This may imply that dysfunction of *Glo 1* in the human retina/RPE might lead to accumulation of methylglyoxal in these tissues and compromise retinal function. The bovine S1929 was an orthologue of ACP33, a CD4 interacting protein that inhibits CD4 function in T cells [29]. ACP33 is widely expressed in human tissues [29], and its bovine orthologue was expressed in the bovine RPE and retina in the present study. The RPE cells do not express CD4 [30], however, the expression of ACP33 in bovine RPE suggests that it may interact with other proteins in the RPE. Another cDNA expressed in the bovine retina and brain in our study was an orthologue of *TTYH1* cloned from human brain [31]. TTYH1 is a transmembrane protein and has structural similarity to yeast iron-transporter proteins [31]. The putative function of TTYH1 as a transporter and retinal expression of its bovine orthologue warrants investigation of its expression in the human retina.

Novel genes expressed in bovine RPE/retina: Twenty-four bovine clones expressed in the RPE and/or retina (Figure 1) did not have significant homology with known gene sequences in the databases and therefore appear to be novel. The sequences of these novel cDNAs have been submitted to the GenBank (NCBI) and their GenBank accession numbers are listed in Table 3. Although these cDNAs had no homology to "known genes," some bovine cDNAs exhibited significant homology to uncharacterised human cDNAs or to human genomic sequences in the database (Table 3) suggesting that latter are the human orthologues of the bovine clones. A number of bovine genes expressed in the retina or RPE have led to the identification of important human retinal and RPE genes such as rhodopsin and RPE65 [32,33]. Mutations in the genes encoding the human rhodopsin and RPE65 lead to degenerative retinal disease [34]. We anticipate that the human orthologues of the subtracted bovine cDNAs would be expressed in the human RPE and/or retina similar to their bovine counterparts and represent novel RPE/retinal genes and potential candidates for retinal disease.

S696, expressed in the bovine RPE (Figure 1), showed significant sequence identity to a human cDNA present in the UniGene cluster Hs.157211 that is mapped at 11q23.3. The human cDNA exhibits some similarity to human complement-C1q tumor necrosis factor related protein 5 [35]. Several inherited retinal dystrophies have been mapped to chromosome

11, however, the human orthologue of S696 does not map to a disease locus on this chromosome and is therefore unlikely to be a retinal disease candidate. The Hs.157211 is constituted by ESTs from various human tissues including RPE and brain, indicating that besides its expression in non-ocular tissues, the gene represented by this cluster is also expressed in neural tissues. Bovine cDNAs S788 and S1945 expressed in the retina and RPE, respectively (Figure 1), had significant sequence similarity with regions of human bacterial chromosome (BAC) clones (Table 3). This nucleotide homology suggests the existence of human orthologues of S788 and S1945, which are expected to express in the human retina and RPE, respectively. S812 expressed in the bovine RPE (Figure 1) had significant nucleotide and amino acid similarity to an uncharacterised hypothetical protein AdRab-G identified from rabbit intestine [36]. It was also homologous to human ESTs from neuroglioma and retinoblastoma cell lines. Likewise, S762, S832, S1997, and S2006 exhibited homologies to uncharacterized cDNAs from human brain. These homologies indicate that the human orthologues of these bovine clones are expressed in neuronal tissues and are likely to be expressed in human RPE/retina. However, the Unigene clusters consisting of these uncharacterized human cDNAs also include ESTs from non-ocular tissues. Though we observed predominant expression of S762, S812, S832, S1997, and S2006 in the bovine RPE/retinal, their human orthologues may be more widely expressed in human tissues. This does not preclude these genes from being potentially important in retinal function, as widely expressed genes can be vital for normal retinal function. For example, mutations in TIMP-3, a widely expressed human gene, lead to Sorsby's fundus dystrophy that is characterised by accumulation of lipid deposits in Bruch's membrane beneath RPE and sub-retinal neovascularisation [37,38]. Thus, investigation of the expression and function of the human orthologues of bovine RPE/retinal genes identified in this study is likely to yield potentially important genes in these tissues.

Sixteen bovine cDNAs did not have any significant match in the databases at NCBI. The reason for not identifying the human orthologues of these bovine cDNAs can be absence of ESTs from human orthologues of bovine cDNAs in the database. Furthermore, some subtracted bovine cDNAs may include the 3'-untranslated region of the gene and not the coding region that is more likely to be conserved between bovine and human and thus likely to reveal the human orthologue. Additional sequence information of these bovine cDNAs will facilitate the identification of their respective potentially novel human orthologues.

In conclusion, all the subtracted bovine cDNAs whose expression was detectable by Northern blotting were expressed in the RPE and/or retina, demonstrating the efficacy of the subtraction method. The homology searches revealed the human orthologues of about twenty percent of these bovine clones, present as uncharacterised cDNAs in the database. Approximately forty percent of bovine cDNAs represent novel genes. These bovine cDNAs predominantly expressed in the RPE/retina will serve as a valuable resource for the identification of their human counterparts, likely to be expressed in the RPE or retina. Earlier, the RPE-specific genes *SFRP5*, *BMP-4* and *Kir7.1* were cloned from this subtracted library [19,39,40]. The possibility of detecting human RPE/retinal genes as orthologues of subtracted bovine RPE/retinal cDNAs extends a useful strategy for identifying novel genes as well as candidates for retinal disease without using human RPE/retina as the starting material.

ACKNOWLEDGEMENTS

This work is dedicated in memory of Neil Della, M.D., Ph.D., dear friend, brilliant scientist, and wonderful colleague. The work was supported by the Foundation Fighting Blindness, National Eye Institute (NIH, USA), unrestricted funds from Research to Prevent Blindness, Inc., National Health and Medical Research Council (Australia; Project grant ID: 991335), Viertel Foundation (Australia), Ophthalmic Research Institute of Australia and Flinders Medical Centre Foundation (Adelaide, Australia). PAC is the George S. and Dolores Dore Eccles Professor of Ophthalmology. DJZ is the Guerrieri Professor of Genetic Engineering and Molecular Ophthalmology. A part of this data was presented at the Australasian Ophthalmic and Vision Science Meeting 1999, Canberra, Australia.

REFERENCES

1. Swaroop A, Xu JZ, Agarwal N, Weissman SM. A simple and efficient cDNA library subtraction procedure: isolation of human retina-specific cDNA clones. Nucleic Acids Res 1991; 19:1954.
2. Swanson DA, Freund CL, Steel JM, Xu S, Ploder L, McInnes RR, Valle D. A differential hybridization scheme to identify photoreceptor-specific genes. Genome Res 1997; 7:513-21.
3. den Hollander AI, van Driel MA, de Kok YJ, van de Pol DJ, Hoyng CB, Brunner HG, Deutman AF, Cremers FP. Isolation and mapping of novel candidate genes for retinal disorders using suppression subtractive hybridization. Genomics 1999; 58:240-9.
4. Sinha S, Sharma A, Agarwal N, Swaroop A, Yang-Feng TL. Expression profile and chromosomal location of cDNA clones, identified from an enriched adult retina library. Invest Ophthalmol Vis Sci 2000; 41:24-8.
5. Imamura Y, Kubota R, Wang Y, Asakawa S, Kudoh J, Mashima Y, Oguchi Y, Shimizu N. Human retina-specific amine oxidase (RAO): cDNA cloning, tissue expression, and chromosomal mapping. Genomics 1997; 40:277-83.
6. Swaroop A, Xu JZ, Pawar H, Jackson A, Skolnick C, Agarwal N. A conserved retina-specific gene encodes a basic motif/leucine zipper domain. Proc Natl Acad Sci U S A 1992; 89:266-70.
7. Higashide T, Murakami A, McLaren MJ, Inana G. Cloning of the cDNA for a novel photoreceptor protein. J Biol Chem 1996; 271:1797-804.
8. Chang JT, Milligan S, Li Y, Chew CE, Wiggs J, Copeland NG, Jenkins NA, Campochiaro PA, Hyde DR, Zack DJ. Mammalian homolog of Drosophila retinal degeneration B rescues the mutant fly phenotype. J Neurosci 1997; 17:5881-90.
9. den Hollander AI, ten Brink JB, de Kok YJ, van Soest S, van den Born LI, van Driel MA, van de Pol DJ, Payne AM, Bhattacharya SS, Kellner U, Hoyng CB, Westerveld A, Brunner HG, Bleeker-Wagemakers EM, Deutman AF, Heckenlively JR, Cremers FP, Bergen AA. Mutations in a human homologue of Drosophila crumbs cause retinitis pigmentosa (RP12). Nat Genet 1999; 23:217-21.

10. Gieser L, Swaroop A. Expressed sequence tags and chromosomal localization of cDNA clones from a subtracted retinal pigment epithelium library. Genomics 1992; 13:873-6.
11. Chomczynski P, inventor; Product and process for isolating RNA. US patent 4,843,155. 1989 Jun 27.
12. Rubenstein JL, Brice AE, Ciaranello RD, Denney D, Porteus MH, Usdin TB. Subtractive hybridization system using single-stranded phagemids with directional inserts. Nucleic Acids Res 1990; 18:4833-42.
13. Bouillet P, Sapin V, Chazaud C, Messaddeq N, Decimo D, Dolle P, Chambon P. Developmental expression pattern of Stra6, a retinoic acid-responsive gene encoding a new type of membrane protein. Mech Dev 1997; 63:173-86.
14. Kuo CH, Yamagata K, Moyzis RK, Bitensky MW, Miki N. Multiple opsin mRNA species in bovine retina. Brain Res 1986; 387:251-60.
15. Kobayashi M, Takezawa S, Hara K, Yu RT, Umesono Y, Agata K, Taniwaki M, Yasuda K, Umesono K. Identification of a photoreceptor cell-specific nuclear receptor. Proc Natl Acad Sci U S A 1999; 96:4814-9.
16. Rubboli F, Bulfone A, Bogni S, Marchitiello A, Zollo M, Borsani G, Ballabio A, Banfi S. A mammalian homologue of the Drosophila retinal degeneration B gene: implications for the evolution of phototransduction mechanisms. Genes Funct 1997; 1:205-13.
17. Cheetham ME, Brion JP, Anderton BH. Human homologues of the bacterial heat-shock protein DnaJ are preferentially expressed in neurons. Biochem J 1992; 284:469-76.
18. Ong OC, Yamane HK, Phan KB, Fong HK, Bok D, Lee RH, Fung BK. Molecular cloning and characterization of the G protein gamma subunit of cone photoreceptors. J Biol Chem 1995; 270:8495-500.
19. Ovchinnikov YuA, Lipkin VM, Kumarev VP, Gubanov VV, Khramtsov NV, Akhmedov NB, Zagranichny VE, Muradov KG. Cyclic GMP phosphodiesterase from cattle retina. Amino acid sequence of the gamma-subunit and nucleotide sequence of the corresponding cDNA. FEBS Lett 1986; 204:288-92.
20. Chang JT, Esumi N, Moore K, Li Y, Zhang S, Chew C, Goodman B, Rattner A, Moody S, Stetten G, Campochiaro PA, Zack DJ. Cloning and characterization of a secreted frizzled-related protein that is expressed by the retinal pigment epithelium. Hum Mol Genet 1999; 8:575-83.
21. Jiang M, Pandey S, Fong HK. An opsin homologue in the retina and pigment epithelium. Invest Ophthalmol Vis Sci 1993; 34:3669-78.
22. Chen P, Hao W, Rife L, Wang XP, Shen D, Chen J, Ogden T, Van Boemel GB, Wu L, Yang M, Fong HK. A photic visual cycle of rhodopsin regeneration is dependent on Rgr. Nat Genet 2001; 28:256-60.
23. Morimura H, Saindelle-Ribeaudeau F, Berson EL, Dryja TP. Mutations in RGR, encoding a light-sensitive opsin homologue, in patients with retinitis pigmentosa. Nat Genet 1999; 23:393-4.
24. Xu S, Ladak R, Swanson DA, Soltyk A, Sun H, Ploder L, Vidgen D, Duncan AM, Garami E, Valle D, McInnes RR. PHR1 encodes an abundant, pleckstrin homology domain-containing integral membrane protein in the photoreceptor outer segments. J Biol Chem 1999; 274:35676-85.
25. Bessant DA, Payne AM, Mitton KP, Wang QL, Swain PK, Plant C, Bird AC, Zack DJ, Swaroop A, Bhattacharya SS. A mutation in NRL is associated with autosomal dominant retinitis pigmentosa. Nat Genet 1999; 21:355-6.
26. Kobayashi A, Higashide T, Hamasaki D, Kubota S, Sakuma H, An W, Fujimaki T, McLaren MJ, Weleber RG, Inana G. HRG4 (UNC119) mutation found in cone-rod dystrophy causes retinal degeneration in a transgenic model. Invest Ophthalmol Vis Sci 2000; 41:3268-77.
27. Ranganathan S, Walsh ES, Godwin AK, Tew KD. Cloning and characterization of human colon glyoxalase-I. J Biol Chem 1993; 268:5661-7.
28. Thornalley PJ. The glyoxalase system: new developments towards functional characterization of a metabolic pathway fundamental to biological life. Biochem J 1990; 269:1-11.
29. Zeitlmann L, Sirim P, Kremmer E, Kolanus W. Cloning of ACP33 as a novel intracellular ligand of CD4. J Biol Chem 2001; 276:9123-32.
30. Canki M, Sparrow JR, Chao W, Potash MJ, Volsky DJ. Human immunodeficiency virus type 1 can infect human retinal pigment epithelial cells in culture and alter the ability of the cells to phagocytose rod outer segment membranes. AIDS Res Hum Retroviruses 2000; 16:453-63.
31. Campbell HD, Kamei M, Claudianos C, Woollatt E, Sutherland GR, Suzuki Y, Hida M, Sugano S, Young IG. Human and mouse homologues of the Drosophila melanogaster tweety (tty) gene: a novel gene family encoding predicted transmembrane proteins. Genomics 2000; 68:89-92.
32. Nathans J, Hogness DS. Isolation and nucleotide sequence of the gene encoding human rhodopsin. Proc Natl Acad Sci U S A 1984; 81:4851-5.
33. Nicoletti A, Wong DJ, Kawase K, Gibson LH, Yang-Feng TL, Richards JE, Thompson DA. Molecular characterization of the human gene encoding an abundant 61 kDa protein specific to the retinal pigment epithelium. Hum Mol Genet 1995; 4:641-9.
34. Rattner A, Sun H, Nathans J. Molecular genetics of human retinal disease. Annu Rev Genet 1999; 33:89-131.
35. Kishore U, Reid KB. C1q: Structure, function, and receptors. Immunopharmacology 2000; 49:159-70.
36. Boll W, Schmid-Chanda T, Semenza G, Mantei N. Messenger RNAs expressed in intestine of adult but not baby rabbits. Isolation of cognate cDNAs and characterization of a novel brush border protein with esterase and phospholipase activity. J Biol Chem 1993; 268:12901-11.
37. Apte SS, Mattei MG, Olsen BR. Cloning of the cDNA encoding human tissue inhibitor of metalloproteinases-3 (TIMP-3) and mapping of the TIMP3 gene to chromosome 22. Genomics 1994; 19:86-90.
38. Della NG, Campochiaro PA, Zack DJ. Localization of TIMP-3 mRNA expression to the retinal pigment epithelium. Invest Ophthalmol Vis Sci 1996; 37:1921-4.
39. Mathura JR Jr, Jafari N, Chang JT, Hackett SF, Wahlin KJ, Della NG, Okamoto N, Zack DJ, Campochiaro PA. Bone morphogenetic proteins-2 and -4: negative growth regulators in adult retinal pigmented epithelium. Invest Ophthalmol Vis Sci 2000; 41:592-600.
40. Shimura M, Yuan Y, Chang JT, Zhang S, Campochiaro PA, Zack DJ, Hughes BA. Expression and permeation properties of the K(+) channel Kir7.1 in the retinal pigment epithelium. J Physiol 2001; 531:329-46.
41. Li D, Burch P, Gonzalez O, Kashork CD, Shaffer LG, Bachinski LL, Roberts R. Molecular cloning, expression analysis, and chromosome mapping of WDR6, a novel human WD-repeat gene. Biochem Biophys Res Commun 2000; 274:117-23.
42. Zhu H, Qiu H, Yoon HW, Huang S, Bunn HF. Identification of a cytochrome b-type NAD(P)H oxidoreductase ubiquitously ex-

pressed in human cells. Proc Natl Acad Sci U S A 1999; 96:14742-7.

43. Strittmatter P, Kittler JM, Coghill JE, Ozols J. Characterization of lysyl residues of NADH-cytochrome b5 reductase implicated in charge-pairing with active-site carboxyl residues of cytochrome b5 by site-directed mutagenesis of an expression vector for the flavoprotein. J Biol Chem 1992; 267:2519-23.
44. Duncan LM, Deeds J, Hunter J, Shao J, Holmgren LM, Woolf EA, Tepper RI, Shyjan AW. Down-regulation of the novel gene melastatin correlates with potential for melanoma metastasis. Cancer Res 1998; 58:1515-20.

The print version of this article was created on 16 July 2002. This reflects all typographical corrections and errata to the article through that date. Details of any changes may be found in the online version of the article.

Genomics 72, 193–202 (2001)
doi:10.1006/geno.2000.6476, available online at http://www.idealibrary.com on IDEAL®

Cloning and Characterization of a Human β,β-Carotene-15, 15′-Dioxygenase That Is Highly Expressed in the Retinal Pigment Epithelium

Weiming Yan,* Geeng-Fu Jang,† Françoise Haeseleer,† Noriko Esumi,* Jinghua Chang,* Michelle Kerrigan,* Michael Campochiaro,* Peter Campochiaro,*·‡ Krzysztof Palczewski,†·§·¶ and Donald J. Zack*·‡·‖·[1]

*Department of Ophthalmology, ‡Department of Neuroscience, and ‖Department of Molecular Biology and Genetics, Johns Hopkins University School of Medicine, Baltimore, Maryland 21287; and †Department of Ophthalmology, §Department of Chemistry, and ¶Department of Pharmacology, University of Washington, Seattle, Washington 98195

Received October 5, 2000; accepted December 12, 2000; published online March 1, 2001

Retinoids play a critical role in vision, as well as in development and cellular differentiation. β,β-Carotene-15,15′-dioxygenase (Bcdo), the enzyme that catalyzes the oxidative cleavage of β,β-carotene into two retinal molecules, plays an important role in retinoid synthesis. We report here the first cloning of a mammalian *Bcdo*. Human *BCDO* encodes a protein of 547 amino acid residues that demonstrates 68% identity with chicken Bcdo. It is expressed highly in the retinal pigment epithelium (RPE) and also in kidney, intestine, liver, brain, stomach, and testis. The gene spans approximately 20 kb, is composed of 11 exons and 10 introns, and maps to chromosome 16q21–q23. A mouse orthologue was also identified, and its predicted amino acid sequence is 83% identical with human *BCDO*. Biochemical analysis of baculovirus expressed human BCDO demonstrates the predicted β,β-carotene-15,15′-dioxygenase activity. The expression pattern of *BCDO* suggests that it may provide a local supplement to the retinoids available to photoreceptors, as well as a supplement to the retinoid pools utilized elsewhere in the body. In addition, the finding that many of the enzymes involved in retinoid metabolism are mutated in retinal degenerations suggests that *BCDO* may also be a candidate gene for retinal degenerative disease. © 2001 Academic Press

INTRODUCTION

Vertebrate phototransduction, the process by which light energy is converted into a neurochemical signal, is carried out by photoreceptor cells within the retina (Koutalos and Yau, 1996; Lagnado and Baylor, 1992; Palczewski *et al.*, 2000; Polans *et al.*, 1996; Pugh *et al.*, 1999; Rattner *et al.*, 1999) and is supported by the underlying cells of the retinal pigment epithelium (RPE) (Bok, 1993). It is initiated when a visual pigment, rhodopsin in rods or one of the color pigments in cones, absorbs a photon of light. These pigments consist of an opsin apoprotein joined in a Schiff base linkage to the chromophore 11-*cis*-retinal. Upon photoisomerization of the 11-*cis*-retinylidine group to an all-*trans*-retinylidine group, the pigment undergoes a sequence of conformational changes. These changes eventually result in the activation of the retinal G-protein transducin, and amplification of the light signal. A hydrolysis step then leads to the release of free all-*trans*-retinal.

Regeneration of fresh rhodopsin from opsin requires a constant supply of 11-*cis*-retinal. The major mechanism for supplying photoreceptors with fresh chromophore, which is known as the visual cycle (or retinoid cycle), involves recycling from the released all-*trans*-retinal (Crouch *et al.*, 1996). Upon release from the binding pocket of rhodopsin, the potentially reactive all-*trans*-retinal is transported to the cytoplasm by a mechanism that is thought to involve a photoreceptor-specific ATP-binding cassette transporter (ABCR) (Ahn and Molday, 2000; Haeseleer *et al.*, 1998; Rattner *et al.*, 2000; Sun and Nathans, 1997, 2000; Weng *et al.*, 1999). It is then reduced to all-*trans*-retinol (Haeseleer *et al.*, 1998; Rattner *et al.*, 2000) and subsequently translocated to the RPE. Within the RPE, a putative retinol isomerase catalyzes the conversion of all-*trans*-retinol into 11-*cis*-retinol (Bernstein *et al.*, 1987; Deigner *et al.*, 1989; Winston and Rando, 1998). It has been suggested that the esterified form of all-*trans*-retinol serves as the immediate substrate for the putative isomerohydrolase (Canada *et al.*, 1990; Ruiz *et al.*, 1999; Trehan *et al.*, 1990), but this issue is controversial (McBee *et al.*, 2000; Stecher *et al.*, 1999). RPE65, a protein of unknown function that is prefer-

[1] To whom correspondence should be addressed at Johns Hopkins University School of Medicine, 809 Maumenee, 600 N. Wolfe Street, Baltimore, MD 21287. Telephone: (410) 502-5230. Fax: (410) 502-5382. E-mail: dzack@bs.jhmi.edu.

0888-7543/01 $35.00

entially expressed in the RPE (Hamel *et al.*, 1993; Nicoletti *et al.*, 1995), appears to be required for isomerization. RPE65 null mice accumulate all-*trans*-retinyl esters in their RPE cells and are deficient in 11-*cis*-retinal (Redmond *et al.*, 1998; Van Hooser *et al.*, 2000). Finally, 11-*cis*-retinol generated by the isomerase reaction is oxidized to 11-*cis*-retinal by 11-*cis*-RDH (Simon *et al.*, 1995) and other oxidizing systems (Driessen *et al.*, 2000; Jang *et al.*, 2000) and transported back to the photoreceptor cells.

A second complementary mechanism for providing retinoids involves their generation from dietary retinoids and retinoid precursors. Since animals cannot synthesize vitamin A (retinol) *de novo*, vitamin A and its derivatives are derived from the oxidative cleavage of C_{40} carotenoids. In one pathway, the enzyme β,β-carotene-15,15′-dioxygenase (EC 1.13.11.21; β,β-carotene dioxygenase; Bcdo) catalyzes the conversion of β,β-carotene into two molecules of all-*trans*-retinal. However, the biochemistry and molecular biology of this pathway and its biological importance in vertebrates are not well understood, partly due to difficulties in purifying and studying the enzyme(s) *in vitro*. In fact, it was only recently that cDNAs for vertebrate (chicken) and invertebrate (*Drosophila*) *Bcdo* were cloned (von Lintig and Vogt, 2000a; Wyss *et al.*, 2000). Of particular interest to the studies presented here is the recent finding that mutations in *Drosophila Bcdo* are responsible for the *ninaB* photoreceptor degeneration (von Lintig *et al.*, 2000b).

In the process of characterizing clones from a human RPE cDNA library that are preferentially expressed in the RPE, we identified a clone that shows homology with *RPE65* and also with chicken *Bcdo* and other retinoid dioxygenases. In this paper we present the initial molecular characterization of the murine and human cDNAs and the human *BCDO* gene, explore the expression pattern of the human gene, and demonstrate that human *BCDO* does indeed encode a protein with Bcdo activity, thus providing the first evidence for a cloned mammalian *Bcdo*. We also suggest that Bcdo in the RPE may play an important role in a local secondary pathway for the synthesis of all-*trans*-retinal, particularly under bright-light conditions where the normal visual cycle may be stressed.

MATERIALS AND METHODS

Cloning of the human BCDO gene. A human RPE cDNA library in Uni-ZAP XR (Stratagene) was *in vivo* excised, and 2000 random clones were grown on LB/ampicillin plates. Using a subtracted bovine RPE cDNA library as template (Chang *et al.*, 1997, 1999), polymerase chain reaction (PCR) products were generated with primers (W8, 5′-AGGAATTCGGCACGAGNN-3′ and W9, 5′-CGGGCCCCCCCTCGAGTT-3′) and labeled with [α-^{32}P]dCTP by random prime labeling. The labeled products were used as probes to screen the above-mentioned human RPE cDNA library, and selected clones were sequenced by standard methods (Thermo Sequenase Cycle Sequencing Kit, Amersham, Piscataway Pharmacia Biotech). BCDO 5′-RACE (Marathon-ready cDNA, Clontech) was conducted according to the manufacturer's instructions using the following primers: adaptor primer 1 (5′-CCATCCTAATACGACTCACTATAGGGC-3′); *BCDO* antisense primer 1 (W121, 5′-CGGGCACAAACAGGGGTTCC-3′; adaptor primer 2, 5′-ACTCACTATAGGGCTCGAGCGGC-3′); and *BCDO* antisense primer 2 (5′-ACCCGTGGAAGCTCTAAGCCTTCA-3′). Resulting PCR products were subcloned into the pCR2.1 vector using a TA cloning kit (Invitrogen) according to the manufacturer's direction and sequenced.

To obtain the gene structure of *BCDO*, RPCI-11 Human Male BAC library high-density filters (Segment 1, Bacpac Resource) were screened using a ^{32}P-labeled PCR fragment generated with the primers W131 (5′-AAAGGAGGTTTCTTAGAAGGACTG-3′) and W133 (5′-CAGCCATTGTCTCTACTGATCC-3′). Four clones containing the entire human *BCDO* gene were isolated, and intron/exon boundaries were determined by sequencing the BAC clones directly or PCR products generated using the BAC clones as templates.

A mouse orthologue was also identified by searching the EST database (National Center for Biotechnology Information) (Altschul *et al.*, 1990, 1997), and the EST clone was obtained and sequenced on both strands.

Northern blot hybridization. Total RNA from human RPE and neural retina was extracted from human donor eyes (Maryland Eye Bank) using Trizol reagent (Life Technologies); all other total RNA used was purchased from Clontech. Northern blots with 10 μg of total RNA from RPE, retina, liver, brain, and testis were prepared and hybridized by standard methods using either a PCR-generated PCR probe (primers W78, 5′-CCAGGACTTCAAGGAGAACTCCAG-3′, and W121) or a human β-actin probe. A human Multiple Tissue Northern blot (MTN) (Clontech), containing 2 μg poly(A)$^+$ RNA from a variety of tissues, was also hybridized with the same probes as previously described (Chang *et al.*, 1999).

Reverse transcription-PCR (RT-PCR) analysis. One microgram of total RNA was reverse transcribed with an oligo(dT) primer using SuperScript II reverse transcriptase (Life Technologies) according to the manufacturer's protocol. Aliquots of first-strand cDNA were PCR amplified using primers for human *BCDO* (W78 and W121) and for human glyceraldehyde phosphate dehydrogenase (GAPD) (W226 5′-GGGGGAGCCAAAAGGGTCAT-3′ and W227 5′-GCCCCAGCGTCAAAGGTGGA-3′) and then analyzed by agarose gel electrophoresis.

Chromosomal localization of the human BCDO gene. Radiation hybrid mapping of the human *BCDO* gene was carried out using the Stanford G3 panel and primers W131 and W133, following the supplier's instructions (Research Genetics). A Chinese hamster–human somatic cell hybrid panel was also analyzed with the same set of human *BCDO* primers as used for the G3 panel, according to the supplier's instructions (Coriell).

Primer extension. Primer W180 (5′-TTCCCTCCTTCACATCTCTG-3′) was labeled with [γ-^{32}P]ATP by T4 polynucleotide kinase. Ten micrograms of total human RPE RNA was denatured with 5 pmol of labeled primer at 80°C for 90 s and annealed at 50°C for 20 min. Primer extension was carried out with ThermoScript reverse transcriptase (Life Technologies) at 45°C for 15 min and then at 65°C for 60 min, and the resulting products were incubated with RNase A1/H at 37°C for 15 min, extracted with phenol/chloroform, ethanol precipitated, and separated on a 6% sequencing gel. The sequence ladder was created using the same primer (W180) with one of the human *BCDO* clones as template.

Generation of anti-BCDO polyclonal antibody. A rabbit polyclonal antibody against BCDO was generated by standard methods. The peptide RLTSVPTLRRFAVPLHVDK, corresponding to human *BCDO* codons 348–367, was synthesized, purified to greater than 90% by HPLC, and then conjugated to keyhole limpet hemocyanin (KLH) as carrier. Two rabbits were immunized with the KLH peptide. Hyperimmune serum was processed over an immunosorbent to capture antibodies specific for the peptide. The affinity-purified antibody was then titered by ELISA methods.

Immunoblot analysis of Bcdo protein expression. Bovine tissues were sonicated in buffer (50 mM sodium phosphate, pH 7.8, 300 mM NaCl, 1 μg/ml leupeptin, 1 μg/ml aprotinin, 0.1 mM PMSF) and

centrifuged at 14,000*g* for 30 min at 4°C to separate soluble and insoluble fractions. The protein concentration of the supernatant and pellet extracts was determined by the Bradford method (Bio-Rad Laboratories). Ten micrograms of protein from each set of extracts was electrophoresed on 4–15% gradient Bio-Rad Ready gels by standard methods. After electrophoresis, the gel was soaked in transfer buffer (25 mM Tris–HCl, 192 mM glycine, 20% methanol) and semi-dry transferred to a nitrocellulose membrane following the manufacturer's instructions (Bio-Rad Laboratories). The nitrocellulose membrane was fixed in methanol destain solution (25% methanol, 10% acetic acid) for 10 min at room temperature. After being blocked with 5% dry milk in 1× TBST (50 mM Tris–HCl, pH 7.4, 200 mM NaCl, 0.1% Tween 20) for 1 h at room temperature, the membrane was incubated overnight at 4°C with the rabbit polyclonal antibody against BCDO (1:8000) in 5% dry milk, washed four times with 1× TBST, and incubated with horseradish peroxidase-conjugated anti-rabbit antibody (1:2000) in 5% dry milk in 1× TBST for 1 h at room temperature. After washing, antibody binding was visualized using ECL plus reagent (Amersham Pharmacia Biotech).

Expression of human BCDO in insect cells. DNA containing the entire human *BCDO* coding region was amplified by PCR from a pBluescript *BCDO* cDNA containing plasmid using primers FH350 (5'-GCAATGGATATAATATTTGGCAGG-3') and FH351 (5'-CCATCAGGTCAGAGGAGCC-3') and 25 cycles at 94°C for 30 s, 60°C for 30 s, and 68°C for 2 min. The PCR product was cloned into the pCRII-TOPO vector (Invitrogen) and sequenced using the BigDye Terminator Cycle Sequencing Kit (Applied Biosystems). The coding region of human *BCDO* was then transferred as a *Bam*HI–*Xho*I fragment into the *Bam*HI–*Xho*I sites of pFASTBac (Life Technologies). A *BCDO* recombinant baculovirus was obtained by transposition in DH10BAC bacteria and amplified after transfection into Sf9 cells. The expression of recombinant proteins was tested 3 days postinfection.

Assay for BCDO activity. Sf9 cells containing either the *BCDO* recombinant baculovirus or the empty bacmid were solubilized with 0.1% Triton X-100 in 20 mM BTP (1,3-bis[tris(hydroxymethyl)-methylamino]propane) (pH 7.4) in a 1:9 ratio (cell pellet to buffer) at 0°C for 30 min. The solubilization mixture was then centrifuged at 98,600*g*, and the resulting supernatant was used to assay for BCDO activity. The unused supernatant was aliquoted and flash-frozen with liquid nitrogen without affecting the enzymatic activity. The assay mixture (100 μl) contained BTP (final concentration, 45–70 mM, pH 7.4), NaCl (33–65 mM), Triton X-100 (0.095%), $FeSO_4$ (10 μM), ascorbic acid (10 mM), the solubilized enzyme (33–132 μg protein), and 2 μl of β,β-carotene (40 μM) in *N,N'*-dimethylformamide, which was added last to initiate the reaction. The reaction was incubated at 37°C for various times and terminated with 300 μl of methanol and 200 μl of 0.4 M NH_2OH (pH 6.5, freshly prepared). The mixture was then placed on a mixer at room temperature for 30 min and extracted with 500 μl hexane. After mixing and separating phases, 400 μl of the upper phase was removed and dried using a Speedvac. The extraction was repeated once. The residue was dissolved in 120 μl hexane. One hundred microliters of the hexane solution was analyzed by normal-phase HPLC (Alltech, silica 5 μm, 2.1 × 250 mm) with 4% ethyl acetate/96% hexane at a flow rate of 0.5 ml/min using an HP1100 with a diode-array detector and HP Chemstation A.06.03 software. The (*syn*) all-*trans*-retinal oxime fraction (the major product) was collected and quantified for the β,β-carotene-15,15'-dioxygenase activity.

RESULTS

Cloning of a Human cDNA with Homology to Bcdo

To identify human cDNAs representing genes that are preferentially expressed in the RPE, a nonsubtracted human RPE cDNA library was screened with a PCR probe generated from a previously described subtracted bovine RPE cDNA library (Chang *et al.*, 1997, 1999). Among the multiple novel positive clones identified, the sequence of one showed 37% identity with human RPE65 at the deduced amino acid level. Based on the findings described below, we called this clone *BCDO*.

The open reading frame of the human *BCDO* cDNA encodes a predicted protein of 547 amino acids with a calculated molecular mass of 62 kDa. The predicted amino acid sequence shows 67% identity and 80% similarity with a recently published chicken Bcdo sequence (Wyss *et al.*, 2000) (Fig. 1). Homology between human and chicken *Bcdo* is distributed fairly equally throughout the entire protein, but human BCDO has an extra 20 amino acid residues at its carboxyl terminus. Recent analysis of GenBank entries identified both human and murine *Bcdo* EST clones (GenBank Accession Nos. AK001592 and AW107279, respectively). The open reading frame of the full-length murine EST clone, which we obtained and sequenced, encodes a protein of 566 amino acids that has 83 and 66% identity with the human and chicken clones, respectively (Fig. 1). Most of the sequence variation between the murine and the human clones is located at the carboxyl terminus. Overall, chicken Bcdo, murine Bcdo, and human BCDO appear to be orthologues of one another. A *Drosophila* β,β-carotene dioxygenase was also recently cloned (von Lintig and Vogt, 2000a). The amino acid homology between human BCDO and *Drosophila* Bcdo is 24%, while the homology between chicken Bcdo and *Drosophila* Bcdo is 31%.

The alignment of the BCDOs and human RPE65 shown in Fig. 1 reveals four areas of increased sequence conservation (labeled A–D). The homology of regions A and D is high and specific enough that database analysis using these regions with Blastp and an Expect (*E*) value of 1000 (Altschul *et al.*, 1990, 1997) yields significant matches only with dioxygenases and RPE65 homologues. Among the real and "hypothetical" dioxygenases that show homology to region A are proteins/genes from *Caenorhabditis elegans* (Accession Nos. CAB60367 and AAC67462), *Arabidopsis thaliana* (T10688), *Synechocystis* sp. (S76206 and S76169), and *Streptomyces coelicolor* (CAB56138). Since all these proteins presumably use iron cation as part of their oxidative mechanism, it is possible that region A or one of the other conserved sequences might be involved in iron cation binding.

Genomic Structure of the Human BCDO Gene

To explore its possible relationship to human disease, the gene structure and chromosomal localization of human *BCDO* were determined. Four BAC clones containing the entire human *BCDO* gene were identified by screening a set of high-density BAC filters. The exon/intron boundaries of human *BCDO* were determined by sequence comparison of the genomic and cDNA clones. *BCDO* spans approximately 20 kb and consists of 11 exons and 10 introns (Table 1). The exons

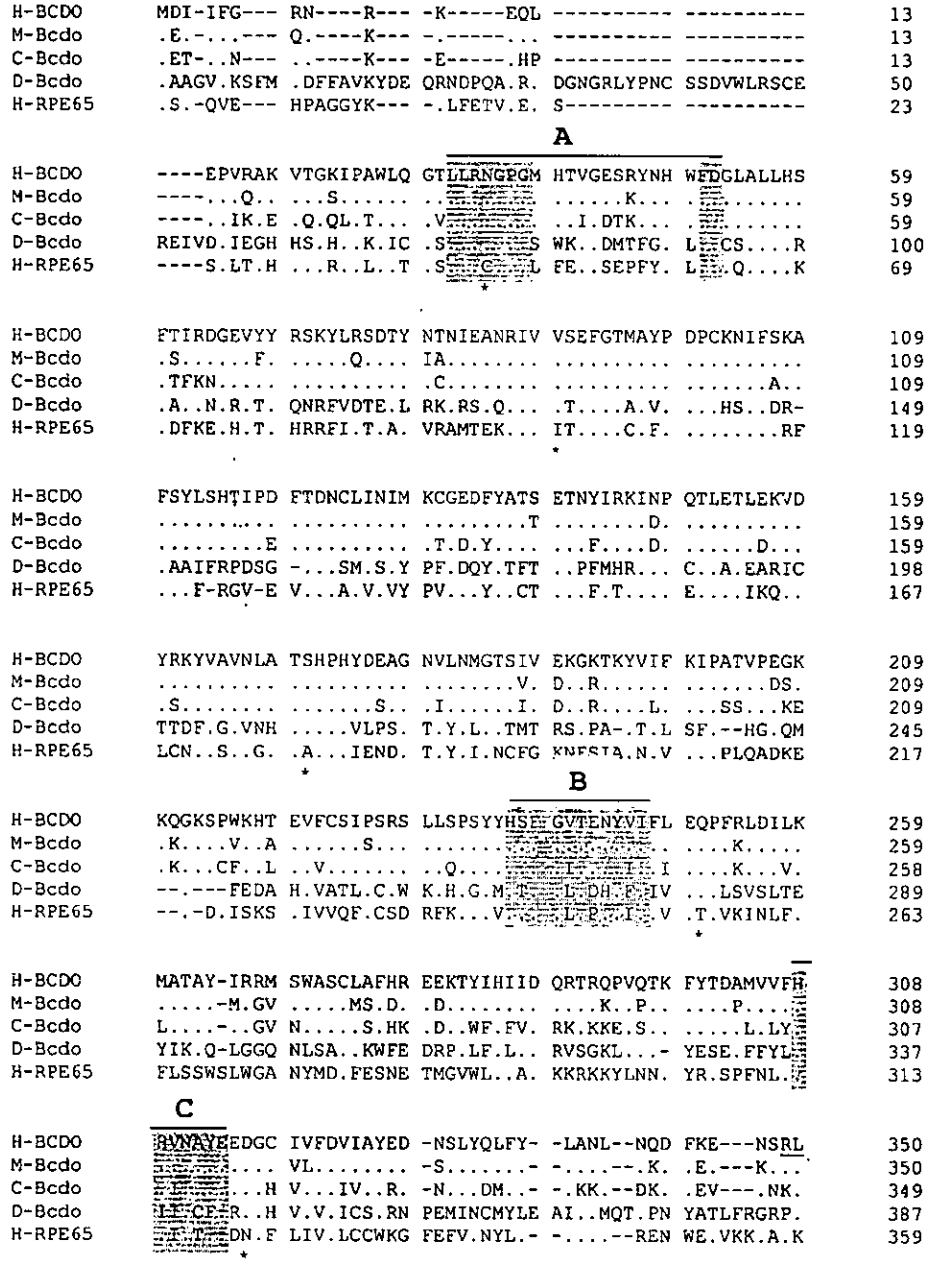

FIG. 1. Sequence comparison of human, mouse, chicken, and *Drosophila* BCDO and human RPE65. The most conserved regions are shaded and labeled A–D. H-BCDO, human BCDO; M-Bcdo, mouse Bcdo; C-Bcdo, chicken Bcdo; D-Bcdo, *Drosophila* Bcdo; H-RPE65, human RPE65. A period represents a residue that is identical to the human BCDO sequence, and a dash represents a site at which a space was introduced to maximize alignment. An asterisk indicates a position that is conserved in all Bcdo proteins but not in human RPE65. The sequence of the peptide used as an immunogen is shaded and underlined. The alignment was generated using GeneWorks 2.5.1 (Oxford Scientific) and modified to maximize homology.

range in size from 95 to 795 bp. Intron sizes, which were determined by PCR and confirmed by GenBank analysis, range from approximately 660 bp to 3 kb. All the 5′-donor and 3′-acceptor sites are consistent with the GT-AG consensus for pre-mRNA splicing recognition sequences.

Primer extension was used to identify the transcription start sites for human *BCDO*. Several potential initiation sites were identified, with the major site 216 bp upstream of the initiation methionine (Fig. 2). This is consistent with the existence of a typical TATA box 30 bp upstream of the transcription start site. Another weaker start site was identified 185 bp upstream of the ATG translation start codon (data not shown).

Human BCDO Gene Maps to 16q21–q23

The chromosomal localization of human *BCDO* was determined using a combination of somatic cell and radiation hybrid analyses. The gene maps to chromosome 16q21–q23. This position is close to the BBS2 locus for Bardet–Biedl syndrome, an autosomal recessive disease associated with pigmentary retinopathy, mental retardation, polydactyly, obesity, and hypogen-

```
H-BCDO       TSVPTLRRFA VPLHVDKNAE VGTNLIKVAS TTATALKEED GQVYCQPEFL      400
M-Bcdo       .......... .......D.. ..S..V..S. ........K. .H......V.      400
C-Bcdo       ..I..CK..V ...QY..D.. ..S..V.L-P .S...V..K. .SI.....I.      398
D-Bcdo       RF.LP.GTIP PASIAKRGLV KSFS.AGLSA PQVSRTMKHS VSQ.ADITYM      437
H-RPE65      APQ.EV..YV L..NI..-.D T.K..VTLPN .....ILCS. ETIWLE..V.      408

H-BCDO       -YEG----L- -ELPRVNY-- A-HNGKQYRY VFATGVQWSP IPTKIIKYDI      440
M-Bcdo       -...-----.- -....T..-- .-Y...P... I..AE..... V....L....      440
C-Bcdo       -C..-----I- -....V..-- D-Y...K.K. .Y.TE..... V....A.LNV      438
D-Bcdo       PTN.KQATAG E.S.KRDAKR GRYEEENLVN LVTMEGSQAE AFQGTNGIQL      487
H-RPE65      -FS.PRQAF. -.F.QI..-- QKYC..P.T. AYGL.LNHF- V.DRLC.LNV      452

                                      D
Human        LTKSSLKWRE DDCWPAPPLF VPAP----GA KDEDDSVILS AIVSTDP-QK      485
Mouse        ........S. ES....     T.----.           ....  .......-..      485
Chicken      Q..EV.H.G. .H...S     S.----D  RE  E.V.T CV.VSE.-N.      483
Drosopholia  RPEMLCD.GC ETPRIYYRY-MGKNYRYFY  ISS VDAVNP GTLIKVDVWN      537
Human RPE65  K..ETWV.Q. P.SY.S  I  SH.----D  LE  .V.. VV..PGAG..      498

H-BCDO       LPFLLILDAK SFTELARASV DVDMHMDLHG LEITDMDWDT KKQ--AASE-      532
M-Bcdo       .......... .......... .A...L.... ...P.A..NA V..--TPA.T      533
C-Bcdo       A......... T.K..G..T. N.E..L.... M..PQN.LGA ETE-------      526
D-Bcdo       KSC.TWCEEN VYPSEPIFVP SP.PKSEDD. VILAS.VLGG LNDRYVGLIV      587
H-RPE65      PAY....N.. DLS.V...E. EINIPVTF.. ..-------- ..S-------      533

H-BCDO       ---EQRDRAS D--------- ------CHGA PLT        547
M-Bcdo       QEV.NS.HPT .PTAPELSHS ENDFTAG..G SSL        566
C-Bcdo       ---------- ---------- ---------- ---        526
D-Bcdo       LCAKTMTELG RCDFHTNGPV PKCLHGWFAP NAI        620
H-RPE65      ---------- ---------- ---------- ---        533
```

FIG. 1—*Continued*

italism (Beales *et al.*, 1997; Bruford *et al.*, 1997; Kwitek-Black *et al.*, 1993). Whether *BCDO* mutations are associated with some cases of Bardet–Biedl syndrome is currently under investigation.

Human BCDO mRNA Is Highly Expressed in the RPE

Northern analysis indicates that *BCDO* is highly expressed in human RPE as a 2.4-kb transcript (Fig. 3A), which is 0.7 kb shorter than the chicken *Bcdo* transcript. *BCDO* was not detected in retina, liver, brain, or testis in our human total RNA blot (Fig. 3A) nor in heart, brain, placenta, lung, liver, skeletal muscle, kidney, or pancreas in a Clontech human poly(A)$^+$ RNA MTN blot (data not shown). To analyze further the expression pattern of human *BCDO*, RT-PCR was carried out with total RNAs from a variety of human tissues (Fig. 3B). Consistent with the Northern result, human *BCDO* is preferentially expressed in the RPE, but also expressed at lower levels in kidney, testis, liver, and brain. Since it is reported that chicken *Bcdo* is expressed primarily in duodenum, we also analyzed the expression of human *BCDO* mRNA in small intestine by RT-PCR. Although our RT-PCR is not quantitative, the level of *BCDO* in intestine seems similar to that in kidney and lower than that in RPE (Fig. 3B). We also performed RT-PCR for human *RPE65* and found that its expression pattern is more restricted

TABLE 1

Exon/intron Boundaries of the Human *BCDO* Gene

Exon	Exon size (bp)	Intron	Intron size (kb)	5′ donor	3′ acceptor
1	282	A	0.63	TGACAG**gtgagc**	**tct**cagGCAAGA
2	129	B	1.4	GAGACC**gtgaga**	**ttg**cagGTGAAG
3	130	C	2.4	TTCCAA**gtaact**	**ccc**cagAGCTTT
4	148	D	2.4	GAGAAG**gtatca**	**ttg**cagGTTGAT
5	148	E	2.8	TACCAG**gtaggc**	**tgc**tagAGGGCA
6	224	F	2.2	GAGAAG**gtgagg**	**ttt**cagACTTAT
7	258	G	1.1	GACAAG**gtaatg**	**ttt**cagAATGCA
8	106	H	2.0	ATGAAG**gtaaaa**	**ttg**tagGCTTAC
9	95	I	0.68	ACCAAG**gtactg**	**gta**cagATAATA
10	112	J	2.7	ATGACG**gtaaga**	**cta**aagGAGTAA
11	795				

Note. The exon sequences are shown in uppercase letters, and the intron sequences are displayed in lowercase letters. The gt-ag consensus sequences in the splicing sites are shown in boldface type.

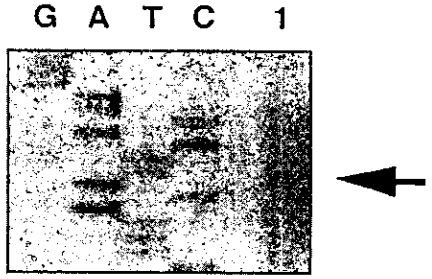

FIG. 2. Primer extension analysis of the *Bcdo* transcription start site. The arrow indicates the position of the band in lane **1** corresponding to the major transcription start site, at 216 bp upstream of the initiation methionine. Sequencing lanes that were used for orientation are shown.

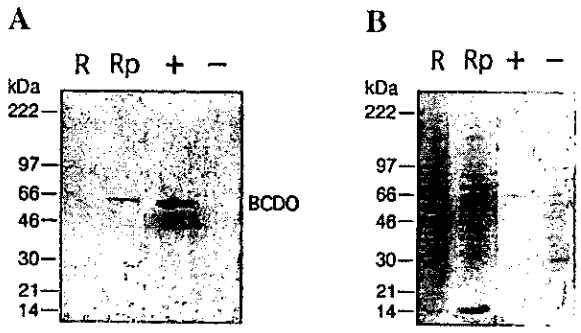

FIG. 4. BCDO protein is expressed by bovine RPE. (A) Immunoblot analysis of Bcdo expression. Ten micrograms of protein from bovine retina ("**R**") and RPE ("**Rp**") was loaded in the indicated lanes. The apparent molecular mass of the band in the RPE lane representing Bcdo is approximately 65 kDa, and its position is indicated on the right side of the panel. As positive and negative controls, respectively, Sf9 cell extract (0.2 μg protein total) from cells infected with BCDO expressing baculovirus ("+") and baculovirus without insert ("−") were also run. (B) Coomassie blue stained protein gel containing the same samples as in "A," except that 2 μg Sf9 extract was loaded in lane "+."

than that for *BCDO* (data not shown), consistent with the fact that so far *RPE65* expression outside the RPE has been reported only in transformed kidney cells and cone photoreceptors (Ma *et al.*, 1998, 1999).

Bovine RPE Expresses Bcdo Protein

To confirm at the protein level that Bcdo is expressed in the RPE, we generated a polyclonal anti-Bcdo antibody. The antibody was raised against a Bcdo synthetic peptide containing a sequence that is 100% conserved between human and mouse Bcdo and is minimally homologous to RPE65 (see Fig. 1). As a positive control, the antibody detected a 65-kDa band in total cell extract from BCDO expressing Sf9 cells (see below), but not in an extract from Sf9 cells infected with an empty bacmid vector (Fig. 4). As expected, a band with similar mobility was detected with bovine RPE extract. No immunoreactivity was seen with bovine retinal extract.

Human BCDO Has Dioxygenase Activity

To study the biochemical characteristics of human BCDO, the enzyme was expressed using a baculovirus system. The majority (>75%) of BCDO activity was extracted without detergent, suggesting that the enzyme is a soluble protein. To improve delivery of β,β-carotene, extracts were supplemented with Triton X-100. The crude 0.1% Triton X-100 soluble fractions were then tested for BCDO activity using a HPLC assay. Extracts from cells containing the BCDO recombinant baculovirus (Fig. 5A, a), but not from control cells containing the empty bacmid (Fig. 5A, d), demonstrated conversion of the β,β-carotene substrate into a major peak representing (*syn*) all-*trans*-retinal oxime and minor peaks representing (*anti*) all-*trans*-retinal oxime, (*syn*) 13-*cis*-retinal oxime, and (*anti*) 13-*cis*-retinal oxime. The retinoids were identified by their characteristic absorption spectra and elution times of authentic standards. For example, the absorption spectrum of peak 2 (Fig. 5A, inset) is consistent with all-*trans*-retinal, and peak 3 represented 13-*cis*-retinal oximes (data not shown). The activity was significantly reduced by the addition of EDTA (Fig. 5A, b) and eliminated by prior boiling of the extract (Fig. 5A, c). As expected, the enzyme activity was also time- (Fig. 5B) and concentration-dependent (Fig. 5C).

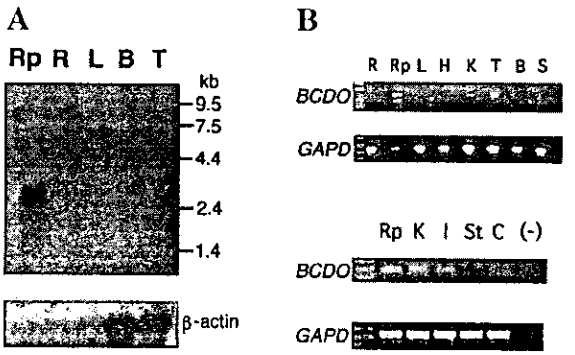

FIG. 3. Human *BCDO* gene is highly expressed in the RPE. (A) Northern analysis of human total RNA probed with labeled human *BCDO* cDNA. Lanes: **Rp**, RPE; **R**, retina; **L**, liver; **B**, brain; and **T**, testis. β-actin probe (**bottom**) was used to control for the amount of RNA loaded. (B) Expression of human *BCDO* gene analyzed by RT-PCR. The *BCDO* primers yielded a 364-bp fragment, and the control *GAPD* primers yielded a 556-bp fragment. Lanes: **R**, retina; **Rp**, RPE; **L**, liver; **H**, heart; **K**, kidney; **T**, testis; **B**, brain; **S**, spleen; **I**, small intestine; **St**, stomach; **C**, colon; and (−), negative control.

The formation of small amounts of 13-*cis*-retinal is consistent with an equilibrium between all-*trans*-retinal and 13-*cis*-retinal. The formation of the equilibrium is accelerated by the presence of membranes, and standard all-*trans*-retinal was converted to 13-*cis*-retinal even in the presence of boiled membranes. Similarly, the formation of 13-*cis*-retinal has been observed in similar assays carried out with the *Drosophila* enzyme (von Lintig and Vogt, 2000a).

The substrate specificity of BCDO was explored using other carotenoids and found to be specific toward β-carotene. No detectable activity was observed with the β,β-carotene-related compounds lutein (hydroxylated form) or lycopene, using the same HPLC assay under similar conditions as used for β,β-carotene (data

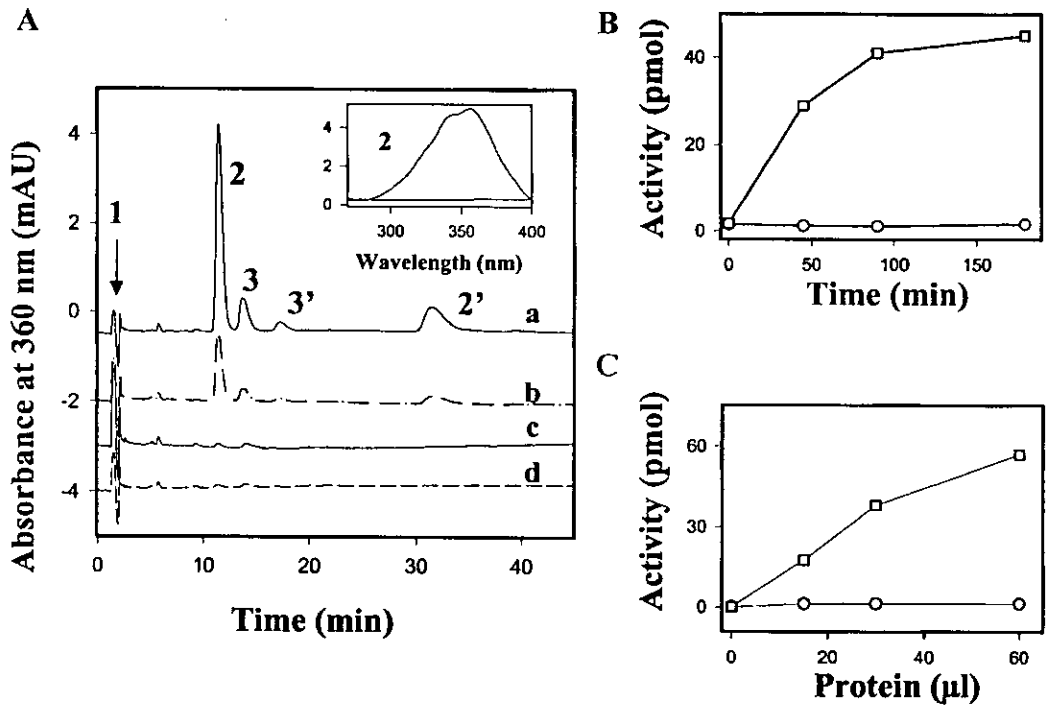

FIG. 5. BCDO protein has β,β-carotene 15,15′-dioxygenase activity. (A) The assay and HPLC conditions were as described under Materials and Methods. Numbered peaks represent: 1, β,β-carotene; 2, (*syn*) all-*trans*-retinal oxime; 2′, (*anti*) all-*trans*-retinal oxime; 3, (*syn*) 13-*cis*-retinal oxime; and 3′, (*anti*) 13-*cis*-retinal oxime. (**Inset**) UV spectrum of peak 2. Triton X-100 (0.1%) solubilized extract (66 μg protein) was assayed for β,β-carotene 15,15′-dioxygenase at 37°C for 70 min with 10 μM $FeSO_4$, 10 mM ascorbic acid, and 40 μM β,β-carotene (a) and in the presence of 5 mM EDTA (b). The same assays were also performed after boiling (c) and with 0.1% Triton X-100-soluble fraction from control cells infected with an empty bacmid (d). (B) The recombinant 0.1% Triton X-100-solubilized β,β-carotene 15,15′-dioxygenase (66 μg protein, top trace) and control (empty bacmid) (108 μg protein, bottom trace) extracts were assayed at 37°C for the indicated times with 10 μM $FeSO_4$, 10 mM ascorbic acid, and 40 μM β,β−carotene. Enzymatic activity was expressed as picomoles of (*syn*) all-*trans*-retinal oxime produced. (C) Increasing amounts of recombinant 0.1% Triton X-100-solubilized β,β-carotene-15,15′-dioxygenase (2.2 μg protein/μl, top trace) and control (empty bacmid) (3.6 μg protein/μl, bottom trace) extracts were assayed at 37°C for 65 min with 10 μM $FeSO_4$, 10 mM ascorbic acid, 1 mM DTT, and 40 μM β,β-carotene.

not shown). These results are similar to those observed with the *Drosophila* enzyme (von Lintig and Vogt, 2000a) and with crude preparations of rat liver and intestine (Nagao and Olson, 1994).

DISCUSSION

Since mammals cannot synthesize vitamin A or other retinoids *de novo*, the major source of new retinoids is dietary intake of plant-derived C_{40} carotenoids, with subsequent oxidative cleavage. Although the ability of certain mammalian tissues to convert β,β-carotene into vitamin A has been known for well over 50 years, its mechanism has been controversial, with an active debate about whether the cleavage was central or eccentric (Sivakumar, 1998). Recently, however, there were significant developments in this field with the first cloning of invertebrate (*Drosophila*) (von Lintig and Vogt, 2000a) and vertebrate (chicken) (Wyss *et al.*, 2000) Bcdos and demonstration that the *Drosophila* enzyme works via a central cleavage mechanism.

In this paper, we describe the first cloning of a mammalian *Bcdo*. Based on their high level of sequence and biochemical similarity with chicken *Bcdo* (Wyss *et al.*, 2000), we suggest that the human and murine genes are orthologues of the chicken gene and probably also orthologues of the *Drosophila* gene (von Lintig and Vogt, 2000a). Like chicken and *Drosophila* Bcdo, human BCDO uses a central cleavage mechanism at the 15,15′ double bond, to produce two molecules of retinal from each molecule of β,β-carotene, and is highly restricted in terms of substrate specificity. Also, like chicken and *Drosophila* Bcdo, the mammalian enzyme is soluble rather than membrane-associated, as shown by the solubility of the baculovirus expressed human BCDO as well as by immunoblot analysis of membrane-associated and soluble fractions of bovine RPE (data not shown).

Interestingly, the homology between human BCDO and human RPE65 is at least as high as, and probably higher than, that between human BCDO and *Drosophila* Bcdo, suggesting the possibility that RPE65 might have Bcdo activity. However, direct testing of *in vitro* expressed RPE65 protein failed to identify any such activity (von Lintig and Vogt, 2000a). Perhaps related to this lack of Bcdo activity, there is a central asparagine in the sequence of region A that is conserved in all homologous dioxygenases that is changed to a cysteine in all known RPE65s (Fig. 1).

Although the function of Bcdo is at this point unclear, we suggest that it may, in part, act as a component of a local supply pathway to supplement the visual cycle in providing 11-*cis*-retinal to photoreceptors. Such a mechanism would be particularly important under bright-light conditions when the ability of the visual cycle to provide sufficient substrate might be limited. As a precedent demonstrating that some retinoid metabolizing enzymes might be important mainly in times of stress, 11-*cis*-retinol dehydrogenase null mice appeared to have normal dark adaptation kinetics under typical light conditions, but when subjected to a strong bleach they demonstrate significantly delayed dark adaptation kinetics (Driessen *et al.*, 2000). Perhaps also of relevance to the situation with Bcdo, 11-*cis*-retinol dehydrogenase is expressed in a number of tissues outside the eye, but no extraocular phenotypes have been reported in the knockout mice.

The human *BCDO* gene maps to chromosome 16q21–q23, which is near the recessive BBS2 locus for Bardet–Biedl syndrome (Beales *et al.*, 1997; Bruford *et al.*, 1997; Kwitek-Black *et al.*, 1993). *BCDO* is a reasonable candidate gene for BBS, not only because of its map location, but also because several of the characteristics of the syndrome, such as retinal degeneration and polydactyly, could be related to abnormalities of the retinoid metabolism. In addition, *BCDO* could be considered as a candidate gene for a number of other retinal diseases both because of the earlier mentioned association with the *Drosophila ninaB* phenotype (von Lintig *et al.*, 2000b) and because many retinal degenerations have been associated with mutations in genes involved in the visual cycle and retinoid metabolism and transport. For example, mutations in ABCR have been associated with Stargardt's disease (Allikmets *et al.*, 1997b) and possibly, but controversially, with age-related macular degeneration (Allikmets, 2000; Allikmets *et al.*, 1997a; Dryja *et al.*, 1998; Stone *et al.*, 1998); mice null for interphotoreceptor retinoid binding protein (IRBP) develop an early retinal degeneration (Liou *et al.*, 1998) (although surprisingly the visual cycle appears to function fairly normally in the absence of IRBP) (Palczewski *et al.*, 1999; Ripps *et al.*, 2000); mutations in 11-*cis*-retinol dehydrogenase have been reported in patients with fundus albipunctatus (Gonzalez-Fernandez *et al.*, 1999; Yamamoto *et al.*, 1999); mutations in CRALBP have been reported in cases of autosomal recessive retinitis pigmentosa (Maw *et al.*, 1997) and retinitis punctata albescens (Burstedt *et al.*, 1999; Morimura *et al.*, 1999); mutations in RPE65 cause a childhood retinal degeneration (Gu *et al.*, 1997; Marlhens *et al.*, 1997); and mutations in serum retinol-binding protein are associated with night blindness and RPE atrophy (Biesalski *et al.*, 1999; Seeliger *et al.*, 1999). These last two findings are potentially the most relevant to BCDO because of its homology to RPE65 and because, even though serum retinol-binding protein is widely expressed outside the eye, the clinical phenotype almost exclusively affects the eye. Also of potential interest, carotenoids have been implicated in age-related macular degeneration (Seddon *et al.*, 1994).

The cloning of the human *BCDO* gene allows direct testing of whether mutations in this gene are associated with retinal diseases or other diseases. Availability of the mouse gene makes analysis of Bcdo function possible through generation of null mice. In addition, the ability to express the protein *in vitro* will allow detailed studies of enzyme kinetics, mechanism, and structure–function relationships to be performed.

ACKNOWLEDGMENTS

This research was supported, in part, by funds from The Foundation Fighting Blindness (Wilmer AMD Center Grant), NIH vision training grants (J.K.M. and J.C.), NIH (EY08061 and Core Grant EY01765), unrestricted grants from Research to Prevent Blindness, Inc. (RPB), and grants from the Ruth and Milton Steinbach Fund, the E. K. Bishop Foundation, and the Macula Vision Foundation. W.Y. is a recipient of fellowship from Fight-For-Sight, and D.J.Z. is a recipient of a Career Development Award from RPB.

REFERENCES

Ahn, J., and Molday, R. S. (2000). Purification and characterization of ABCR from bovine rod outer segments. *Methods Enzymol* **315:** 864–879.

Allikmets, R. (2000). Further evidence for an association of ABCR alleles with age-related macular degeneration. *Am. J. Hum. Genet.* **67:** 487–491.

Allikmets, R., Shroyer, N. F., Singh, N., Seddon, J. M., Lewis, R. A., Bernstein, P. S., Peiffer, A., Zabriskie, N. A., Li, Y., Hutchinson, A., Dean, M., Lupski, J. R., and Leppert, M. (1997a). Mutation of the Stargardt disease gene (ABCR) in age-related macular degeneration. *Science* **277:** 1805–1807.

Allikmets, R., Singh, N., Sun, H., Shroyer, N. F., Hutchinson, A., Chidambaram, A., Gerrard, B., Baird, L., Stauffer, D., Peiffer, A., Rattner, A., Smallwood, P., Li, Y., Anderson, K. L., Lewis, R. A., Nathans, J., Leppert, M., Dean, M., and Lupski, J. R. (1997b). A photoreceptor cell-specific ATP-binding transporter gene (ABCR) is mutated in recessive Stargardt macular dystrophy. *Nat. Genet.* **15:** 236–246.

Altschul, S. F., Gish, W., Miller, W., Myers, E. W., and Lipman, D. J. (1990). Basic local alignment search tool. *J. Mol. Biol.* **215:** 403–410.

Altschul, S. F., Madden, T. L., Schaffer, A. A., Zhang, J., Zhang, Z., Miller, W., and Lipman, D. J. (1997). Gapped BLAST and PSI-BLAST: A new generation of protein database search programs. *Nucleic Acids Res.* **25:** 3389–3402.

Beales, P. L., Warner, A. M., Hitman, G. A., Thakker, R., and Flinter, F. A. (1997). Bardet–Biedl syndrome: A molecular and phenotypic study of 18 families. *J. Med. Genet.* **34:** 92–98.

Bernstein, P. S., Law, W. C., and Rando, R. R. (1987). Biochemical characterization of the retinoid isomerase system of the eye. *J. Biol. Chem.* **262:** 16848–16857.

Biesalski, H. K., Frank, J., Beck, S. C., Heinrich, F., Illek, B., Reifen, R., Gollnick, H., Seeliger, M. W., Wissinger, B., and Zrenner, E. (1999). Biochemical but not clinical vitamin A deficiency results from mutations in the gene for retinol binding protein. *Am. J. Clin. Nutr.* **69:** 931–936.

Bok, D. (1993). The retinal pigment epithelium: A versatile partner in vision. *J. Cell Sci. Suppl.* **17:** 189–195.

Bruford, E. A., Riise, R., Teague, P. W., Porter, K., Thomson, K. L., Moore, A. T., Jay, M., Warburg, M., Schinzel, A., Tommerup, N., Tornqvist, K., Rosenberg, T., Patton, M., Mansfield, D. C., and Wright, A. F. (1997). Linkage mapping in 29 Bardet–Biedl syndrome families confirms loci in chromosomal regions 11q13, 15q22.3–q23, and 16q21. *Genomics* **41:** 93–99.

Burstedt, M. S., Sandgren, O., Holmgren, G., and Forsman-Semb, K. (1999). Bothnia dystrophy caused by mutations in the cellular retinaldehyde-binding protein gene (RLBP1) on chromosome 15q26. *Invest. Ophthalmol. Vis. Sci.* **40:** 995–1000.

Canada, F. J., Law, W. C., Rando, R. R., Yamamoto, T., Derguini, F., and Nakanishi, K. (1990). Substrate specificities and mechanism in the enzymatic processing of vitamin A into 11-*cis*-retinol. *Biochemistry* **29:** 9690–9697.

Chang, J. T., Esumi, N., Moore, K., Li, Y., Zhang, S., Chew, C., Goodman, B., Rattner, A., Moody, S., Stetten, G., Campochiaro, P. A., and Zack, D. J. (1999). Cloning and characterization of a secreted frizzled-related protein that is expressed by the retinal pigment epithelium. *Hum. Mol. Genet.* **8:** 575–583.

Chang, J. T., Milligan, S., Li, Y., Chew, C. E., Wiggs, J., Copeland, N. G., Jenkins, N. A., Campochiaro, P. A., Hyde, D. R., and Zack, D. J. (1997). Mammalian homolog of *Drosophila* retinal degeneration B rescues the mutant fly phenotype. *J. Neurosci.* **17:** 5881–5890.

Crouch, R. K., Chader, G. J., Wiggert, B., and Pepperberg, D. R. (1996). Retinoids and the visual process. *Photochem. Photobiol.* **64:** 613–621.

Deigner, P. S., Law, W. C., Canada, F. J., and Rando, R. R. (1989). Membranes as the energy source in the endergonic transformation of vitamin A to 11-*cis*-retinol. *Science* **244:** 968–971.

Driessen, C. A., Winkens, H. J., Hoffmann, K., Kuhlmann, L. D., Janssen, B. P., Van Vugt, A. H., Van Hooser, J. P., Wieringa, B. E., Deutman, A. F., Palczewski, K., Ruether, K., and Janssen, J. J. (2000). Disruption of the 11-*cis*-retinol dehydrogenase gene leads to accumulation of *cis*-retinols and *cis*-retinyl esters. *Mol. Cell. Biol.* **20:** 4275–4287.

Dryja, T. P., Briggs, C. E., Berson, E. L., Rosenfeld, P. J., and Abitbol, M. (1998). ABCR gene and age-related macular degeneration. *Science* **279:** 1107.

Gonzalez-Fernandez, F., Kurz, D., Bao, Y., Newman, S., Conway, B. P., Young, J. E., Han, D. P., and Khani, S. C. (1999). 11-*cis* retinol dehydrogenase mutations as a major cause of the congenital night-blindness disorder known as fundus albipunctatus. *Mol. Vis.* **5:** 41.

Gu, S. M., Thompson, D. A., Srikumari, C. R., Lorenz, B., Finckh, U., Nicoletti, A., Murthy, K. R., Rathmann, M., Kumaramanickavel, G., Denton, M. J., and Gal, A. (1997). Mutations in RPE65 cause autosomal recessive childhood-onset severe retinal dystrophy. *Nat. Genet.* **17:** 194–197.

Haeseleer, F., Huang, J., Lebioda, L., Saari, J. C., and Palczewski, K. (1998). Molecular characterization of a novel short-chain dehydrogenase/reductase that reduces all-*trans*-retinal. *J. Biol. Chem.* **273:** 21790–21799.

Hamel, C. P., Tsilou, E., Pfeffer, B. A., Hooks, J. J., Detrick, B., and Redmond, T. M. (1993). Molecular cloning and expression of RPE65, a novel retinal pigment epithelium-specific microsomal protein that is post-transcriptionally regulated in vitro. *J. Biol. Chem.* **268:** 15751–15757.

Jang, G-F., McBee, J. K., Alekseev, A. M., Haeseleer, F., and Palczewski, K. (2000). Stereoisomeric specificity of retinoid cycle in the vertebrate retina. *J. Biol. Chem.* **275:** 28128–28138.

Koutalos, Y., and Yau, K. W. (1996). Regulation of sensitivity in vertebrate rod photoreceptors by calcium. *Trends Neurosci.* **19:** 73–81.

Kwitek-Black, A. E., Carmi, R., Duyk, G. M., Buetow, K. H., Elbedour, K., Parvari, R., Yandava, C. N., Stone, E. M., and Sheffield, V. C. (1993). Linkage of Bardet–Biedl syndrome to chromosome 16q and evidence for non-allelic genetic heterogeneity. *Nat. Genet.* **5:** 392–396.

Lagnado, L., and Baylor, D. (1992). Signal flow in visual transduction. *Neuron* **8:** 995–1002.

Liou, G. I., Fei, Y., Peachey, N. S., Matragoon, S., Wei, S., Blaner, W. S., Wang, Y., Liu, C., Gottesman, M. E., and Ripps, H. (1998). Early onset photoreceptor abnormalities induced by targeted disruption of the interphotoreceptor retinoid-binding protein gene. *J. Neurosci.* **18:** 4511–4520.

Ma, J., Xu, L., Othersen, D. K., Redmond, T. M., and Crouch, R. K. (1998). Cloning and localization of RPE65 mRNA in salamander cone photoreceptor cells. *Biochim. Biophys. Acta* **1443:** 255–261.

Ma, J. X., Zhang, D., Laser, M., Brownlee, N. A., Re, G. G., Hazen-Martin, D. J., Redmond, T. M., and Crouch, R. K. (1999). Identification of RPE65 in transformed kidney cells. *FEBS Lett.* **452:** 199–204.

Marlhens, F., Bareil, C., Griffoin, J. M., Zrenner, E., Amalric, P., Eliaou, C., Liu, S. Y., Harris, E., Redmond, T. M., Arnaud, B., Claustres, M., and Hamel, C. P. (1997). Mutations in RPE65 cause Leber's congenital amaurosis. *Nat. Genet.* **17:** 139–141.

Maw, M. A., Kennedy, B., Knight, A., Bridges, R., Roth, K. E., Mani, E. J., Mukkadan, J. K., Nancarrow, D., Crabb, J. W., and Denton, M. J. (1997). Mutation of the gene encoding cellular retinaldehyde-binding protein in autosomal recessive retinitis pigmentosa. *Nat. Genet.* **17:** 198–200.

McBee, J. K., Kuksa, V., Alvarez, R., de Lera, A. R., Prezhdo, O., Haeseleer, F., Sokal, I., and Palczewski, K. (2000). Isomerization of all-trans-retinol to cis-retinols in bovine retinal pigment epithelial cells: Dependence on the specificity of retinoid-binding proteins. *Biochemistry* **39:** 11370–11380.

Morimura, H., Berson, E. L., and Dryja, T. P. (1999). Recessive mutations in the RLBP1 gene encoding cellular retinaldehyde-binding protein in a form of retinitis punctata albescens. *Invest. Ophthalmol. Vis. Sci.* **40:** 1000–1004.

Nagao, A., and Olson, J. A. (1994). Enzymatic formation of 9-*cis*, 13-*cis*, and all-*trans* retinals from isomers of β-carotene. *FASEB J.* **8:** 968–973.

Nicoletti, A., Wong, D. J., Kawase, K., Gibson, L. H., Yang-Feng, T. L., Richards, J. E., and Thompson, D. A. (1995). Molecular characterization of the human gene encoding an abundant 61 kDa protein specific to the retinal pigment epithelium. *Hum. Mol. Genet.* **4:** 641–649.

Palczewski, K., Polans, A. S., Baehr, W., and Ames, J. B. (2000). Ca(2+)-binding proteins in the retina: Structure, function, and the etiology of human visual diseases. *BioEssays* **22:** 337–350.

Palczewski, K., Van Hooser, J. P., Garwin, G. G., Chen, J., Liou, G. I., and Saari, J. C. (1999). Kinetics of visual pigment regeneration in excised mouse eyes and in mice with a targeted disruption of the gene encoding interphotoreceptor retinoid-binding protein or arrestin. *Biochemistry* **38:** 12012–12019.

Polans, A., Baehr, W., and Palczewski, K. (1996). Turned on by Ca^{2+}! The physiology and pathology of Ca(2+)-binding proteins in the retina. *Trends Neurosci.* **19:** 547–554.

Pugh, E. N., Jr., Nikonov, S., and Lamb, T. D. (1999). Molecular mechanisms of vertebrate photoreceptor light adaptation. *Curr. Opin. Neurobiol.* **9:** 410–418.

Rattner, A., Smallwood, P. M., and Nathans, J. (2000). Identification and characterization of all-*trans*-retinol dehydrogenase from photoreceptor outer segments, the visual cycle enzyme that reduces all-*trans*-retinal to all-*trans*-retinol. *J. Biol. Chem.* **275:** 11034–11043.

Rattner, A., Sun, H., and Nathans, J. (1999). Molecular genetics of human retinal disease. *Annu. Rev. Genet.* **33:** 89–131.

Redmond, T. M., Yu, S., Lee, E., Bok, D., Hamasaki, D., Chen, N., Goletz, P., Ma, J. X., Crouch, R. K., and Pfeifer, K. (1998). Rpe65 is necessary for production of 11-*cis*-vitamin A in the retinal visual cycle. *Nat. Genet.* **20:** 344–351.

Ripps, H., Peachey, N. S., Xu, X., Nozell, S. E., Smith, S. B., and Liou, G. I. (2000). The rhodopsin cycle is preserved in IRBP "knockout" mice despite abnormalities in retinal structure and function. *Vis. Neurosci.* **17:** 97–105.

Ruiz, A., Winston, A., Lim, Y. H., Gilbert, B. A., Rando, R. R., and Bok, D. (1999). Molecular and biochemical characterization of lecithin retinol acyltransferase. *J. Biol. Chem.* **274:** 3834–3841.

Seddon, J. M., Ajani, U. A., Sperduto, R. D., Hiller, R., Blair, N., Burton, T. C., Farber, M. D., Gragoudas, E. S., Haller, J., Miller, D. T., *et al.* (1994). Dietary carotenoids, vitamins A, C, and E, and advanced age-related macular degeneration. Eye Disease Case-Control Study Group *J. Am. Med. Assoc.* **272:** 1413–1420.

Seeliger, M. W., Biesalski, H. K., Wissinger, B., Gollnick, H., Gielen, S., Frank, J., Beck, S., and Zrenner, E. (1999). Phenotype in retinol deficiency due to a hereditary defect in retinol binding protein synthesis. *Invest. Ophthalmol. Vis. Sci.* **40:** 3–11.

Simon, A., Hellman, U., Wernstedt, C., and Eriksson, U. (1995). The retinal pigment epithelial-specific 11-*cis* retinol dehydrogenase belongs to the family of short chain alcohol dehydrogenases. *J. Biol. Chem.* **270:** 1107–1112.

Sivakumar, B. (1998). Current controversies in carotene nutrition. *Ind. J. Med. Res.* **108:** 157–166.

Stecher, H., Gelb, M. H., Saari, J. C., and Palczewski, K. (1999). Preferential release of 11-*cis*-retinol from retinal pigment epithelial cells in the presence of cellular retinaldehyde-binding protein. *J. Biol. Chem.* **274:** 8577–8585.

Stone, E. M., Webster, A. R., Vandenburgh, K., Streb, L. M., Hockey, R. R., Lotery, A. J., and Sheffield, V. C. (1998). Allelic variation in ABCR associated with Stargardt disease but not age-related macular degeneration. *Nat. Genet.* **20:** 328–329.

Sun, H., and Nathans, J. (1997). Stargardt's ABCR is localized to the disc membrane of retinal rod outer segments. *Nat. Genet.* **17:** 15–16. [Letter]

Sun, H., and Nathans, J. (2000). ABCR: Rod photoreceptor-specific ABC transporter responsible for Stargardt disease. *Methods Enzymol.* **315:** 879–897.

Trehan, A., Canada, F. J., and Rando, R. R. (1990). Inhibitors of retinyl ester formation also prevent the biosynthesis of 11-*cis*-retinol. *Biochemistry* **29:** 309–312.

Van Hooser, J. P., Aleman, T. S., He, Y. G., Cideciyan, A. V., Kuksa, V., Pittler, S. J., Stone, E. M., Jacobson, S. G., and Palczewski, K. (2000). Rapid restoration of visual pigment and function with oral retinoid in a mouse model of childhood blindness. *Proc. Natl. Acad. Sci. USA* **97:** 8623–8628.

von Lintig, J., and Vogt, K. (2000a). Filling the gap in vitamin A research. Molecular identification of an enzyme cleaving β-carotene to retinal. *J. Biol. Chem.* **275:** 11915–11920.

von Lintig, J., Dreher, A., Kiefer, C., Wernet, M. F., and Vogt, K. (2000b). Analysis of the blind *Drosophila* mutant *ninaB* identifies the gene encoding the key enzyme for vitamin A formation *in vivo*. *Proc. Natl. Acad. Sci. USA*, in press.

Weng, J., Mata, N. L., Azarian, S. M., Tzekov, R. T., Birch, D. G., and Travis, G. H. (1999). Insights into the function of Rim protein in photoreceptors and etiology of Stargardt's disease from the phenotype in abcr knockout mice. *Cell* **98:** 13–23.

Winston, A., and Rando, R. R. (1998). Regulation of isomerohydrolase activity in the visual cycle. *Biochemistry* **37:** 2044–2050.

Wyss, A., Wirtz, G., Woggon, W., Brugger, R., Wyss, M., Friedlein, A., Bachmann, H., and Hunziker, W. (2000). Cloning and expression of β,β-carotene 15,15′-dioxygenase. *Biochem. Biophys. Res. Commun.* **271:** 334–336.

Yamamoto, H., Simon, A., Eriksson, U., Harris, E., Berson, E. L., and Dryja, T. P. (1999). Mutations in the gene encoding 11-*cis* retinol dehydrogenase cause delayed dark adaptation and fundus albipunctatus. *Nat. Genet.* **22:** 188–191.

Expression and permeation properties of the K^+ channel Kir7.1 in the retinal pigment epithelium

Masahiko Shimura*, Yukun Yuan*, Jinghua T. Chang‡, Suiyuan Zhang‡, Peter A. Campochiaro‡§, Donald J. Zack‡§‖ and Bret A. Hughes*†

*W. K. Kellogg Eye Center, Department of Ophthalmology and Visual Sciences and †Department of Physiology, University of Michigan, Ann Arbor, MI and ‡ Wilmer Eye Institute and Departments of § Neuroscience and ‖ Molecular Biology and Genetics, Johns Hopkins University School of Medicine, Baltimore, MD, USA

(Received 30 June 2000; accepted after revision 31 October 2000)

1. Bovine *Kir7.1* clones were obtained from a retinal pigment epithelium (RPE)-subtracted cDNA library. Human RPE cDNA library screening resulted in clones encoding full-length human *Kir7.1*.

2. Northern blot analysis indicated that bovine *Kir7.1* is highly expressed in the RPE.

3. Human Kir7.1 channels were expressed in *Xenopus* oocytes and studied using the two-electrode voltage-clamp technique.

4. The macroscopic Kir7.1 conductance exhibited mild inward rectification and an inverse dependence on extracellular K^+ concentration ($[K^+]_o$). The selectivity sequence based on permeability ratios was K^+ (1.0) ≈ Rb^+ (0.89) > Cs^+ (0.013) > Na^+ (0.003) ≈ Li^+ (0.001) and the sequence based on conductance ratios was Rb^+ (9.5) ≫ K^+ (1.0) > Na^+ (0.458) > Cs^+ (0.331) > Li^+ (0.139).

5. Non-stationary noise analysis of Rb^+ currents in cell-attached patches yielded a unitary conductance for Kir7.1 of ~2 pS.

6. In whole-cell recordings from freshly isolated bovine RPE cells, the predominant current was a mild inwardly rectifying K^+ current that exhibited an inverse dependence of conductance on $[K^+]_o$. The selectivity sequence based on permeability ratios was K^+ (1.0) ≈ Rb^+ (0.89) > Cs^+ (0.021) > Na^+ (0.003) ≈ Li^+ (0.002) and the sequence based on conductance ratios was Rb^+ (8.9) ≫ K^+ (1.0) > Na^+ (0.59) > Cs^+ (0.23) > Li^+ (0.08).

7. In cell-attached recordings with Rb^+ in the pipette, inwardly rectifying currents were observed in nine of 12 patches of RPE apical membrane but in only one of 13 basolateral membrane patches.

8. Non-stationary noise analysis of Rb^+ currents in cell-attached apical membrane patches yielded a unitary conductance for RPE Kir of ~2 pS.

9. On the basis of this molecular and electrophysiological evidence, we conclude that Kir7.1 channel subunits comprise the K^+ conductance of the RPE apical membrane.

The retinal pigment epithelium (RPE) is a simple cuboidal epithelium in the distal retina that separates the photoreceptor cells from their main blood supply in the choroid. From this strategic position, the RPE carries out a host of functions that are critical to the visual process. One of these is the transepithelial transport of fluid, ions and metabolites, which serves to control the composition and volume of the extracellular fluid that surrounds the photoreceptor outer segments (Hughes *et al.* 1998).

It is well established that K^+ channels play a central role in the vectorial transport of K^+ across the RPE. At the apical membrane, the net flux of K^+ into or out of the subretinal space is determined by the balance between K^+ efflux through Ba^{2+}-sensitive K^+ channels (Lasansky & De Fisch, 1966; Miller & Steinberg, 1977; Griff *et al.* 1985; Joseph & Miller, 1991; Quinn & Miller, 1992) and K^+ influx via the electrogenic Na^+–K^+ pump (Miller *et al.* 1978) and Na^+–K^+–$2Cl^-$ cotransporter (Miller & Edelman,

1990; Joseph & Miller, 1991). At light onset, a decrease in subretinal K^+ concentration, originating from a change in photoreceptor activity, causes an increase in the efflux of K^+ through the apical K^+ channels, leading to the reversal of net K^+ transport from absorption to secretion (Bialek & Miller, 1994).

In patch-clamp studies on RPE cells isolated from a variety of vertebrate species, we have shown that the predominant conductance in the physiological voltage range is an inwardly rectifying K^+ (Kir) conductance (Hughes & Steinberg, 1990; Hughes & Takahira, 1996, 1998). The inward rectification of this K^+ conductance is relatively weak, such that it supports substantial outward K^+ current at voltages positive to the K^+ equilibrium potential. This conductance has several remarkable properties, including an inverse dependence on extracellular K^+ concentration (Segawa & Hughes, 1994; Hughes & Takahira, 1996) and an intracellular Mg-ATP requirement for sustained activity (Hughes & Takahira, 1998). Blocker sensitivity studies on the intact RPE sheet preparation indicate that these Kir channels underlie that apical membrane K^+ conductance (Hughes *et al.* 1995*a*).

In the mid-1990s, expressional cloning of the inwardly rectifying K^+ channels ROMK1 (Ho *et al.* 1993), IRK1 (Kubo *et al.* 1993) and GIRK (Kofuji *et al.* 1995) established the existence of a new gene family distinct from the voltage-gated K^+ channel family. Since then, several other members of the Kir channel family have been identified, increasing the number of members to 15 (Reimann & Ashcroft, 1999). The most recent addition is Kir7.1, an inwardly rectifying K^+ channel with several novel properties, including a macroscopic conductance with low dependence on extracellular K^+ concentration ($[K^+]_o$) (Döring *et al.* 1998; Krapivinsky *et al.* 1998), a low unitary conductance estimated to be ~50 fS (Krapivinsky *et al.* 1998), and an unusually large Rb^+-to-K^+ conductance ratio (Wischmeyer *et al.* 2000). Kir7.1 expression has been reported in certain epithelia such as choroid plexus and small intestine, as well as in stomach, kidney, thyroid follicular cells, brain, spinal chord and testis (Döring *et al.* 1998; Krapivinsky *et al.* 1998; Partiseti *et al.* 1998; Nakamura *et al.* 1999, 2000). The capacity of this channel to pass large outward K^+ currents makes it well suited to function in epithelial ion transport processes (Döring *et al.* 1998).

In this study, we have cloned bovine Kir7.1 from a subtracted RPE cDNA library (Chang *et al.* 1997, 1999), obtained its human orthologue and confirmed its expression in the RPE by Northern blot analysis. Furthermore, we have compared the permeation properties of the native Kir channel in freshly dissociated bovine RPE cells to those of cloned Kir7.1 channels expressed in *Xenopus* oocytes and find that they are nearly identical. Some of these results have been published in abstract form (Shimura *et al.* 1999; Yuan *et al.* 2000).

METHODS

Isolation of human Kir7.1 cDNA

Over a thousand clones from a bovine RPE cDNA library that had been 'subtracted' with biotinylated heart and liver RNA were partially sequenced using a combination of manual and automated (Beckman CEQ2000) dideoxy sequencing (Chang *et al.* 1997, 1999). Using as a probe the insert of a clone having sequence homology to ROMK2, a human RPE cDNA library was screened. Resultant positive clones were plaque purified and sequenced. Methods used for library screening and other routine recombinant DNA analyses were essentially as described in standard laboratory manuals (Sambrook *et al.* 1989; Ausubel *et al.* 1996).

Northern analysis

For Northern analysis, an RNA blot was prepared by loading 10 μg total mRNA isolated from various bovine tissues. The blot was sequentially hybridized with a partial-length bovine Kir7.1 cDNA probe at 42 °C in 50 % formamide, 6 × SSPE (saline–sodium phosphate–EDTA buffer) and 0.5 % SDS. After 24 h of hybridization, membranes were washed twice at low stringency (42 °C, 2 × SSPE with 0.1 % SDS). Blots were then exposed to X-ray film for 24 h.

Expression of Kir7.1 in *Xenopus* oocytes

For the construction of a transcription plasmid, the coding region of human Kir7.1 cDNA (nucleotides 90–1303 of pc84 cDNA) was PCR amplified with the Expand High Fidelity PCR system (Boerhinger Meinheim, Indianapolis, IN, USA) and subcloned into the polyadenylating transcription vector pBSTA (Goldin, 1992) at the *Bgl*II site using a blunt end-ligation procedure. The resulting plasmid contained the cloned cDNA insert flanked by the 5′ and 3′ untranslated regions of the *Xenopus* β-globin gene and allowed sense-strand cDNA to be transcribed by T7 RNA polymerase. Capped poly(A)$^+$ RNA was synthesized from plasmid cDNA linearized at the *Sac*I site using a commercially available cRNA capping kit (Ambion Inc., Austin, TX, USA). cRNA was precipitated in 70 % ethanol and re-dissolved in diethyl pyrocarbonate (DEPC)-treated water.

All experiments with *Xenopus* frogs were carried out following protocols approved by the University of Michigan Committee on the Use and Care of Animals. *Xenopus laevis* oocytes were surgically removed from adult females anaesthetized with topical tricaine methane sulfonate (0.15 % for 15–30 min) and defolliculated by incubating clusters of oocytes in 0.2 % collagenase (type IV, Sigma Chemical Co., St Louis, MO, USA) in calcium-free ND96 solution (96 mM NaCl, 2 mM KCl, 1 mM $MgCl_2$, 10 mM Hepes (pH 7.4), 300 mg ml^{-1} gentamicin and 550 mg ml^{-1} sodium pyruvate). Incisions were sutured and frogs were allowed to recover with aftercare. Healthy stage V–VI oocytes were collected and stored overnight at 18 °C in ND96 solution plus 1 mM $CaCl_2$. Defolliculated oocytes were injected with 5–10 ng of Kir 7.1 cRNA in 50 nl and maintained at 18 °C in incubation solution for up to 72 h before recording. Oocytes injected with the same volume of DEPC-treated water served as controls.

Experiments on Kir7.1 cRNA-injected oocytes

Solutions. The standard bath solution for *Xenopus* oocyte recordings consisted of (mM): 96 NaCl, 2 KCl, 10 Na-Hepes, 1.0 $CaCl_2$, 1.0 $MgCl_2$, pH 7.4. To study the dependence of Kir7.1 currents on extracellular K^+, the concentration of K^+ ($[K^+]_o$) was varied by equimolar replacement with Na^+. In experiments investigating the permeability of Kir7.1 to monovalent cations, the solution consisted of (mM): 98 X, 10 NMDG-Hepes, 1.0 $CaCl_2$, and 1.0 $MgCl_2$, where X is KCl, NaCl, RbCl, LiCl, or CsCl. When indicated, 10 mM $BaCl_2$ was added directly to the external solution.

Electrophysiology. Whole-cell currents were recorded using the two-electrode voltage-clamp technique (Stuhmer, 1992). Microelectrodes, pulled from thick-wall borosilicate glass (o.d. = 1.0 mm, i.d. = 0.5 mm) with a multistage programmable puller (Sutter Instruments, San Rafael, CA, USA) and having an impedance of 0.5–1.5 MΩ when filled with 3 M KCl, were used as voltage-sensing and current-passing electrodes. Signals from the current-passing electrode were amplified using a GeneClamp 500 amplifier (Axon Instruments, Inc., Burlingame, CA, USA) with the built-in low pass filter set to 0.5–1 kHz and stored on a computer hard drive for later analysis. To avoid voltage errors due to large currents (Baumgartner *et al.* 1999), data from oocytes exhibiting currents $> 25\ \mu$A at −160 mV were rejected. Data acquisition and analysis were performed with pCLAMP 6.0 software (Axon Instruments, Foster City, CA, USA).

For cell-attached patch recordings, the vitelline membrane was manually removed after exposing oocytes to a hypertonic solution (400 mosmol (kg H_2O)$^{-1}$: 220 mM NMDG-Cl, 5 mM EGTA-KOH, 1 mM $MgCl_2$, 10 mM Hepes) for 5–10 min. Patch pipettes were pulled from 7052 glass tubing (o.d. = 1.65 mm, i.d. = 1.2 mm, Garner Glass, Claremont, CA, USA) and heat-polished to a resistance in the range 0.5–2 MΩ. Currents were recorded with an Axopatch 200 amplifier (Axon Instruments) with the built-in low pass filter set to 4 kHz.

Experiments on isolated bovine RPE cells

Cell isolation. Adult bovine eyes were obtained from a local abattoir within 30 min of death and placed on ice. Cells were isolated by enzymatic dispersion as described previously (Hughes & Takahira, 1998). Briefly, 5 mm-square pieces of RPE–choroid were dissected from the inferior and superior pigmented regions of bovine eyecups and incubated for 30 min at 37 °C in cell isolation medium (135 mM NMDG-Cl, 5 mM KCl, 10 mM Hepes, 3 mM EDTA-KOH, 10 mM glucose, 3 mM cysteine, 0.2 mg ml^{-1} papain (type III), titrated to pH 7.4 with NMDG-free base). The tissue was then incubated in standard bath solution containing 0.1 % BSA for 3 min and finally in standard bath solution alone for another 10 min before dislodging cells by gentle vortexing. As described previously for frog (Hughes & Steinberg, 1990) and human RPE cells (Hughes *et al.* 1995*b*), isolated bovine RPE cells had a 'dumb-bell' shape, with a smooth basolateral membrane domain and an apical membrane domain often containing long processes. Cells were stored in standard bath solution at 4 °C for up to 24 h before use.

Solutions. The standard bath solution for experiments on isolated RPE cells consisted of (mM): 135 NaCl, 5 KCl, 10 Hepes, 10 glucose, 1.8 $CaCl_2$, 1.0 $MgCl_2$, titrated to pH 7.4 with NaOH. To study the dependence of the native Kir conductance on extracellular K^+, $[K^+]_o$ was varied by equimolar replacement with Na^+. In experiments investigating the permeability of Kir conductance to monovalent cations, the control solution consisted of (mM): 140 X, 10 NMDG-Hepes, 10 mM glucose, 1.8 $CaCl_2$, and 1.0 $MgCl_2$, where X is KCl, NaCl, RbCl, LiCl, or CsCl (pH 7.4). In an effort to isolate Kir currents, Cl^- channels and the electrogenic Na^+–HCO_3^- cotransporter were blocked by adding 250 μM 4,4′-diisothiocyanato-stilbene-2,2′-disulfonic acid (DIDS) to all solutions as a concentrated DMSO stock solution (final concentration of DMSO was 0.05 %). In addition, 100 μM $GdCl_3$ was added to block non-specific cation channels. Neither of these blockers had obvious effects on either the kinetics or voltage dependence of inwardly rectifying K^+ currents.

The pipette solution used for whole-cell recording consisted of (mM): 30 KCl, 83 potassium gluconate, 10 Hepes, 5.5 EGTA-KOH, 0.5 $CaCl_2$, 2 $MgCl_2$, 4 ATP dipotassium salt, titrated to pH 7.2 with KOH. The osmolarities of external and internal solutions were 290 ± 10 and 245 ± 5 mosmol (kg H_2O)$^{-1}$, respectively. All chemicals were of reagent grade and obtained from Sigma Chemical except for papain, which was obtained from Aldrich Chemical (Milwaukee, WI, USA).

Electrophysiological recording. Isolated RPE cells were transferred to a continuously perfused Lucite recording chamber on the stage of an inverted microscope (Segawa & Hughes, 1994). All experiments were conducted at room temperature (23–25 °C). Pipettes were pulled from 7052 glass tubing (o.d.= 1.65 mm, i.d. = 1.2 mm, Garner Glass) with a multistage programmable puller and heat-polished to a resistance in the range 1–3 MΩ before use. Membrane currents were recorded using the conventional whole-cell or cell-attached patch recording configuration of the patch-clamp technique (Hamill *et al.* 1981). Currents were amplified with an Axopatch 200 amplifier (Axon Instruments) with the built-in low pass filter set to 1 kHz (unless noted otherwise), digitized and stored on a computer hard drive for later analysis. In whole-cell recordings, series resistance (R_s) and membrane capacitance (C_m) averaged 6.5 ± 5.2 MΩ and 63.4 ± 12.6 pF, respectively ($n = 25$). To minimize voltage errors when recording large inward Rb^+ currents, R_s was compensated 70–80 % with the internal circuitry of the amplifier. Command potentials were generated by software control (pCLAMP 6, Axon Instruments).

In addition to the inwardly rectifying K^+ (Kir) current, most bovine RPE cells also expressed a delayed rectifier K^+ current and some had an M-type K^+ current as well (Takahira & Hughes, 1997). The delayed rectifier current was inactivated by holding the membrane potential at 0 mV between voltage steps and ramps. Cells exhibiting M-type K^+ currents were excluded from the present study.

Voltage-clamp protocols and analysis

Current voltage (I–V) relationships were constructed using data obtained from either voltage-ramp or voltage-step protocols. In the voltage-ramp protocol, the membrane potential was held at 0 mV and then ramped every 15 s from +60 to −160 mV over a 4 s period. In the voltage-step protocol, the membrane potential was held at 0 mV and stepped for 1 s to voltages ranging from +50 to −150 mV in 10 mV steps (oocyte) or from +40 to −160 mV in 20 mV steps (RPE).

Selectivity for monovalent cations was determined under bi-ionic conditions by substituting Rb^+, Na^+, Li^+, or Cs^+ for K^+ in the bathing solution. Permeability ratios, P_X/P_K, were calculated according to a modified form of the Goldman-Hodgkin-Katz voltage equation (Hille, 1992):

$$E_X - E_K = (RT/zF)\ln(P_X/P_K), \quad (1)$$

where E_X is the reversal potential with 98 mM (oocytes) or 140 mM (RPE cells) cation X in the bath, z is the valancy, and R, T and F have their usual meanings. Relative conductance was calculated by measuring the inward slope conductance (g_X) between −140 and −160 mV for each monovalent cation and normalizing it to the slope conductance obtained with K^+ in the bath.

To investigate the relationship between membrane voltage (V_m), conductance and $[K^+]_o$, the chord conductance (G_X) was determined according to the equation:

$$G_X = I/(V_m - E_X), \quad (2)$$

where I is the amplitude of the whole-cell current and E_X is the apparent reversal potential with 98 mM (oocytes) or 140 mM (RPE cells) cation X in the bath.

Non-stationary noise analysis was carried out essentially as described (Heinemann & Conti, 1992; Jackson & Strange, 1996; Traynelis & Jaramillo, 1998). The activity of a specific population of channels gives rise to a macroscopic current (I), which can be defined as:

$$I = N i P_o, \quad (3)$$

where N is the number of channels in the membrane, i is the current flowing through a single channel and P_o is the channel open

probability. Analysis of 'noise' in macroscopic current can be used to estimate the single-channel current (and, therefore, the unitary conductance) and the number of channels in the membrane. Assuming that the membrane contains N independent and identical channels having two conductance states, open and closed, and that graded changes in macroscopic current are due to graded changes in channel open probability, then the current noise or variance, σ^2, is given by:

$$\sigma^2 = iI - I^2/N. \quad (4)$$

By measuring the variance of the mean macroscopic current during different levels of channel activity, channel size and density can be estimated. Because both Kir7.1 and RPE Kir currents are essentially time independent, we applied Ba^{2+}, a voltage-dependent blocker, to produce a time-dependent change in channel open probability.

Data are given as means ± S.E.M. and were fitted using computer software (SigmaPlot 4.0, SPSS Inc., Chicago, IL, USA).

RESULTS

Identification and cloning of human Kir7.1

Random sequencing of cDNA clones from a subtracted bovine RPE cDNA library (Chang *et al.* 1997, 1999) led to the identification of a novel cDNA having sequence similarity with ROMK2. We used this cDNA as a probe to screen a human RPE cDNA library and identified more than 10 positive clones. One of the cDNA clones, pc84, contained the largest cDNA insert (2.4 kb) and was completely sequenced. Analysis of the sequencing data indicated that pc84 contained the entire coding sequence for a Kir7.1 channel subunit as well as a partial 3′ end-sequence (data not shown). The open reading frame encodes a 360-amino acid polypeptide that is identical to that reported previously for human Kir7.1 (Döring *et al.* 1998; Krapivinsky *et al.* 1998; Partiseti *et al.* 1998).

Tissue distribution

Figure 1*A* shows a Northern blot of RNA isolated from various bovine tissues hybridized with a *Kir7.1* probe. A strong 1.6 kb signal was detected in the RPE but not the neural retina or any other tissues examined, despite the fact that the RPE lane contained less RNA (Fig. 1*B*). These results indicate that *Kir7.1* is highly expressed in the RPE. It should be noted, however, that previous studies reported a wider expression pattern for *Kir7.1* (Döring *et al.* 1998; Krapivinsky *et al.* 1998; Partiseti *et al.* 1998; Nakamura *et al.* 1999, 2000). The reason for the apparent difference from our results is unclear. Although our Northern blot did not include several of the tissues in which *Kir7.1* expression has been reported, it did include brain, kidney and testis. It is possible that our Northern blots were less sensitive than the reverse transcription and Northern assays used by others. In addition, the results presented here may reflect species-specific differences in expression pattern because the previous studies were done with rat and/or human tissues while our studies were done with bovine tissues.

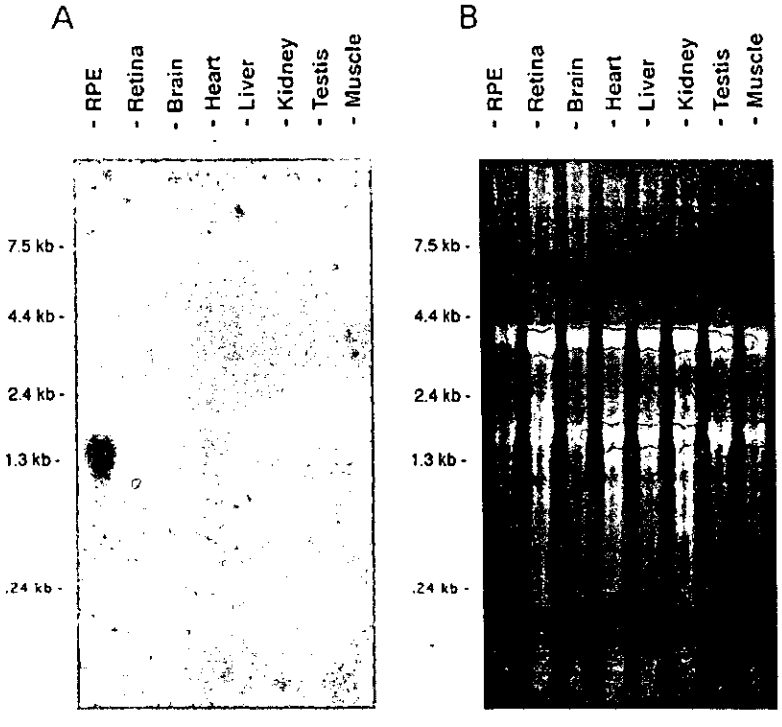

Figure 1. Kir7.1 is highly expressed in the RPE

A, Northern blot analysis of total RNA (10 μg lane^{-1}) extracted from bovine RPE, retina and other tissues and hybridized with human *Kir7.1* probe. *B*, the same RNA gel stained with ethidium bromide.

Functional expression of Kir7.1 in *Xenopus* oocytes

Basic properties

When bathed in the standard 2 mM K^+ solution, Kir7.1 cRNA-injected oocytes typically had a large negative membrane potential and exhibited inwardly rectifying currents. Figure 2*A* (upper panel) depicts a representative family of currents recorded from a Kir7.1 cRNA-injected oocyte. Inward currents activated rapidly in response to hyperpolarizing voltage pulses, whereas outward currents evoked by depolarizing pulses underwent a time-dependent inactivation. The steady-state I–V relationship generated by a 4 s voltage ramp in the same oocyte exhibited mild inward rectification, with relatively large outward currents at voltages positive to V_0, the zero current potential (Fig. 2*B*). Addition of 10 mM Ba^{2+} to the bath blocked virtually all of the Kir7.1 current, unmasking an endogenous Ca^{2+}-activated Cl^- current at voltages positive to about −20 mV. For 10 Kir7.1 cRNA-injected oocytes, V_0 averaged −99.5 ± 6.8 mV and the chord conductance (G) measured at −160 mV averaged 18.4 ± 1.5 μS (mean ± S.E.M.).

Permeation properties

Previous studies by Krapavinsky *et al.* (1998) and Döring *et al.* (1998) showed that, unlike other native and cloned Kir channels, the macroscopic Kir7.1 conductance exhibits a low dependence on extracellular K^+ concentration ($[K^+]_o$). In addition, Wischmeyer *et al.* (2000) recently reported that although Kir7.1 has a monovalent cation permeability sequence of $K^+ > Rb^+$, it has a macroscopic Rb^+ conductance that is about 8-fold larger than its K^+ conductance. To allow a direct comparison to the native Kir conductance in RPE cells (see *Properties of native Kir channels in bovine RPE* below), we re-examined the dependence of macroscopic Kir7.1 conductance on $[K^+]_o$ as well as its permselectivity to monovalent cations.

Figure 3*A* shows a series of representative I–V relationships obtained from a single Kir7.1 cRNA-injected oocyte. Increases in $[K^+]_o$ caused positive shifts in V_0 and decreased the slope of the I–V relationship in the vicinity of V_0. Outward currents, however, were affected, becoming smaller as $[K^+]_o$ was increased. Figure 3*B* plots the mean values of V_0 ($n = 6$) as a function of $[K^+]_o$, and the straight line is the least squares fit of the data with a slope of 55.6 mV per 10-fold change in $[K^+]_o$. This K^+-induced change in V_0 coincides well with the change in E_K calculated by the Nernst equation (58 mV), indicating that the Kir7.1 conductance is highly selective for K^+ over Na^+.

To evaluate the dependence of Kir7.1 conductance on $[K^+]_o$, we calculated chord conductance (G) from the data in Fig. 3*A* and plotted it as a function of membrane voltage (V). Figure 3*C* shows that both the shape of the G–V curve and its position along the x-axis changed as $[K^+]_o$ was varied. In the presence of 1 and 2 mM K^+, the shape of the G–V curve was sigmoidal, but at higher

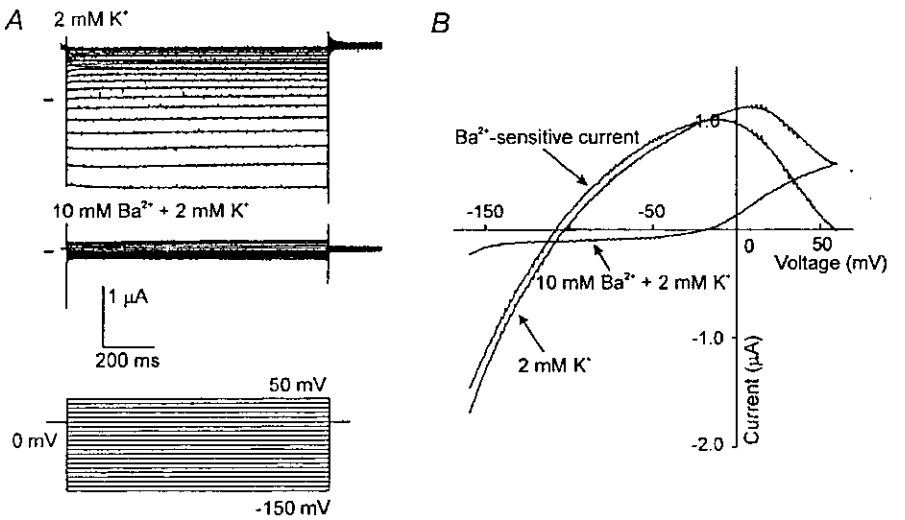

Figure 2. Characterization of macroscopic Kir7.1 currents

A, families of currents measured from a Kir7.1 cRNA-injected *Xenopus* oocyte bathed with standard (2 mM K^+) solution in the absence (upper panel) and presence (middle panel) of 10 mM Ba^{2+}. The horizontal line to the left of the records indicates the zero-current level. The voltage protocol used to evoke these currents is shown below. *B*, I–V relationships obtained from the same oocyte using the voltage-ramp method.

concentrations the curve was exponential, perhaps because the test voltages were not large enough to produce saturation. As a consequence of the G–V curves crossing over at large negative potentials, the relationship between $[K^+]_o$ and conductance depended on voltage. At −160 mV, the most negative voltage examined, chord conductance increased slightly with increasing $[K^+]_o$, as reported previously (Döring *et al.* 1998). In contrast, at more positive potentials, the macroscopic Kir7.1 conductance decreased with increasing $[K^+]_o$.

In order to differentiate between the effects of $[K^+]_o$ on outward and inward conductances, we re-plotted the data as a function of driving force, $V_m - E_K$ (Fig. 3*D*). The results demonstrate that at voltages near E_K, both outward and inward conductances decreased with increasing $[K^+]_o$, although the changes were small at concentrations greater than 50 mM. Similar results were obtained in five other oocytes. This behaviour is contrary to that of other members of the Kir channel family, whose macroscopic conductance typically saturates with voltage and increases in proportion to the square root of $[K^+]_o$. The mechanism underlying the unusual behaviour of Kir7.1 is not known, but obviously must involve changes in single-channel conductance, open probability, or both.

We investigated the permselectivity of Kir7.1 channels under bi-ionic conditions by superfusing oocytes with solutions containing various monovalent cations (intracellular $[K^+]$ was presumed to remain constant). Figure 4*A* shows families of whole-cell currents recorded from an oocyte bathed with either K^+, Rb^+, Li^+, Na^+, or Cs^+ as the sole monovalent cation; the corresponding I–V relationships averaged from nine oocytes are shown in Fig. 4*B* and, at a different scale, Fig. 4*C*. Compared to the currents in K^+, the maximal inward currents in Na^+, Li^+ and Cs^+ external solutions were smaller, whereas those in Rb^+ were nearly 10 times larger. It is interesting to note that at depolarized voltages, the Rb^+ slope conductance was actually somewhat smaller than the K^+ conductance (not apparent in averaged experiments) and that it increased dramatically near −50 mV, roughly 40 mV negative to the apparent reversal potential. The significance of this

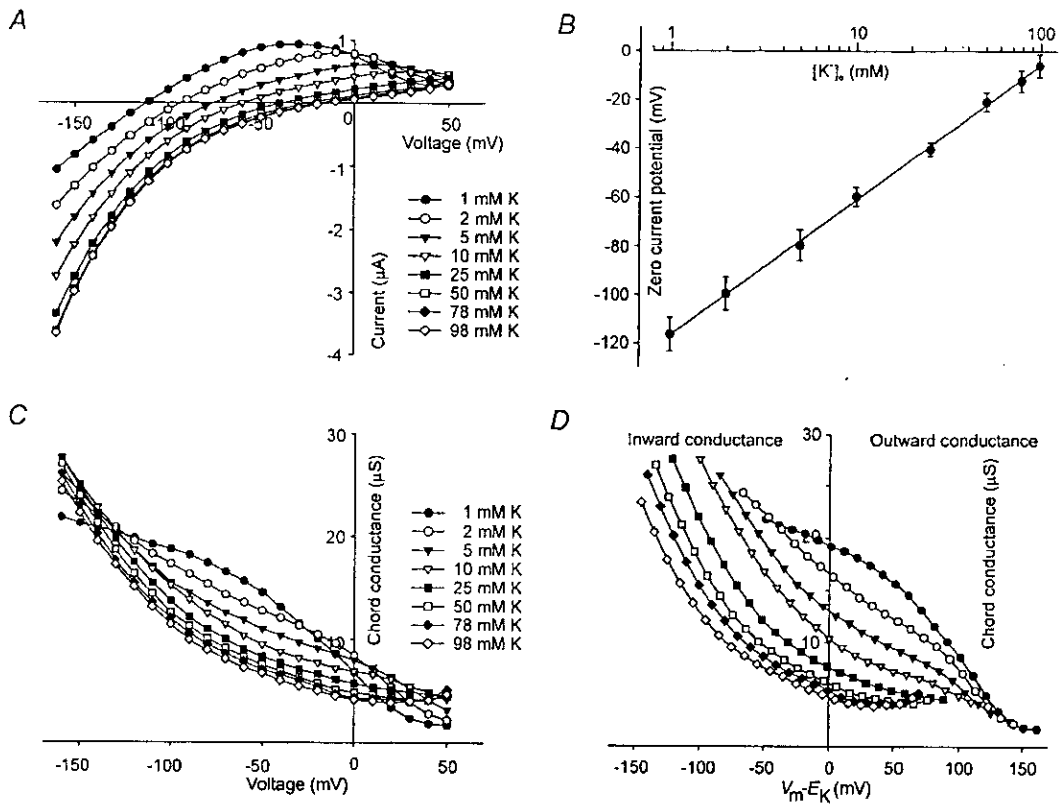

Figure 3. Dependence of Kir7.1 current and conductance on $[K^+]_o$

A, current–voltage relationships obtained from a single Kir7.1 cRNA-injected oocyte bathed with various $[K^+]_o$. Data were generated from currents evoked by voltage steps. *B*, relationship between zero current potential and $[K^+]_o$. Each filled circle and vertical bar indicates the mean and S.E.M. for 12 oocytes. The continuous line shows the linear regression fit to the data. *C*, relationship between conductance and membrane voltage. Chord conductance was calculated from the data in *A*. *D*, relationship between conductance and driving force. The same data in *C* plotted as a function of $V_m - E_K$.

'activation potential' is unclear, but may reflect channel gating or the relief from block by some intracellular ion. The selectivity sequence calculated from relative slope conductances (g_X/g_K) in the voltage range −140 to −160 mV was: Rb^+ (9.5) ≫ K^+ (1.0) > Na^+ (0.46) > Cs^+ (0.33) > Li^+ (0.14) (Table 1). These results are similar to those previously reported by Wischmeyer *et al.* 2000).

Replacement of external K^+ with Na^+, Li^+, or Cs^+ caused V_0 to shift to more negative potentials, whereas replacement with Rb^+ left V_0 virtually unchanged (Fig. 4*C*). Although it is common to substitute V_0 for reversal potential (E_{rev}) in the calculation of permeability ratios (eqn (1)), this practice can lead to significant errors due to the impact of endogenous channels, particularly when the current of interest is small. In an attempt to circumvent this problem, we applied 10 mM Ba^{2+} to the bath in the presence of various monovalent cations and measured the reversal potential of Ba^{2+}-sensitive currents. When Na^+, Li^+, or Cs^+ was in the bath, E_{rev} was significantly more negative than the corresponding value of V_0 (Fig. 5*C*, *D* and *E*; Table 1). In contrast, when K^+ or Rb^+ was in the bath, E_{rev} could not be estimated by this method because the Ba^{2+}-induced block of current was strongly voltage dependent (Fig. 5*A* and *B*). The relationship between V_0 and $\log[K^+]_o$ (Fig. 3*B*) indicates

Table 1. Permeability and conductance ratios for the Kir7.1 conductance

Ion (X)	V_0 (mV) ($n = 9$)	E_{rev} (mV) ($n = 5$)	P_X/P_K	g_X/g_K
K^+	−8.4 ± 2.3	—	1	1
Rb^+	−10.8 ± 1.1	—	0.886 ± 0.045	9.503 ± 1.548
Na^+	−136.9 ± 6.4	−156.1 ± 3.3	0.003 ± 0.001	0.458 ± 0.011
Li^+	−126.6 ± 5.6	−160.5 ± 2.0	0.002 ± 0.001	0.139 ± 0.012
Cs^+	−37.6 ± 3.7	−116.6 ± 3.2	0.013 ± 0.004	0.331 ± 0.035

that for external K^+, E_{rev} must lie close to the measured value of V_0. Assuming that this is also true for Rb^+, we obtain a permeability sequence of K^+ (1.0) ≈ Rb^+ (0.89) > Cs^+ (0.013) > Na^+ (0.003) ≈ Li^+ (0.002) ($n = 5$) (Table 1), in agreement with the results of Wischmeyer *et al.* (2000).

In addition to changes in V_0 and inward slope conductance, substitution of K^+ with other monovalent cations also affected the size of outward currents (Fig. 4*C*). The magnitude of outward current was considerably larger in the presence of extracellular Na^+ or Li^+ than it was in K^+, Rb^+, or Cs^+, and most of this current was blocked by 10 mM Ba^{2+} (Fig. 5*C* and *D*), indicating that it represented outward K^+ current through Kir7.1 channels. The magnitude of outward Kir7.1 current in the presence of

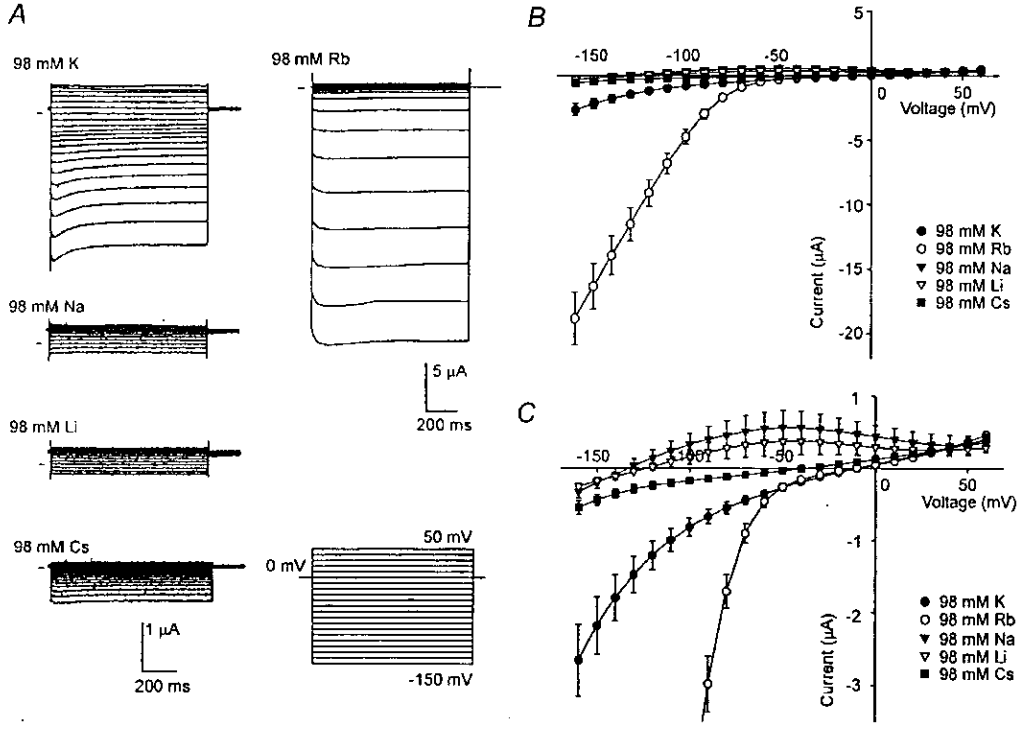

Figure 4. Effect of cation substitution on Kir7.1 conductance

A, macroscopic currents recorded from a representative Kir7.1 cRNA-injected oocyte bathed in 98 mM K^+, Na^+, Li^+, Cs^+, or Rb^+. Currents were evoked by the voltage-step protocol indicated. *B*, current–voltage relationships obtained with various monovalent cations in the bath. Each point and vertical bar represents the mean ± S.E.M. for 9 oocytes. *C*, same data as in *B* but at a higher gain to show zero current potentials. Connecting lines have no theoretical significance.

external K^+ or Rb^+ is difficult to estimate because the Ba^{2+}-induced block was strongly voltage dependent in these cases. It seems likely, however, that a significant fraction of K^+ outward current observed in the presence of external K^+ or Rb^+ was mediated by endogenous channels. In the presence of external Cs^+, only inward currents at large negative potentials were blocked (Fig. 5*E*), suggesting that Cs^+ behaves as a permeant blocker. We conclude that outward K^+ current through Kir.71 channels is considerably greater in the presence of external Na^+ and Li^+ than it is in the presence of external K^+, Rb^+, or Cs^+. The reason for these differences is unclear, but the mechanism might involve specific cation interactions with extracellular domains of the channel, influencing gating or perhaps the permeation pathway itself.

Non-stationary noise analysis

In a previous study on Kir7.1 channels expressed in mammalian cells, Krapivinsky and colleagues (1998) recorded currents from cell-attached patches and used non-stationary noise analysis to estimate that Kir7.1 has a single-channel conductance of ~50 fS. We attempted to confirm these results in cell-attached recordings from Kir7.1 cRNA-injected oocytes, but when the pipette contained 98 mM K^+, we failed to observe inwardly rectifying currents in 12 patches. Because the macroscopic Kir7.1 current increased roughly 10-fold when Rb^+ was substituted for K^+ (Fig. 4), we reasoned that Kir7.1 currents in cell-attached patches might be better resolved by using Rb^+ as the charge carrier. Indeed, when K^+ in the pipette was replaced with Rb^+, we routinely recorded inwardly rectifying currents. Figure 6*A* shows

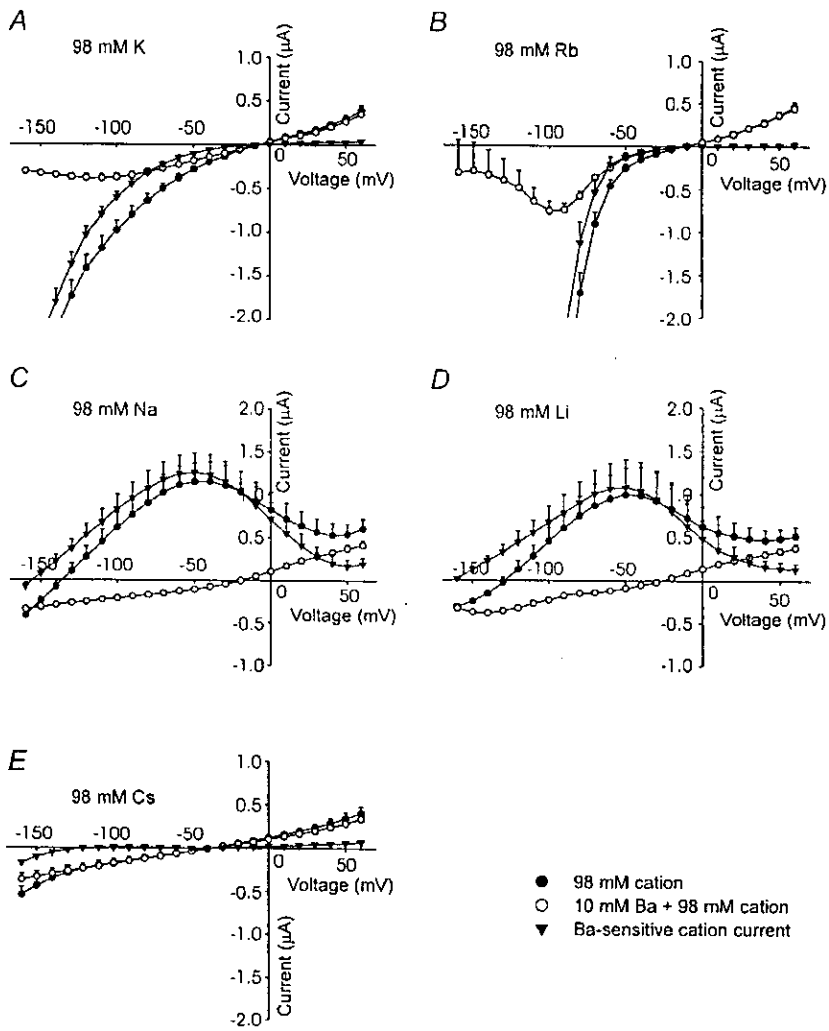

Figure 5. Determination of the reversal potential of Kir7.1 currents from Ba^{2+}-sensitive currents

Panels depict averaged I–V relationships obtained in the presence and absence of 10 mM Ba^{2+} with either 98 mM K^+ (*A*), Rb^+ (*B*), Na^+ (*C*), Li^+ (*D*) or Cs^+ (*E*) as the sole monovalent cation ($n = 5$). Ba^{2+}-sensitive currents are also depicted.

representative recordings obtained with 98 mM Rb^+ and 1 mM Ba^{2+} in the recording pipette. Instantaneous currents were inwardly rectifying, with a sharp increase in conductance at about −50 mV (Fig. 6*B*, ○), reminiscent of whole-cell Rb^+ currents (Fig. 4*B*). Inward Rb^+ currents exhibited a time-dependent decay due to a voltage-dependent block by Ba^{2+} (Fig. 6*C*, ●), allowing the estimation of single-channel current (i) and number of channels (N) by non-stationary noise analysis. Figure 6*C* plots current variance *vs.* mean current amplitude calculated from 40 successive current records elicited by voltage steps from 0 mV to −100 mV and the smooth curve is the least squares fit of the data to eqn (4), with values for i and N of 0.31 pA and 2861, respectively. Similar results were obtained in five other cell-attached patches, yielding an average single-channel chord conductance of 2.27 ± 0.26 pS.

Properties of native Kir channels in bovine RPE

Basic properties

As reported previously, isolated bovine RPE cells exhibited a prominent inwardly rectifying K^+ current (Hughes & Takahira, 1998). Figure 7 shows that in the presence of 5 mM $[K^+]_o$, the I–V relationship was mildly inwardly rectifying, with substantial outward currents at voltages positive to V_0. Most of this current was blocked by the addition of 10 mM Ba^{2+} to the bath, which unmasked a small outwardly rectifying current that reversed near the Cl^- equilibrium potential.

Permeation properties

We previously showed that the Kir conductances in toad (Segawa & Hughes, 1994) and human RPE cells (Hughes & Takahira, 1996) are inversely dependent on extracellular $[K^+]_o$. We confirmed and extended these findings in bovine RPE cells by measuring changes in conductance over a wider range of $[K^+]_o$. Figure 8*A* shows that increasing $[K^+]_o$ shifted the I–V relationship obtained from a representative cell to the right and decreased the slope of the I–V relationship near V_0. A plot of V_0 *vs.* $\log[K^+]_o$ (Fig. 8*B*) revealed a linear relationship that was close to that predicted by the Nernst equation (55.6 mV *vs.* 58 mV per 10-fold change in $[K^+]_o$), indicating that under our present recording conditions, the K^+

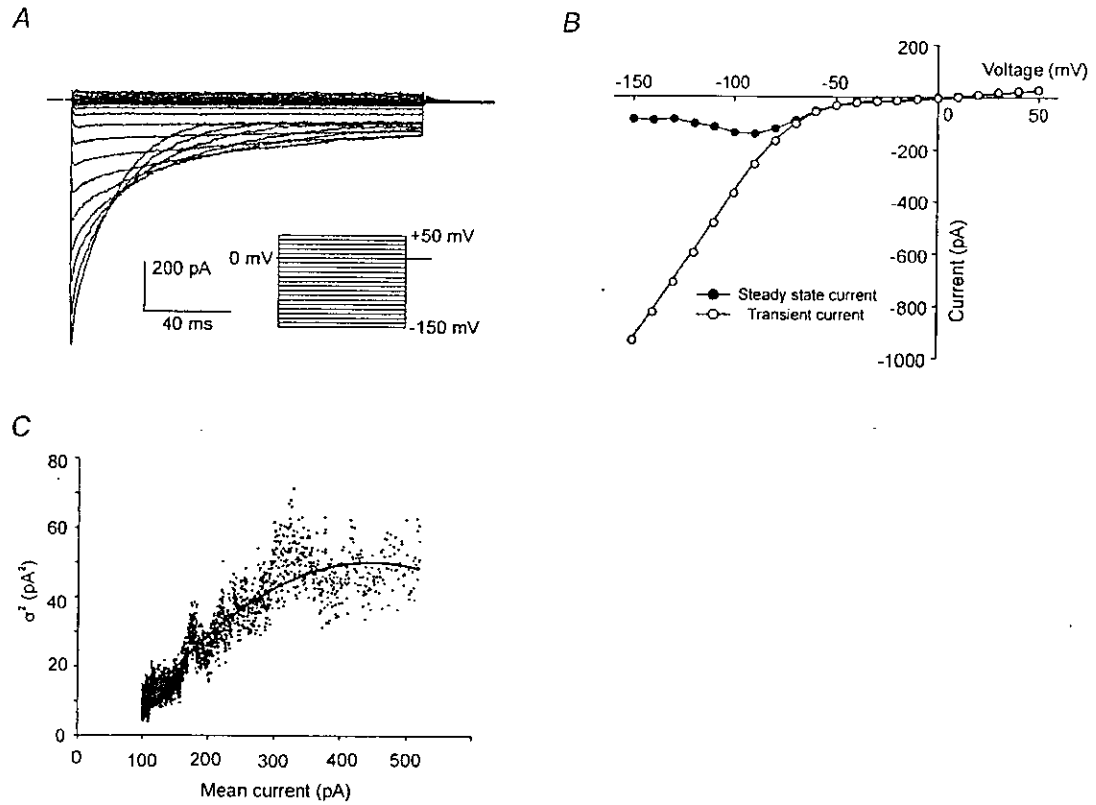

Figure 6. Non-stationary noise analysis of Kir7.1 Rb^+ currents

A, family of currents recorded from a cell-attached patch on a Kir7.1 cRNA injected oocyte with 98 mM Rb^+ and 1 mM Ba^{2+} in the pipette. The bath contained 98 mM K^+ external solution to depolarize the membrane potential. *B*, I–V relationships obtained from the currents in *A* measured 2.5 ms (○) and 167 ms (●) after the onset of the voltage step. *C*, relationship between current variance (σ^2) and mean current from the same patch as in *A*. See text for additional details.

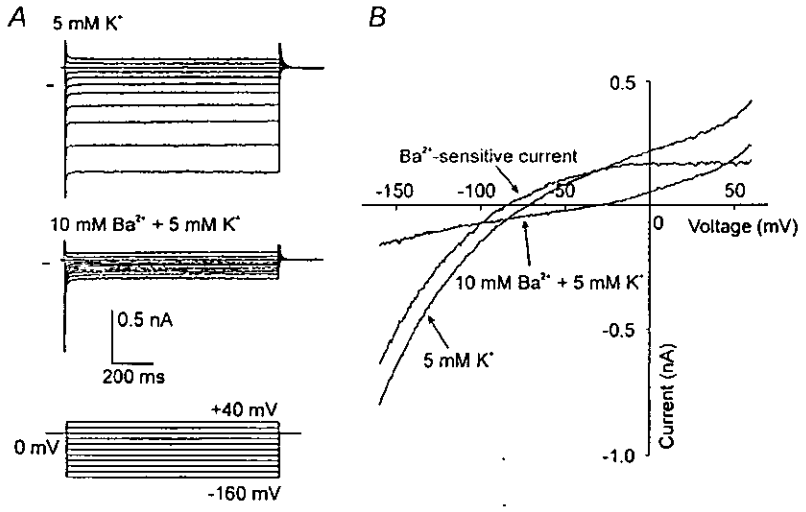

Figure 7. Properties of the Kir current in the RPE

A, families of whole-cell currents recorded from an isolated bovine RPE bathed with standard (5 mM K^+) solution in the absence (upper panel) and presence of 10 mM Ba^{2+} (middle panel). The voltage protocol used to evoke these currents is shown below. *B*, *I–V* relationships obtained from the same cell as in *A* using a voltage-ramp protocol.

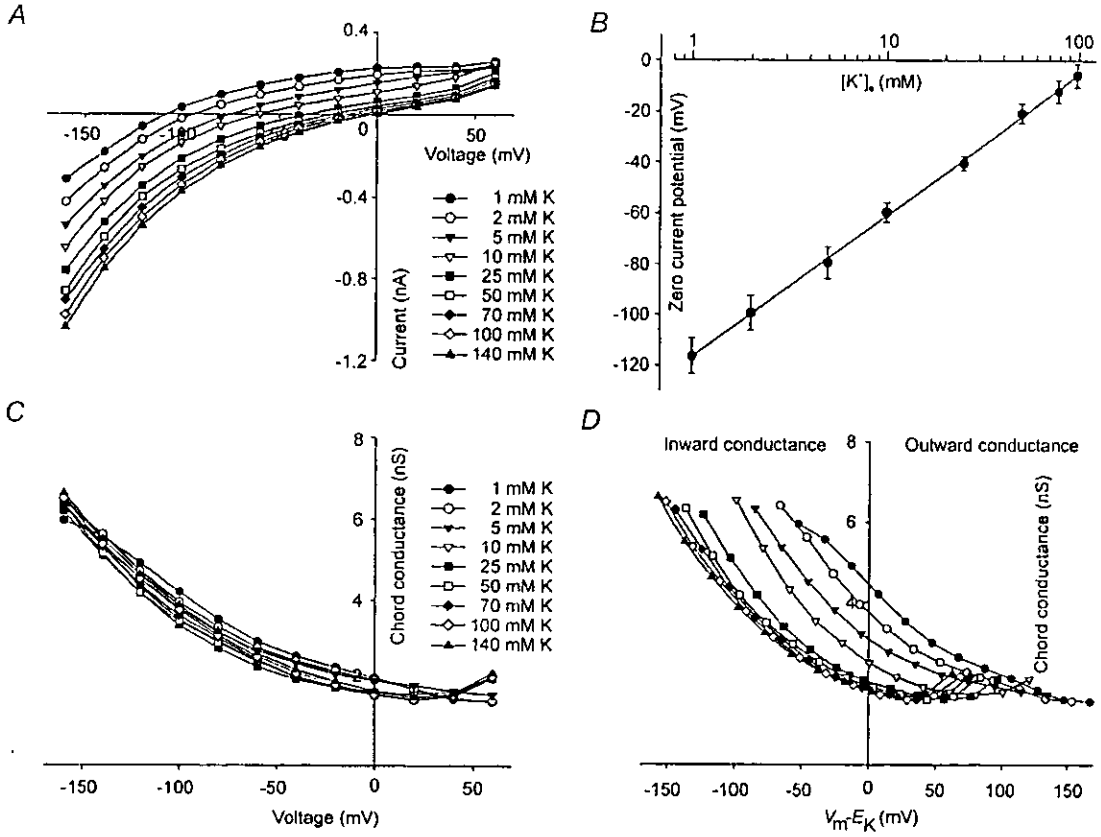

Figure 8. Dependence of RPE Kir currents on $[K^+]_o$

A, *I–V* relationships obtained from a single bovine RPE cell bathed with various $[K^+]_o$. Data were generated from currents evoked by voltage steps. *B*, relationship between zero current potential and $[K^+]_o$. Each filled circle and vertical bar indicates the mean ± S.E.M. for 8 cells. The continuous line shows the linear regression fit to the data. *C*, relationship between conductance and membrane voltage. Chord conductance was calculated from the data in *A*. *D*, relationship between conductance and driving force. The same data in *C* plotted as a function of $V_m - E_K$.

conductance accounted for roughly 95 % of the whole-cell conductance of bovine RPE cells.

To evaluate the dependence of the Kir conductance on $[K^+]_o$ and voltage, we calculated chord conductance from the data in Fig. 8*A* and plotted it as a function of membrane voltage (Fig. 8*C*). The *G–V* curve was nearly the same at all K^+ concentrations, although conductance at given voltage in the range −120 to + 10 mV was slightly higher at lower concentrations. When conductance was plotted as a function of driving force (Fig. 8*D*), an effect $[K^+]_o$ on inward and outward conductances could be clearly seen. In the K^+ concentration range 1–25 mM, inward and outward conductances decreased with increases in $[K^+]_o$, but they changed little when $[K^+]_o$ was increased further. Similar results were obtained in five other cells. Thus, despite some quantitative differences, the RPE Kir conductance responds to changes in $[K^+]_o$ in a manner that is qualitatively similar to that of Kir7.1 but opposite to that typical of other Kir channels.

In addition to its similarity to the Kir7.1 conductance with regard to its inverse dependence on $[K^+]_o$, the RPE

Table 2. Permeability and conductance ratios for the RPE Kir conductance

Ion (X)	V_0 (mV) ($n = 11$)	E_{rev} (mV) ($n = 5$)	P_X/P_K	g_X/g_K
K^+	−7.3 ± 0.7	—	1	1
Rb^+	−10.4 ± 1.3	—	0.811 ± 0.138	8.889 ± 0.041
Na^+	−141.9 ± 2.4	−153.2 ± 6.3	0.003 ± 0.001	0.585 ± 0.097
Li^+	−123.1 ± 1.8	−157.4 ± 3.3	0.002 ± 0.001	0.083 ± 0.012
Cs^+	−41.4 ± 2.9	−105.8 ± 3.9	0.021 ± 0.006	0.225 ± 0.053

Kir conductance also shares other unusual permeation properties. Figure 9*A* shows a representative family of *I–V* relationships recorded from a single bovine RPE cell under bi-ionic conditions. For all monovalent cations tested, the *I–V* curve showed inward rectification, but the magnitude of inward currents was substantially greater when Rb^+ was in the bath (Fig. 9*B*). As was true for the macroscopic Kir7.1 conductance, inward Rb^+ current through RPE Kir conductance exhibited an activation potential near −50 mV. The selectivity sequence calculated from inward slope conductances in the voltage range −140 to −160 mV was: Rb^+ (8.9) ≫ K^+ (1.0) > Na^+

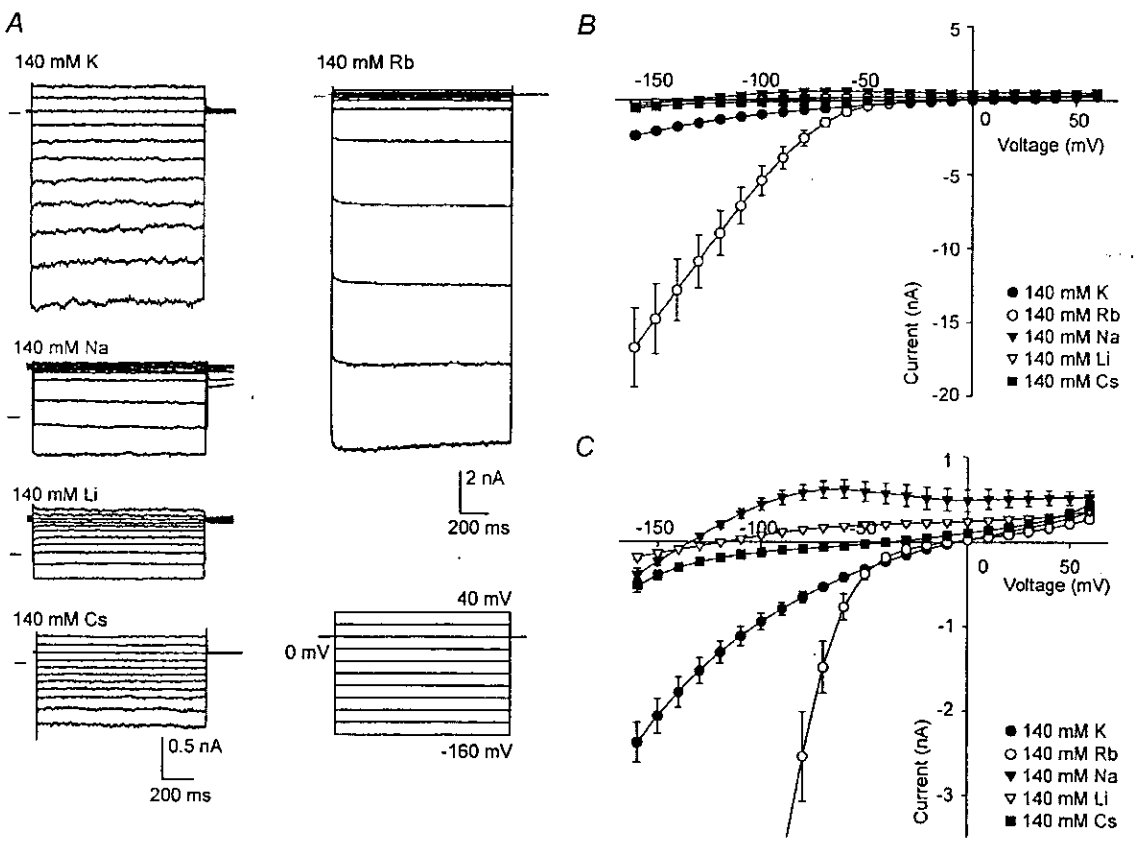

Figure 9. Effect of cation substitution on the RPE Kir conductance

A, macroscopic currents recorded from a representative bovine RPE cell bathed in 140 mM K^+, Na^+, Li^+, Cs^+, or Rb^+. Currents were evoked by the voltage-step protocol indicated. *B*, *I–V* relationships obtained with various monovalent cations in the bath. Each point and vertical bar represent mean and S.E.M. for 11 RPE cells. *C*, same data as in *B* but at a higher gain to show zero current potentials. Connecting lines have no theoretical significance.

(0.59) > Cs^+ (0.23) > Li^+ (0.08) (Table 2). These values are nearly identical to those obtained for Kir7.1 (Table 1).

Figure 9*C* depicts the same *I–V* curves as in Fig. 9*B* but at a higher gain to show the effect of cation substitution on V_0. Replacement of external K^+ with Rb^+ had little effect on V_0, but replacement with Na^+, Li^+, or Cs^+ caused V_0 to shift to more negative potentials (Table 2). Because of the influence of residual Cl^- and Na^+ currents, these changes in V_0 may underestimate the actual changes in E_{rev}. Therefore, we applied 10 mM Ba^{2+} in the continued presence of the various monovalent cations (Fig. 10) to allow the estimation of E_{rev} from the reversal of Ba^{2+}-sensitive currents. When K^+ or Rb^+ was in the bath, the Ba^{2+} block was strongly voltage dependent, making it impossible to estimate E_{rev} from Ba^{2+}-sensitive currents. With external Cs^+, Na^+, or Li^+, however, the Ba^{2+}-sensitive current reversed at a potential that was significantly more negative than the corresponding value of V_0 (Fig. 10*C*, *D* and *E*; Table 2). Using these E_{rev} values for external Cs^+, Na^+ and Li^+ and V_0 values for K^+ and Rb^+, we calculate a permeability sequence of K^+ (1.0) ≈ Rb^+ (0.81) > Cs^+ (0.021) > Na^+ (0.003) ≈ Li^+ (0.002) (Table 2), which is nearly identical to that obtained for the cloned Kir 7.1 channel (Table 1).

The magnitude of outward currents also varied depending on the species of cation in the bath, being considerably larger in the presence of external Na^+ and, to a lesser extent, Li^+, than in the presence of K^+, Rb^+, or Cs^+ (Fig. 9*C*). External Ba^{2+} blocked the outward currents present with Na^+ or Li^+ in the bath (Fig. 10*C* and *D*), but

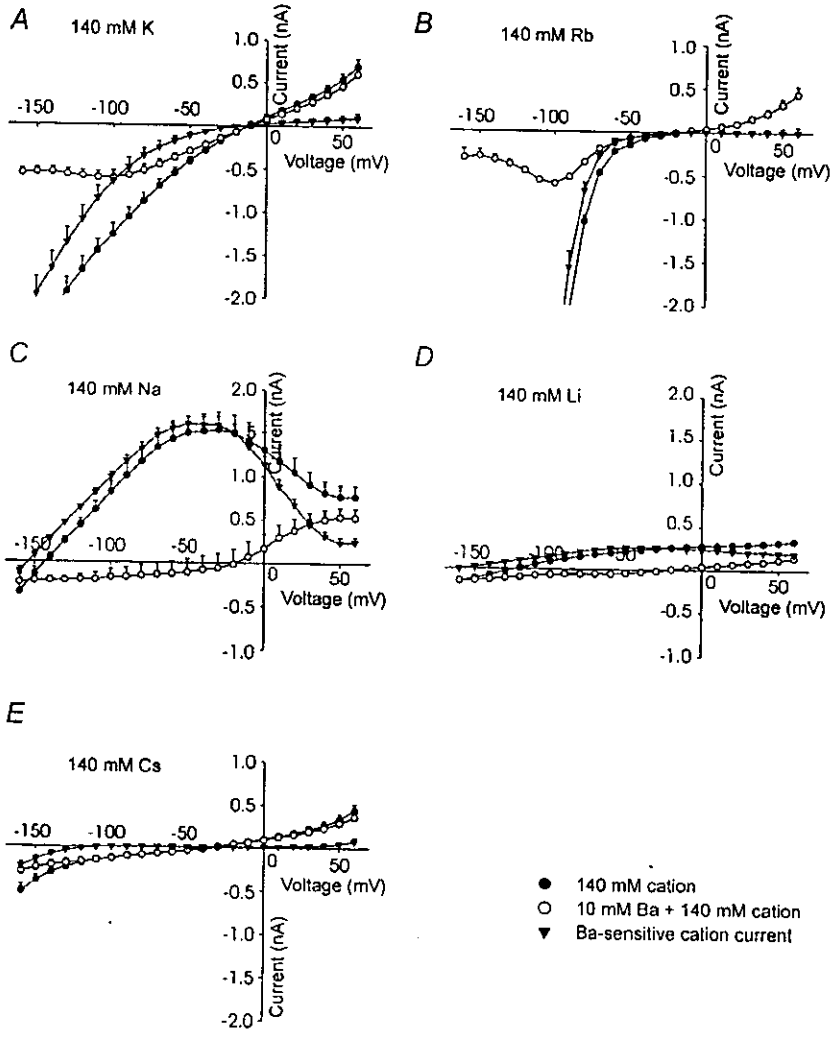

Figure 10. Determination of the reversal potential of RPE Kir currents from Ba^{2+}-sensitive currents

Panels depict averaged *I–V* relationships obtained in the presence and absence of 10 mM Ba^{2+} with either 140 mM K^+ (*A*), Rb^+ (*B*), Na^+ (*C*), Li^+ (*D*) or Cs^+ (*E*) as the sole monovalent cation ($n = 11$). Ba^{2+}-sensitive currents are also depicted.

had little effect on outward currents in the presence of K^+, Rb^+, or Cs^+ (Fig. 10*A*, *B* and *E*). Thus, like the cloned Kir7.1 channel, the RPE Kir channel appears to conduct outward K^+ current when either Na^+ or Li^+ is the sole monovalent cation in the bath, but little or no outward current when the bath contains K^+, Rb^+, or Cs^+.

Non-stationary noise analysis and localization of Kir channels to the RPE apical membrane

Electrophysiological studies on the intact RPE have demonstrated that the apical membrane has a large K^+ conductance (Lasansky & De Fisch, 1966; Miller, Steinberg & Oakley, 1978; Joseph & Miller, 1991) that is probably composed of inwardly rectifying channels (Hughes *et al.* 1995*a*). In numerous recordings from cell-attached patches of apical membrane on isolated bovine RPE cells, however, we failed to record unitary currents that could be attributed to a Kir channel, suggesting that the channel underlying the macroscopic Kir current may have a very low conductance. Consistent with this idea, the 'leak' current in some patches exhibited inward rectification (data not shown), but this was not studied further because of the low frequency of these observations. When we substituted Rb^+ for K^+ in the pipette, however, we routinely observed inwardly rectifying currents in apical membrane patches. Figure 11*A* shows a representative family of currents recorded from a cell-attached apical membrane patch with 140 mM Rb^+ plus 1 mM Ba^{2+} in the pipette. Instantaneous currents were inwardly rectifying, with a sharp increase in conductance at about −50 mV (Fig. 11*B*). With prolonged hyperpolarization, inward currents decayed with a mono-exponential time course, reflecting the voltage-dependent block of Kir channels by Ba^{2+}. Similar results were observed in nine of 12 apical membrane patches but in only one of 13 basolateral membrane patches. Hence, inwardly rectifying K^+ channels appear to be localized to the apical membrane of the RPE.

Figure 11*C* shows the results of non-stationary noise analysis of Kir currents recorded from the same apical membrane patch as that depicted in Fig. 11*A* and *B*. Mean current and variance were calculated from 40 current records evoked by voltage steps to −150 mV from a

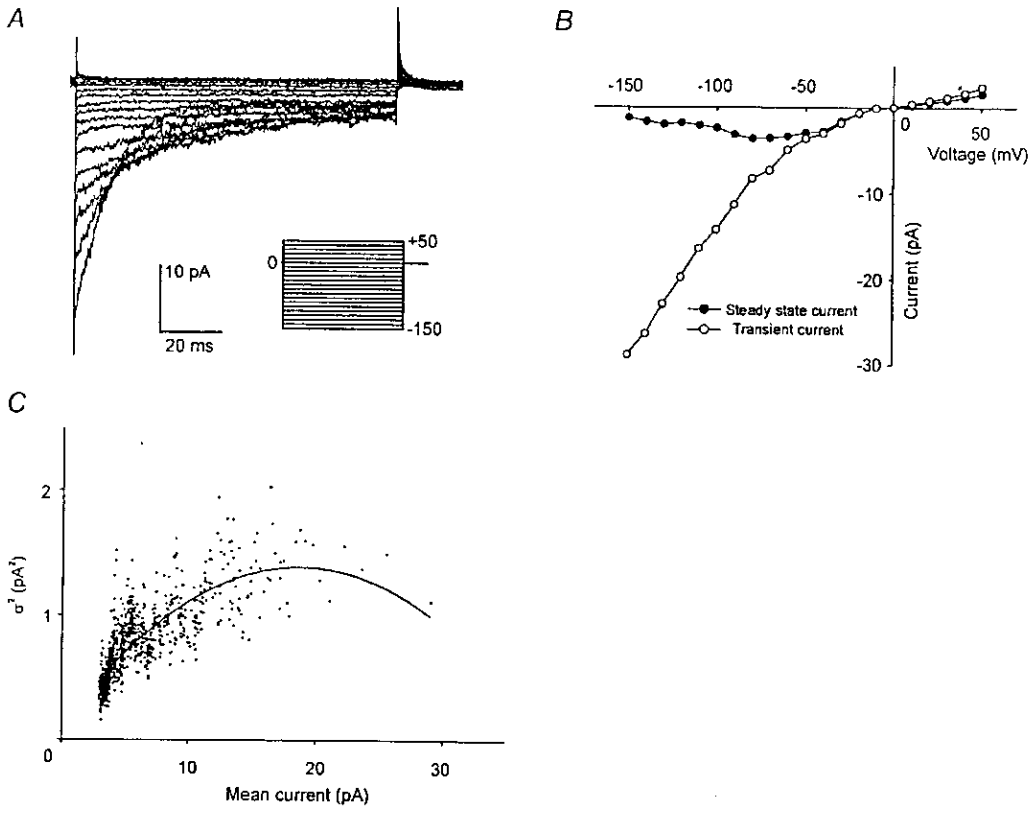

Figure 11. Non-stationary noise analysis of RPE Kir Rb^+ currents

A, family of currents recorded from a cell-attached patch on the apical membrane of a bovine RPE cell with 140 mM Rb^+ and 1 mM Ba^{2+} in the pipette. The bath contained 140 mM K^+ external solution to depolarize the membrane potential. *B*, *I–V* relationships obtained from the currents in *A* measured 2.5 ms (○) and 167 ms (●) after the onset of the voltage step. *C*, relationship between current variance and mean current from the same patch as in *A*. See text for additional details.

holding potential of 0 mV. The smooth curve is the least-squares fit of the data to eqn (4), with values for single-channel current (i) and number of channels (N) of 0.312 pA and 106, respectively. For a total of five apical membrane patches, the unitary chord conductance calculated from estimates of single-channel current averaged 1.70 ± 0.27 pS. Hence, the RPE Kir channel has single-channel Rb^+ conductance that is nearly identical to that of the cloned Kir7.1 channel. From this unitary Rb^+ conductance and the whole-cell Rb^+ chord conductance (104 ± 16.8 nS at −150 mV, $n = 8$), we estimate that each RPE cell contains at least 61 000 Kir channels.

DISCUSSION

We have cloned and sequenced human Kir7.1 from an RPE cDNA library and demonstrated by Northern analysis that Kir7.1 is highly expressed in the RPE. In electrophysiological experiments, we determined that native Kir channels in isolated bovine RPE cells share several unusual permeation properties with heterologously expressed Kir7.1 channels, including an inverse dependence of macroscopic conductance on $[K^+]_o$, a Rb^+-to-K^+ conductance ratio of ~10 and a low single-channel Rb^+ conductance of ~2 pS. Finally, in cell-attached patch recordings, we have localized inwardly rectifying Rb^+ currents to the apical membrane of the RPE. Hence, a major conclusion of this paper is that Kir7.1 channel subunits comprise the Kir conductance of the RPE apical membrane.

Cloning of human Kir7.1 from the RPE

In a 'subtracted' bovine RPE cDNA library (Chang *et al.* 1997, 1999), we identified a clone containing a partial sequence with homology to the Kir channel subunit ROMK2. Subsequently, we used this clone to probe a human RPE cDNA library and isolated a cDNA containing the entire open reading frame encoding a 360-amino acid polypeptide identical to Kir7.1, a new member of the Kir gene family (Döring *et al.* 1998; Krapivinsky *et al.* 1998; Partiseti *et al.* 1998; Nakamura *et al.* 1999). Kir7.1 is the most divergent member of the Kir family, with only a 38% sequence identity at the amino acid level with its closest homologue, human Kir1.3 (Shuck *et al.* 1997). While Kir7.1 contains structural motifs typical of inwardly rectifying K^+ channels, namely two membrane spanning domains and an intervening pore domain, its sequence in the pore region diverges at three locations that are conserved in other cloned Kir channel subunits: S111, M125 and G129 (Krapivinsky *et al.* 1998). It is now well established that M125, which lies two residues downstream from the pore selectivity sequence G-Y-G, is responsible for many of the unique permeation properties of the Kir7.1 channel, including a low dependence of macroscopic conductance on $[K^+]_o$ (Döring *et al.* 1998; Krapivinsky *et al.* 1998), a low single-channel conductance (Krapivinsky *et al.* 1998) and a high Rb^+-to-K^+ conductance ratio (Wischmeyer *et al.* 2000).

Tissue distribution of bovine Kir7.1

We evaluated the tissue distribution of *Kir7.1* by Northern blot analysis of mRNA isolated from various bovine tissues. A single transcript of ~1.4 kb was present in the RPE, but Kir7.1 mRNA could not be detected in neural retina, brain, heart, liver, kidney, testis, or skeletal muscle. These results differ somewhat from reports by other investigators. In a study by Doring *et al.* (1998), three Kir7.1 transcripts were detected in Northern blots of rat mRNA, with a 1.4 kb signal in brain, lung and kidney, a 2.4 kb band in testis and a 3.2 kb band in lung and kidney. In contrast, Northern blot analysis of human RNA detected a single 3.2 kb transcript in brain, small intestine, hippocampus, medulla and thyroid (Partiseti *et al.* 1998; Nakamura *et al.* 1999). These inter- and intra-species differences in the size of Kir7.1 transcripts may reflect different lengths in untranslated regions or poly(A)$^+$ tails (Nakamura *et al.* 2000). Our failure to detect Kir7.1 mRNA in any tissue other than the RPE may be due to the limited exposure time of the blot, or may reflect species-specific differences in expression pattern between rats, cows and humans. This does not affect our conclusion, however, that Kir7.1 is highly expressed in the RPE.

Permeation properties of Kir7.1

Kir7.1 has unique properties with respect to permeant ions. Other native and cloned Kir channels typically exhibit saturation of conductance with voltage and a limiting conductance that is proportional to the square root of $[K^+]_o$ (Lopatin & Nicholas, 1996). In previous studies by other investigators, it was noted that the macroscopic Kir7.1 conductance has an unusually low dependence on $[K^+]_o$ (Döring *et al.* 1998; Krapivinsky *et al.* 1998). Although our results generally agree with this assessment, they reveal that the relationship between Kir7.1 conductance and $[K^+]_o$ is more complex than was previously appreciated. We found that the macroscopic Kir7.1 conductance was non-saturating except at low K^+ concentrations (1 and 2 mM) and exhibited a low dependence on $[K^+]_o$ at very negative potentials (−160 mV) but an inverse dependence on $[K^+]_o$ at voltages positive to about −125 mV. Thus, at physiological voltages, the macroscopic Kir7.1 conductance decreases as $[K^+]_o$ is increased. Obviously, additional information about how single Kir7.1 channel conductance and gating vary with voltage and $[K^+]_o$ are needed before the mechanism(s) responsible for this unconventional behaviour can be elucidated.

In general, the permeation properties of ion channels can be probed in two fundamentally different ways: reversal potentials determined under bi-ionic conditions yield relative permeabilities, whereas current–voltage relationships provide relative conductances. In agreement with the recent report by Wischmeyer *et al.* (2000), we found that Kir7.1 has a Rb^+-to-K^+ permeability ratio of about 1, but a macroscopic Rb^+-to-K^+ conductance ratio of

roughly 10. This is in striking contrast to most other native and cloned Kir channels in which Rb^+ acts as a permeant blocker, giving rise to Rb^+-to-K^+ conductance ratios in the range 0.1–0.5 (Standen & Stanfield, 1980; Zhou *et al.* 1994; Reuveny *et al.* 1996; Löffler & Hunter, 1997; Welling, 1997; Choe *et al.* 1998). It is interesting to note that the macroscopic Rb^+ conductance of Kir7.1 exceeded the K^+ conductance only at voltages negative to about −50 mV; at more positive potentials the Rb^+ and K^+ conductances were quantitatively similar. The basis for the 'activation' of the Rb^+ conductance at −50 mV is unknown, but conceivably could involve the relief of K^+ (or some other ion) binding to a site within the channel that is accessible from the cytoplasmic side. To the extent that it reflects a change in single-channel conductance, the dramatic increase in macroscopic Kir7.1 conductance that occurs when external K^+ is replaced with Rb^+ suggests that the channel pore has a binding site with a higher affinity for K^+, as suggested by Wischmeyer *et al.* (2000). It remains to be determined, however, whether alterations in open probability or the number of functional channels might also be contributing factors.

The sole report of Kir7.1 single-channel conductance comes from the study of Krapivinsky *et al.* (1998), who applied non-stationary noise analysis to K^+ currents recorded from membrane patches of transfected mammalian cells to obtain an estimate of ~50 fS. In the present study, we were unable to confirm these results in the *Xenopus* oocyte expression system. However, when we used Rb^+ as the permeant cation (together with Ba^{2+} to produce a time-dependent change in channel open probability), non-stationary noise analysis yielded a single-channel conductance of ~2 pS. Assuming that channel gating and the number of functional channels are unaffected by Rb^+, our macroscopic conductance measurements would suggest a 10-fold smaller single-channel K^+ conductance of ~200 fS. This value is ~4 times larger than that estimated by Krapivinsky *et al.* (1998) but well within the accuracy of noise measurements. Thus, our results confirm that Kir7.1 has a very low single-channel conductance.

Kir7.1 channels comprise the RPE Kir conductance

It is well established that the membrane properties of isolated RPE cells are dominated by a mild, inwardly rectifying K^+ conductance (Hughes & Steinberg, 1990; Segawa & Hughes, 1994; Hughes, *et al.* 1995*b*; Hughes & Takahira, 1998) and there are several lines of evidence suggesting that this conductance lies in the apical membrane (Segawa & Hughes, 1994; Hughes *et al.* 1995*a*). In previous studies on amphibian (Hughes & Steinberg, 1990; Segawa & Hughes, 1994) and human RPE (Hughes & Takahira, 1996), we demonstrated that, in the vicinity of E_K, this conductance has the unusual property of decreasing in response to increases in $[K^+]_o$. In the present study on bovine RPE cells, we measured Kir conductance over a wider range of K^+ concentrations and confirmed this behaviour. Moreover, we extended these findings by examining the cation selectivity of the RPE Kir conductance and found that although it is nearly equally permeable to Rb^+ and K^+, it is 10 times more conductive to Rb^+ than to K^+. In addition, we estimate that the channel has a unitary Rb^+ conductance of ~2 pS. These values are in close agreement with those obtained for the heterologously expressed Kir7.1 channel, strongly suggesting that Kir7.1 channel subunits comprise the Kir conductance of the RPE apical membrane. This conclusion is supported by the results of cell-attached recordings, which revealed inwardly rectifying Rb^+ currents mainly in apical membrane patches.

Although the Kir conductance in bovine RPE cells was qualitatively similar to the Kir7.1 conductance examined in oocytes, it differed in some respects. Compared to the cloned Kir7.1 conductance, the decrease in RPE Kir conductance produced by increasing $[K^+]_o$ was less pronounced. Moreover, in RPE cells bathed with low $[K^+]$, outward Kir currents were relatively smaller and exhibited less inactivation at positive potentials. The reason for these discrepancies is unknown, but one possibility is that the RPE and oocyte differ with respect to the intracellular concentrations of cytoplasmic blockers such as Mg^{2+} and polyamines, which are known to affect outward currents through other Kir channel types. Alternatively, there may be differences in post-translational modification of the channel subunit protein. Whole-cell recordings of Kir7.1 channels expressed in mammalian cells may help resolve this issue.

Recently, Kusaka *et al.* (1999) presented immunohistochemical and single-channel current data suggesting that Kir4.1 channels are present in the apical processes of neonatal rat RPE. Kir4.1 channels are characterized by moderate inward rectification, a strong dependence of macroscopic conductance on extracellular $[K^+]$, high sensitivity to block by Cs^+ and Ba^{2+}, inactivation at strong negative potentials and a single-channel K^+ conductance of 20–25 pS (Takumi *et al.* 1995). None of these properties, however, are shared by the predominant Kir conductance in amphibian (Hughes & Steinberg, 1990; Segawa & Hughes, 1994), human (Hughes *et al.* 1995*b*) or bovine RPE (Hughes & Takahira, 1998; this study). To reconcile this discrepancy, Kusaka *et al.* (1999) suggested that Kir.4.1 currents are not detected in whole-cell recordings because apical processes are lost from isolated RPE cells. In our experience, however, processes are generally present on the apical surface of isolated RPE cells (Hughes & Steinberg, 1990; Hughes *et al.* 1995*b*), and membrane capacitance measurements indicate that they are voltage clamped in whole-cell recordings. Hence, we conclude that if Kir4.1 channels are present in the RPE apical membrane, their contribution to the macroscopic conductance is minor compared to that of Kir7.1 channels.

Physiological significance

The RPE has an intimate anatomical and functional relationship with the adjacent photoreceptor cells. Microvilli projecting from the apical surface of the RPE interdigitate with the distal third of photoreceptor outer segments. Separating the RPE apical membrane and plasma membrane of the outer segment is a small extracellular compartment called the subretinal space. The RPE provides crucial support to the photoreceptors by regulating this microenvironment through the vectorial transport of fluid, ions and metabolites. K^+ channels in the apical membrane function directly in subretinal K^+ homeostasis by determining the direction and magnitude of net K^+ transport across the RPE (Miller & Edelman, 1990; Joseph & Miller, 1991). They also influence the net transport of HCO_3^- (Hughes *et al.* 1989) and Cl^- (Bialek & Miller, 1994) by affecting the electrochemical driving forces on these anions and also support Na^+–K^+ pump activity by providing a recycling pathway for K^+ across the apical membrane.

One of the unique features of the RPE is that, like the choroid plexus, the Na^+–K^+ pump is localized to the apical rather than the basolateral membrane (Steinberg & Miller, 1973; Okami *et al.* 1990), which is typical of most other transporting epithelia (Rodriguez-Boulan & Zurzolo, 1993). The results of our cell-attached recordings from isolated RPE cells indicate that channels with the hallmarks of Kir7.1 are also localized to the apical membrane. The capacity of the Kir7.1 channel to conduct relatively large outward currents makes it well suited to serve as the obligatory return pathway for K^+ that enters the cell through the Na^+–K^+ pump. On the basis of our meansurements of single-channel and whole-cell Rb^+ conductance, we estimate that there are $> 61\,000$ Kir7.1 channels in the apical membrane of each RPE cell. Assuming that these channels are distributed along the length of the microvilli, then their low unitary conductance and large number might serve to distribute the K^+ conductance and help minimize local K^+ gradients within the processes and extracellular space and thus optimize Na^+–K^+ pump function.

In addition to their function in transport processes, apical membrane K^+ channels also play an important role in RPE–photoreceptor interactions. At light onset, the closure of cGMP-gated cation channels in the photoreceptor outer segments leads to a decrease in subretinal $[K^+]$ from approximately 5 mM to 2 mM. By virtue of the presence of K^+ channels in the apical membrane, this $[K^+]_o$ decrease produces an apical membrane hyperpolarization, which generates the c-wave of the DC electroretinogram (Oakley & Green, 1976). At the same time, it triggers a large efflux of K^+ (and, secondarily, Cl^- and water) from the RPE, leading to reciprocal changes in the volumes of the RPE cell (Bialek & Miller, 1994) and subretinal space (Huang & Karwoski, 1992; Li *et al.* 1994).

One of the important features of the Kir channel in the RPE is that its macroscopic outward conductance increases with decreases in extracellular K^+ concentration (Segawa & Hughes, 1994; Hughes & Takahira, 1996). In the present study, we confirmed this finding in bovine RPE cells (Fig. 8) and show that it is an inherent property of the Kir7.1 channel (Fig. 3). This is opposite to the behaviour of other cloned and native Kir channels, which typically exhibit a decrease in outward (and inward) conductance with decreases in $[K^+]_o$ (Nichols & Lopatin, 1997). Our results suggest that, at light onset, an increase in the outward conductance of Kir7.1 channels might conspire with an increase in electrochemical driving force (Bialek & Miller, 1994) to promote K^+ efflux across the RPE apical membrane.

Ausubel, F. M., Brent, R., Kingston, R. E., Moore, D. D., Seidman, J. G., Smith, J. A. & Struhl, K. (1996). *Current Protocols in Molecular Biology*. John Wiley & Sons, New York.

Baumgartner, W., Isias, L. & Sigworth, F. J. (1999). Two-microelectrode voltage clamp of *Xenopus* oocytes: Voltage errors and compensation for local current flow. *Biophysical Journal* **77**, 1980–1991.

Bialek, S. & Miller, S. (1994). K^+ and Cl^- transport mechanisms in bovine pigment epithelium that could modulate subretinal space volume and composition. *Journal of Physiology* **475**, 53–67.

Chang, J., Milligan, S., Li, Y., Campochiaro, P. A., Hyde, D. & Zack, D. J. (1997). Mammalian homolog of *Drosophila* retinal degeneration B rescues the mutant phenotype in the fly. *Journal of Neuroscience* **17**, 5881–5890.

Chang, J. T., Esumi, N., Moore, K., Li, Y., Zhang, S., Chew, C., Goodman, B., Amir Rattner, A., Moody, S., Stetten, G., Campochiaro, P. A. & Zack, D. J. (1999). Cloning and characterization of a secreted frizzled-related protein that is expressed by the retinal pigment epithelium. *Human Molecular Genetics* **8**, 575–583.

Choe, H., Sackin, H. & Palmer, L. G. (1998). Permeation and gating of an inwardly rectifying potassium channel. Evidence for a variable energy well. *Journal of General Physiology* **112**, 433–446.

Döring, F., Derst, C., Wischmeyer, E., Karschin, C., Schneggenburger, R., Daut, J. & Karschin, A. (1998). The epithelial inward rectifier channel Kir7.1 displays unusual K^+ permeation properties. *Journal of Neuroscience* **18**, 8625–8636.

Goldin, A. L. (1992). Maintenance of *Xenopus laevis* and oocyte injection. *Methods in Enzymology* **207**, 266–279.

Griff, E. R., Shirao, Y. & Steinberg, R. H. (1985). Ba^{2+} unmasks K^+ modulation of the Na^+-K^+ pump in the retinal pigment epithelium. *Journal of General Physiology* **86**, 853–876.

Hamill, O. P., Marty, A., Neher, E., Sakmann, B. & Sigworth, F. J. (1981). Improved patch-clamp techniques for high-resolution current recording from cells and cell-free membrane patches. *Pflügers Archiv* **391**, 85–100.

Heinemann, S. H. & Conti, F. (1992). Nonstationary noise analysis and application to patch clamp recordings. *Methods in Enzymology* **207**, 131–149.

HILLE, B. (1992). *Ionic Channels of Excitable Membranes*, 2nd edn. Sinauer Associates Inc., Sunderland, MA, USA.

HO, K., NICHOLS, C. G., LEDERER, W. J., LYTTON, J., VASSILEV, P. M., KANAZIRSKA, M. V. & HEBERT, S. C. (1993). Cloning and expression of an inwardly rectifying ATP-regulated potassium channel. *Nature* **362**, 31–38.

HUANG, B. & KARWOSKI, C. (1992). Light-evoked expansion of subretinal space volume in the retina of the frog. *Journal of Neuroscience* **12**, 4243–4252.

HUGHES, B. A., ADORANTE, J. S., MILLER, S. S. & LIN, H. (1989). Apical electrogenic $NaHCO_3$ cotransport. A mechanism for HCO_3 absorption across the retinal pigment epithelium. *Journal of General Physiology* **94**, 125–150.

HUGHES, B. A., GALLEMORE, R. P. & MILLER, S. S. (1998). Transport mechanisms in the retinal pigment epithelium. In *The Retinal Pigment Epithelium: Function and Disease*, ed. MARMOR, M. F. & WOLFENSBERGER, T. J., pp. 103–134. Oxford University Press, New York.

HUGHES, B. A., SHAIKH, A. & AHMAD, A. (1995*a*). Effects of Ba^{2+} and Cs^+ on apical membrane K^+ conductance in toad retinal pigment epithelium. *American Journal of Physiology* **268**, C1164–1172.

HUGHES, B. A. & STEINBERG, R. H. (1990). Voltage-dependent currents in isolated cells of the frog retinal pigment epithelium. *Journal of Physiology* **428**, 273–297.

HUGHES, B. A. & TAKAHIRA, M. (1996). Inwardly rectifying K^+ currents in isolated human retinal pigment epithelial cells. *Investigative Ophthalmology and Visual Science* **37**, 1125–1139.

HUGHES, B. A. & TAKAHIRA, M. (1998). ATP-dependent regulation of inwardly rectifying K^+ current in bovine retinal pigment epithelial cells. *American Journal of Physiology* **275**, C1372–1383.

HUGHES, B. A., TAKAHIRA, M. & SEGAWA, Y. (1995*b*). An outwardly rectifying K^+ current active near resting membrane potential in human retinal pigment epithelial cells. *American Journal of Physiology* **269**, 179–187.

JACKSON, P. S. & STRANGE, K. (1996). Single channel properties of a volume sensitive anion channel: Lessons from noise analysis. *Kidney International* **49**, 1695–1699.

JOSEPH, D. P. & MILLER, S. S. (1991). Apical and basement membrane ion transport mechanism in bovine retinal pigment epithelium. *Journal of Physiology* **435**, 439–463.

KOFUJI, P., DAVIDSON, N. & LESTER, H. A. (1995). Evidence that neuronal G-protein-gated inwardly rectifying K^+ channels are activated by G beta gamma subunits and function as heteromultimers. *Proceeding of the National Academy of Sciences of the USA* **92**, 6542–6546.

KRAPIVINSKY, G., MEDINA, I., ENG, L., KRAPIVINSKY, L., YANG, Y. & CLAPHAM, D. E. (1998). A novel inward rectifier K^+ channel with unique pore properties. *Neuron* **20**, 995–1005.

KUBO, Y., BALDWIN, T. J., JAN, Y. N. & JAN, L. Y. (1993). Primary structure and functional expression of a mouse inward rectifier potassium channel. *Nature* **362**, 127–133.

KUSAKA, S., HORIO, Y., FUJITA, A., MATSUSHITA, K., INANOBE, A., GOTOW, T., UCHIYAMA, Y., TANO, Y. & KURACHI, Y. (1999). Expression and polarized distribution of an inwardly rectifying K^+ channel, Kir4.1, in rat retinal pigment epithelium. *Journal of Physiology* **520**, 373–381.

LASANSKY, A. & DE FISCH, F. W. (1966). Potential, current, and ionic influxes across the isolated retinal pigment epithelium and choroid. *Journal of General Physiology* **49**, 913–924.

LI, J. D., GALLEMORE, R. P., DMITRIEV, A. & STEINBERG, R. H. (1994). Light-dependent hydration of the space surrounding the photoreceptors in chick retina. *Investigative Ophthalmology and Visual Science* **35**, 2700–2711.

LÖFFLER, K. & HUNTER, M. (1997). Cation permeation and blockade of ROMK1, a cloned renal potassium channel. *Pflügers Archiv* **434**, 151–158.

LOPATIN, A. N. & NICHOLAS, C. G. (1996). $[K^+]$ dependence of open channel conductance in cloned inward rectifier potassium channels (IRK1, Kir2.1). *Biophysical Journal* **71**, 682–694.

MILLER, S. S. & EDELMAN, J. L. (1990). Active ion transport pathways in the bovine retinal pigment epithelium. *Journal of Physiology* **424**, 283–300.

MILLER, S. S. & STEINBERG, R. H. (1977). Passive ionic properties of frog retinal pigment epithelium. *Journal of Membrane Biology* **36**, 337–372.

MILLER, S. S., STEINBERG, R. H. & OAKLEY, B. I. (1978). The electrogenic sodium pump of the frog retinal pigment epithelium. *Journal of Membrane Biology* **67**, 199–209.

NAKAMURA, N., SUZUKI, Y., IKEDA, Y., NOTOYA, M. & HIROSE, S. (2000). Complete structure and regulation of the rate gene for inward rectifier potassium channel Kir7.1. *Journal of Biological Chemistry* **275**, 28276–28284.

NAKAMURA, N., SUZUKI, Y., SAKUTA, H., OOKATA, K., KAWAHARA, K. & HIROSE, S. (1999). Inwardly rectifying K^+ channel Kir7.1 is highly expressed in thyroid follicular cells, intestinal epithelial cells and choroid plexus epithelial: implication for a functional coupling with Na^+,K^+-ATPase. *Biochemical Journal* **342**, 329–336.

NICHOLS, C. G. & LOPATIN, A. N. (1997). Inward rectifier potassium channel. *Annual Review of Physiology* **59**, 171–191.

OAKLEY, B. I. & GREEN, D. G. (1976). Correlation of light-induced changes in retinal extracellular potassium concentration with c-wave of the electroretinogram. *Journal of Neurophysiology* **39**, 1117–1133.

OKAMI, T., YAMAMOTO, A., OMORI, K., TAKADA, T., UYAMA, M. & TASHIRO, Y. (1990). Immunocytochemical localization of Na^+,K^+-ATPase in rat retinal pigment epithelial cells. *Journal of Histochemistry and Cytochemistry* **38**, 1267–1275.

PARTISETI, M., COLLURA, V., AGNEL, M., CULOUSCOU, J. M. & GRAHAM, D. (1998). Cloning and characterization of a novel human inwardly rectifying potassium channel predominantly expressed in small intestine. *FEBS Letters* **434**, 171–176.

QUINN, R. H. & MILLER, S. S. (1992). Ion transport mechanisms in native human retinal pigment epithelium. *Investigative Ophthalmology and Visual Science* **33**, 3513–3527.

REIMANN, F. & ASHCROFT, F. M. (1999). Inwardly rectifying potassium channels. *Current Opinion in Cell Biology* **11**, 503–508.

REUVENY, E., JAN, Y. N. & JAN, L. Y. (1996). Contributions of a negatively charged residue in the hydrophobic domain of the IRK1 inwardly rectifying K^+ channel to K^+-selective permeation. *Biophysical Journal* **70**, 754–761.

RODRIGUEZ-BOULAN, E. & ZURZOLO, C. (1993). Polarity signals in epithelial cells. *Journal of Cell Science Supplement* **17**, 335–343.

SAMBROOK, J., FRITSCH, F. F. & MANIATIS, T. (1989). *Molecular Cloning, a Laboratory Manual*. Cold Spring Harbor Laboratory Press, New York.

SEGAWA, Y. & HUGHES, B. A. (1994). Properties of the inwardly rectifying K^+ conductance in the toad retinal pigment epithelium. *Journal of Physiology* **476**, 41–53.

SHIMURA, M., YUAN, Y. & HUGHES, B. A. (1999). Cation permeability of the inwardly rectifying potassium conductance in bovine retinal pigment epithelial (RPE) cells. *Investigative Ophthalmology and Visual Science* **40**, S499 (abstract).

SHUCK, M. E., PISER, T. M., BOCK, J. H., SLIGHTOM, J. L., LEE, K. S. & BIENKOWSKI, M. J. (1997). Cloning and characterization of two K^+ inward rectifier (Kir) 1.1 potassium channel homologs from human kidney (Kir1.2 and Kir1.3). *Journal of Biological Chemistry* **272**, 586–593.

STANDEN, N. B. & STANFIELD, P. R. (1980). Rubidium block and rubidium permeability of the inward rectifier of frog skeletal muscle fibers. *Journal of Physiology* **304**, 415–435.

STEINBERG, R. & MILLER, S. (1973). Aspects of electrolyte transport in frog pigment epithelium. *Experimental Eye Research* **16**, 365–372.

STUHMER, W. (1992). Electrophysiological recording from *Xenopus* oocytes. *Methods in Enzymology* **207**, 319–339.

TAKAHIRA, M. & HUGHES, B. A. (1997). Isolated bovine retinal pigment epithelial cells express delayed rectifier type and M-type K^+ currents. *American Journal of Physiology* **273**, C790–803.

TAKUMI, T., ISHII, T., HORIO, Y., MORISHIGE, K., TAKAHASHI, N., YAMADA, M., YAMASHITA, T., KIYAMA, H., SOHMIYA, K., NAKANISHI, S. & KURACHI, Y. (1995). A novel ATP-dependent inward rectifier potassium channel expressed predominantly in glial cells. *Journal of Biological Chemistry* **270**, 16339–16346.

TRAYNELIS, S. F. & JARAMILLO, F. (1998). Getting the most out of noise in the central nervous system. *Trends in Neurosciences* **21**, 137–145.

WELLING, P. A. (1997). Primary structure and functional expression of a cortical collecting duct Kir channel. *American Journal of Physiology* **273**, F825–836.

WISCHMEYER, E., DORING, F. & KARSCHIN, A. (2000). Stable cation coordination at a single outer pore residue defines permeation properties in Kir channels. *FEBS Letters* **466**, 115–120.

YUAN, Y., CHANG, J. T., SHIMURA, M., CAMPOCHIARO, P. A., ZACK, D. J. & HUGHES, B. A. (2000). Molecular cloning and functional expression of Kir7.1, an inwardly rectifying K^+ channel from the retinal pigment epithelium (RPE). *Investigative Ophthalmology and Visual Science* **41**, S613 (*abstract*).

ZHOU, H., TATE, S. S. & PALMER, L. G. (1994). Primary structure and functional properties of an epithelial K channel. *American Journal of Physiology* **266**, C809–824.

Acknowledgements

We thank Anuradha Swaminathan and Drs Gyanendra Kumar, Yasunori Segawa and Masayuki Takahira for their assistance with certain aspects of this study and Dr Alan Goldin (University of California, San Diego) for kindly providing the pBSTA plasmid. This work waas supported by National Eye Institute Grants EY08850 (B.A.H.), EY07703 and P30EY1765, Foundation Fighting Blindness, Macular Vision and Steinbach Foundations and unrestricted funds from Research to Prevent Blindness, Inc. (R.P.B.). D.J.Z. is a recipient of a Career Development Award from RPB and M.S. a recipient of an award from the Naito Foundation.

Corresponding author

B. A. Hughes: W. K. Kellogg Eye Center, Department of Ophthalmology and Visual Sciences, University of Michigan, 1000 Wall Street, Ann Arbor, MI 48105, USA.

Email: bhughes@umich.edu